



BIONATURE 2011

The Second International Conference on Bioenvironment, Biodiversity and
Renewable Energies

May 22-27, 2011

Venice/Mestre, Italy

BIONATURE 2011 Editors

Gianfranco Chicco, Politecnico di Torino, Italy

Son V. Nghiem, Jet Propulsion Laboratory / California Institute of Technology -
Pasadena, USA

BIONATURE 2011

Foreword

The Second International Conference on Bioenvironment, Biodiversity and Renewable Energies (BIONATURE 2011), held between May 22 -27, 2011 in Venice, Italy, covered the these three main areas: environment, biodiversity and invasion, and renewable and sustainable energies.

Environmental change awareness is a key state of spirit and legislation for preventing, protecting, and ultimately saving the planet biodiversity. Technical and practical methods for applying bio-agriculture for the public's health and safety are primary targets. The goal is the use of ecological economic stimuli in tandem with social and governmental actions preventing deforestation, pollution, and global warming. To cope with the climate and landscape changes advanced technical inventory of tools and statistics on lessons learned are needed to derive appropriate measure and plan accordingly.

The biologic equilibrium on its vast immensity is a challenge for both knowledge gathering and its understanding. Preserving the existing species under rapid economy, one the one side, and using the diversity of environmental species for industrial purposes is a very week balance. There is a risk of forever damaging the existence of thousands of species, or miss the opportunity of using them for the benefit of humanity. Therefore, measuring and interpreting the impact of human actions on the diversity on marine and oceanic life, on Arctic and Antarctic bio-climate, or on forest ecosystems represent one way to prevent ecological disasters and predict possible environmental changes. The event deals with such ecosystem diversity, and the use of their existence for humanity in terms of industrial products, drug production, but also in terms of studying and modeling the ecological degradation, such loss of Poles' ice, food-chain dependency survival, wildlife endurance, or ozone holes. It also bring to the stage different disruption side-effect of the landscape changes, detection and warning systems, invasion of alien species, and the need for public awareness and education.

Replacing the classical energy with alternative renewable energy (green energy), such as bioenergy, eolian energy, or solar energy is an ecological and economic trend that suggests important socio-economic advantages: using native renewable resources, increasing of self-sufficiency rate of energy and promoting use of clean energy, and that way, polluting emissions to the air will be reduced. Bioenergy is renewable energy derived from biological sources, to be used for heat, electricity, or vehicle fuel. Biofuel derived from plant materials is among the most rapidly growing renewable energy technologies. In several countries corn-based ethanol is currently the largest source of biofuel as a gasoline substitute or additive. Recent energy legislation mandates further growth of both corn-based and advanced biofuels from other sources. Growing biofuel demand has implications for U.S. and world agriculture. Eolian energy is currently used throughout the world on a large scale. In the past decade, its evolution shows its acceptance as a source of generation, with expressive growth trends in the energy matrices in the countries where this source is used Eolian energy is renewable and has very low environmental impact. To generate it, there are no gas emissions, no effluent refuse, and no other natural resources, such as water, are consumed. Photovoltaic technology makes use of the energy in the sun, and it has little impact on the environment. Photovoltaics can be used in a wide range of products, from small consumer items to large commercial solar electric systems. The event bring together the challenging technical and regulation aspects for supporting and producing renewable energy with less or no impact

on the ecosystems. There are several technical integration barriers and steps for social adoption and governmental legislation to favor and encourage this kind of energy.

We welcomed technical papers presenting research and practical results, position papers addressing the pros and cons of specific proposals, such as those being discussed in the standard forums or in industry consortia, survey papers addressing the key problems and solutions on any of the above topics short papers on work in progress, and panel proposals.

We take here the opportunity to warmly thank all the members of the BIONATURE 2011 technical program committee as well as the numerous reviewers. The creation of such a broad and high quality conference program would not have been possible without their involvement. We also kindly thank all the authors that dedicated much of their time and efforts to contribute to BIONATURE 2011. We truly believe that, thanks to all these efforts, the final conference program consisted of top quality contributions.

We hope that BIONATURE 2011 was a successful international forum for the exchange of ideas and results between academia and industry and to promote further progress in bioenvironment, biodiversity, and renewable energies.

We are certain that the participants found the event useful and communications very open. We also hope the attendees enjoyed the beautiful surroundings of Venice.

BIONATURE 2011 Chairs

Gianfranco Chicco, Politecnico di Torino, Italy

Josean Garrués Irurzun, University of Granada, Spain

Son V. Nghiem, Jet Propulsion Laboratory / California Institute of Technology - Pasadena, USA

Suhkneung Pyo, Sungkyunkwan University - Suwon City, South Korea

Orazio Tagliatela-Scafati, University of Naples "Federico II", Italy

Qian Pei Yuan, The *Hong Kong* University of Science and Technology, Hong Kong

Dilip Khatiwada, Royal Institute of Technology, Stockholm, Sweden

BIONATURE 2011

Committee

BIONATURE Advisory Chairs

Gianfranco Chicco, Politecnico di Torino, Italy
Josean Garrués Irurzun, University of Granada, Spain
Son V. Nghiem, Jet Propulsion Laboratory / California Institute of Technology - Pasadena, USA
Suhkneung Pyo, Sungkyunkwan University - Suwon City, South Korea
Orazio Taglialatela-Scafati, University of Naples "Federico II", Italy
Qian Pei Yuan, The Hong Kong University of Science and Technology, Hong Kong

BIONATURE Publicity Chair

Dilip Khatiwada, Royal Institute of Technology, Stockholm, Sweden

BIONATURE 2011 Technical Program Committee

Omar Badran, German Jordanian University - Amman, Jordan
Rupp Carriveau, Union Gas / University of Windsor University of Windsor, Canada
Longjian Chen, China Agricultural University, China
Yau-Hung Chen, Tamkang University - Taipei Taiwan, ROC
Gianfranco Chicco, Politecnico di Torino, Italy
Alexandre Costa, CIEMAT - Madrid, Spain
Hany A. El-Shemy, Cairo University - Giza, Egypt
Jerekias Gandure, University of Botswana, Botswana
Josean Garrués Irurzun, University of Granada, Spain
Bassim H. Hameed, University of Science Malaysia - Penang, Malaysia
Kathleen Hefferon, Cornell University, USA
Dilip Khatiwada, Royal Institute of Technology (KTH)- Stockholm, Sweden / Nepal Bureau of Standards & Metrology (NBSM)- Kathmandu, Nepal
Keat Teong Lee, Universiti Sains Malaysia, Malaysia
Ana Jesús López, University of Oviedo, Spain
Soteris Kalogirou, Cyprus University of Technology - Limassol, Cyprus
Dilip Khatiwada, Royal Institute of Technology, Stockholm, Sweden
Valentinas Klevas, Kaunas University of Technology / Lithuanian Energy Institute, Lithuania
Villy Kourafalou, University of Miami/ Rosenstiel School of Marine and Atmospheric Science, USA
Hacene Mahmoudi, University of Chlef, Algeria
Arkadiusz Majoch, The Oil and Gas Institute - Warsaw, Poland
Steven E. McMurray, NOAA Fisheries - Silver Spring, USA
Blanca Moreno Cuartas, University of Oviedo, Spain
Ali Mostafaeipour, Yazd University, Iran
Abdeen Mustafa Omer, Energy Research Institute (ERI) - Nottingham, UK
Son V. Nghiem, Jet Propulsion Laboratory / California Institute of Technology - Pasadena, USA
Suhkneung Pyo, Sungkyunkwan University - Suwon City, South Korea
Bale V. Reddy, University of Ontario Institute of Technology - Oshawa, Canada

Joginder S. Saini, Indian Institute of Technology - Roorkee, India
Francisca Segura Manzano, University of Huelva, Spain
Elena Serrano, University of Alicante, Spain
Atul Sharma, Rajiv Gandhi Institute of Petroleum Technology - Rae Bareilly, India
Sungwoo Shin, Hanyang University, South Korea
Vladimir Strezov, Macquarie University - Sydney Australia
Orazio Tagliapietra-Scafati, University of Naples "Federico II", Italy
Qian Pei Yuan, The Hong Kong University of Science and Technology, Hong Kong
Talal Yusaf, University of Southern Queensland - Toowoomba, Australia
Xiangdong Zhang, International Arctic Research Center / University of Alaska Fairbanks, USA

Copyright Information

For your reference, this is the text governing the copyright release for material published by IARIA.

The copyright release is a transfer of publication rights, which allows IARIA and its partners to drive the dissemination of the published material. This allows IARIA to give articles increased visibility via distribution, inclusion in libraries, and arrangements for submission to indexes.

I, the undersigned, declare that the article is original, and that I represent the authors of this article in the copyright release matters. If this work has been done as work-for-hire, I have obtained all necessary clearances to execute a copyright release. I hereby irrevocably transfer exclusive copyright for this material to IARIA. I give IARIA permission to reproduce the work in any media format such as, but not limited to, print, digital, or electronic. I give IARIA permission to distribute the materials without restriction to any institutions or individuals. I give IARIA permission to submit the work for inclusion in article repositories as IARIA sees fit.

I, the undersigned, declare that to the best of my knowledge, the article does not contain libelous or otherwise unlawful contents or invading the right of privacy or infringing on a proprietary right.

Following the copyright release, any circulated version of the article must bear the copyright notice and any header and footer information that IARIA applies to the published article.

IARIA grants royalty-free permission to the authors to disseminate the work, under the above provisions, for any academic, commercial, or industrial use. IARIA grants royalty-free permission to any individuals or institutions to make the article available electronically, online, or in print.

IARIA acknowledges that rights to any algorithm, process, procedure, apparatus, or articles of manufacture remain with the authors and their employers.

I, the undersigned, understand that IARIA will not be liable, in contract, tort (including, without limitation, negligence), pre-contract or other representations (other than fraudulent misrepresentations) or otherwise in connection with the publication of my work.

Exception to the above is made for work-for-hire performed while employed by the government. In that case, copyright to the material remains with the said government. The rightful owners (authors and government entity) grant unlimited and unrestricted permission to IARIA, IARIA's contractors, and IARIA's partners to further distribute the work.

Table of Contents

Production of green energy from co-digestion: perspectives for the province of Cuneo, energetic balance and environmental sustainability <i>Giuseppe Genon, Enrico Brizio, Deborah Panepinto, Daniele Russolillo, and Franco Becchis</i>	1
Development of Complex Technologies for Biomass Processing <i>Konstantin Latinin, Vladimir Sinelshchikov, and Victor Zaichenko</i>	7
CO2 Emission Reduction from Sustainable Energy Systems: Benefits and Limits of Distributed Multi-Generation <i>Pierluigi Mancarella and Gianfranco Chicco</i>	11
Application of sulfated tin oxide in Transesterification of Waste Cooking Oil: An Optimization Study <i>Man Kee Lam and Keat Teong Lee</i>	17
Analysing the effect of Renewable Energy Sources on Electricity Prices in Spain. A Maximum Entropy Econometric Approach. <i>Blanca Moreno and Maria Teresa Garcia-Alvarez Garcia-Alvarez</i>	21
Electrical Prices in the European Union. An Econometric Panel Data Model <i>Blanca Moreno and Ana Jesus Lopez</i>	27
Interactions Between BTEX, TPH, and TCE During Their bio-removal from the Artificially Contaminated Water <i>Yiqin Chen, Junhui Li, Chengkeng Lei, and Shim Hojae</i>	33
Arctic Perennial Sea Ice Crash of the 2000s and its Impacts <i>Son Nghiem, Gregory Neumann, Pablo Clemente-Colon, Ignatius Rigor, and Donald Perovich</i>	38
Complex approach to oil spill utilization <i>Esfir Sulman, Michail Sulman, Ekaterina Prutenskaya, Ekaterina Selivanova, and Michail Rakitin</i>	43
Glycoside hydrolases of marine bacteria are promising tools in haemotherapy <i>Larissa Balabanova, Irina Bakunina, Galina Likhatskaya, Tatyana Zvyagintseva, and Valery Rasskazov</i>	47
Biocalcification of Corals and their Response to Global Climate Change <i>M. Azizur Rahman and Ryuichi Shinjo</i>	51

Production of green energy from Co-digestion: Perspectives for the Province of Cuneo, Energetic Balance and Environmental Sustainability

Genon G. *, Brizio E. **, Panepinto D. *, Russolillo D. ***, Becchis F. ***

* Politecnico di Torino

Torino, Italia

giuseppe.genon@polito.it, deborah.panepinto@polito.it

** ARPA Piemonte

Cuneo, Italia

e.brizio@arpa.piemonte.it

*** Fondazione per l'Ambiente Teobaldo Fenoglio ONLUS

Torino, Italia

daniele.russolillo@fondazioneambiente.org, franco.becchis@fondazioneambiente.org

Abstract - In Italy and many European countries energy production from biomass is encouraged by strong economic subsidies so that biomass energy plants are getting large diffusion. Nevertheless, it is necessary to define the environmental compatibility taking into account global parameters as well as environmental impacts at regional and local scale coming from new polluting emissions. The environmental balances regarding new energy plants are of primary importance within very polluted areas such as Northern Italy where air quality limits are systematically exceeded, in particular for PM₁₀, NO₂ and ozone. The paper analyses the renewable energy scenario relating to manure anaerobic digestion and biogas production for the Province of Cuneo, N-W Italy, and the environmental sustainability of the possible choices. The study is focused on energy producibility, heat and power, nitrogen oxides and ammonia emissions, GHG balances dealing also with indirect releases of CH₄ and N₂O, as well as emissions due to energy crops production. The most important conclusion that can be drawn is that the production of renewable energy from anaerobic digestion could cover up to 13% of the Province electricity consumption but sustainability in terms of CO₂ emissions can be reached only through an overriding use of agricultural waste products (manure and by-products instead of energy crops) and cogeneration of thermal energy at disposal; the application of best available techniques to waste gas cleaning, energy recovery and digestate chemical-physical treatments allows positive emissive balances.

Keywords- *anaerobic digestion; NO_x; ammonia; environmental balances, energy efficiency; biomass*

I. INTRODUCTION

Renewable energy plants (based on biogas produced by anaerobic digestion of manure and energy crops, vegetable oil, wood and solid biomass) are getting large diffusion in Northern Italy because of the benefits deriving from the production of energy on one's own, the reduction of odour nuisance from manure and the increase of its biological stability and, most of all, the economic return (pay-back times can be as short as 4-5 years in Italy) based on electricity production. The new energy scenario has to be considered within the environmental background of the area

where it is introduced, involving air quality limits compliance, the use of best available techniques, energetic efficiency (also thermal), emissive balances, global warming issues, biomass origins, aspects dealing with the use of water and fertilizers for energy crops, nitrates leaching towards groundwater. This is the focus of the present study.

II. STATE OF THE ART

In literature there are many references about bioenergy production and related environmental sustainability, in particular the individuation and utilization of indicators or methodologies corresponding to LCA have been studied; the evaluated aspects concern both the original definition of the evaluation scheme and subsequently the description of many practically interesting applicative situation have been obtained. As far as biogas production and utilization is concerned, in [1], the energy efficiency of different biogas systems was evaluated and specific energy balances were defined; the study provides bases for assessment of environmental compatibility, including management of spent digestate. It has been observed [2] that biogas systems lead to environmental improvements, arising from changed land use and handling of organic waste products, which often exceed the direct benefits from fossil fuel replacement; from the other side an impact factor, of different numerical value, can be originated, arising from the utilized raw material, the energy service that is provided, the replaced reference system. The use of LCA has been suggested by Colin et al. [3] to evaluate the contribution to climate change of biomethane production by monofermentation of cultivated crops, and it resulted absolutely lower than the contribution of natural gas importation; also the effects on ecosystem quality and human health damages were evaluated. In order to define the required information concerning energetic aspects, experiences of co-digestion of energy crops and cow or pig manures have been conducted on different scales [4][5], in order to define the influence of operating parameters on methane yield and post-methanation potential. From a

methodological point of view, a standard methodology has been outlined [6], to compare the greenhouse gas balances of bioenergy systems with those of fossil energy systems: a careful definition of system boundaries, and many operating issues have been dealt with in detail, with the final aim of an optimization from the greenhouse gas emissions point of view. In order to establish a reliable approach to the impact assessment of biomass cultivation phase, different LCA models were developed [7], and data from experimental fields were used for testing. The aspect of GHG balances of bioenergy systems producing electricity, heat and transportation biofuels has been examined in comparison with fossil reference systems in Cherubini [8] from standard LCA. In literature there are a lot of studies relating to this field. From the indicated references it is possible to establish that the environmental balances for energy crops exploitation are well defined and may examples are at disposal for useful comparisons; in any case a specific definition of the local context and the existing operating conditions must be carefully examined, in order to arrive to valid conclusions for a proposed application.

III. ENVIRONMENTAL CONDITIONS OF NORTHERN ITALY

Air quality of Northern Italy is one of the most polluted of the world, maybe the worst in Europe, due to the strong human activities and the orography of its territory. PM₁₀, NO₂ and ozone concentrations measured at the ground level diffusely and permanently go beyond the quality standards. In particular, PM₁₀ concentration is only partly due to particulate primary emissions because the chemical analysis of PM measured in Northern Italy confirm that secondary particles (deriving from NO_x, SO_x, NH₃ and VOC) account for 60-70 % of total PM concentration [9]. Moreover, some European studies report [10] the following aerosol formation factors, to be considered by weight, starting from gaseous pollutants: NO_x 0,88; SO_x 0,54; NH₃ 0,64. As it is clear from the reported figures, in order to control and improve air quality in Northern Italy, the emissions of gaseous compounds such as NO_x and ammonia (mostly emitted by agriculture) should be mainly reduced. Another strong environmental critical issue of Northern Italy is nitrate contamination of surface and ground-water resources mainly due to the use of fertilizers and the land-spreading of animal manures.

IV. ENVIRONMENTAL COMPATIBILITY FOR ANAEROBIC DIGESTION PLANTS

The main environmental concerns referring to animal manure management are odours due to uncontrolled fermentation, ammonia emissions from the storage and the land-spreading and greenhouse gases (GHG) release (CH₄ and N₂O). Anaerobic digestion (AD) can be an answer to odour nuisance but it is totally ineffective on nitrogen content of digested materials; moreover, as we will see later on, also CH₄ and N₂O could be enhanced with respect to the *ante operam* conditions.

Due to obvious economic drivers, manure is rarely digested alone; on the contrary, energy crops such as maize, triticale and sorghum and, sometimes, agro-residues are fed to digesters in order to increase the volatile solid (VS) content and then biogas production (higher methane yields). AD plants formally proposed in Northern Italy in the last months are several and they are all characterised by high crop/manure ratios within the mixture to be digested, (crops sometimes represent more than 50% of the feedstock).

As previously mentioned, within anaerobic digesters, nitrogen contained in the primary mixture is not removed and almost the same amount can be found in the digested material, under different forms: as a matter of fact, a large part of nitrogen contained in proteins is hydrolyzed to ammonium ion (NH₄⁺) and dissolved ammonia (NH₃) that can be volatilized; an increase in pH, NH₃ concentration and temperature, 3 conditions that do occur after anaerobic digestion, enhance ammonia emissions during storage and after field application. Moreover, nitrogen content of the mixture to be digested is strongly increased by the use of energy crops (for example, maize silage contain 4.3 kg N/ton of FM)

This way, the nitrogen amount to be managed along with digested materials can be strongly larger than that in primary manure and it is surely more suitable for volatilization.

Based on reliable emission factors and international studies (CORINAIR, IPCC and IPPC BAT reference documents, Italian experimental results and so on) it is possible to assess that 34 ±11% of nitrogen contained in the storage is emitted as NH₃-N from the storage and land-spreading (almost 15% from the land-spreading) of fresh animal manure. This amount could be strongly enhanced by chemical-physical conditions induced by digestion; as a matter of fact, according to different crop/manure ratios, ammonia emissions can be much larger than those from fresh manure, up to three times when manure represents just one third of the mixture to be digested.

As far as energetic scenarios at the regional scale are concerned, in the case we decide to send 10% of manure produced in the Piedmont region (1300 kt/y) to AD together with the same amount of energy crop (maize), 531 GWh_{el} could be produced but ammonia emissions would show an increase around 2300 t/y and more than 700 t NO_x/y would be emitted from the engine, that corresponds to a huge neo-formation potential of more than 2000 t/y of PM₁₀ (or, more correctly, PM_{2.5}). These data can be also seen as a specific emission of secondary particulates around 4 g/kWh_{el} due to energy production from AD, whereas the average secondary PM emission factor for the Italian national power system (SO₂: 0,67 g/kWh_{el}; NO_x: 0,523 g/kWh_{el}; PM: 0,024 g/kWh_{el}) is 0,85 g/kWh_{el}. As obvious, the reported figures refer to plants without any ammonia abatement devices, that are not generally planned for new installations. The large amount of ammonia release could be strongly reduced by employing stripping-absorbing towers for digested materials

(H₂SO₄ solutions are usually applied as absorbents in order to obtain a fertilising by-product that could be sold); alternatively, the storage tank could be covered (a solid cover should be implemented because straw covers or natural crusts could be less effective in reducing NH₃ emissions and have the potential to increase GHG emissions [11]) and Best Available Techniques to the land spreading of digestates (immediate incorporation, use of deep injectors) should be applied. On the other hand, NO_x emissions could be largely reduced by Selective Catalytic Reduction (up to 90%), but the technical feasibility of this solution depends on the poisoning potential of waste gas and the purification possibilities.

As far as greenhouse gases balances are concerned, 0,0032±0,0012 kg N₂O-N/kg excreted N are expected to be emitted from the storage of fresh manure; moreover, an indirect N₂O should be considered, dealing with volatilised nitrogen: the proposed emission factor is 0.01 kg N₂O-N/(kg NH₃-N + NO_x-N volatilised).

Another environmental aspect that should be analysed when dealing with anaerobic digestion is the post-methanation potential, that is the uncontrolled emission of methane from the storage of digested materials. As a matter of fact, the post-methanation somehow depends on the volatile solid content of the slurry and it is well known that the VS removal efficiency of AD is never 100%; on the contrary VS conversion to biogas is for the most part a function of the biodegradability of the primary mixture to be digested and the dimension of the digester through the hydraulic retention time (HRT). Based on several experimental data, the VS removal efficiency is often lower than 50%.

This way, taking into account the VS content in the digested material that sometimes can be remarkable (more than 50% of the original quantity) on the one hand, given the temperature of digested materials, the presence of specialized anaerobic biomass coming from the digesters and the long time at disposal for the storage (even more than 100 days) on the other hand, the post-methanation could represent a considerable emission.

Some authors [12] report that “typically 5-15% of the total biogas produced can be obtained from post-methanation of residues” while the CROPGEN project [13] inform that up to 12-31% of total methane production can be recovered from post-methanation of digestates. The post-methanation potentials measured within the CROPGEN project for digestates incubated for 100 days at 5, 20 and 35°C were 1-9, 73-120, 133-197 l CH₄/kg VS respectively. As far as the mentioned project is concerned, the post-methanation potential doesn't change during feeding regimes with 30-40% of crops in the feedstock. Other studies [14] report post-methanation potentials of 160-210 at 35-55°C, 53-87 at 15-20 °C and 26 l CH₄/kg VS at 10°C for a storage of 250 days.

In order to develop proper GHG balances around the technical choice of anaerobically digesting manure and

crops, a post-methanation potential of 50 l CH₄/kg VS and a VS removal efficiency of 50% can be used to calculate the indirect GHG emissions from the storage of digested materials. As far as GHG emissions from untreated manure are concerned, the emission factors proposed by IPCC can be considered a good reference: for a mixture of swine and dairy cattle manure and a climate between cool and temperate, an emission around 4 kg CH₄/t of manure can be expected.

As pointed out by Figure 1, co-digestion of manure and energy crops (when energy crops represent from 30 to 70% of feedstock), causes indirect GHG emissions that nullify the “energy bonus” due to CO₂ avoided emissions [15]: based on our assumption the indirect emissions of GHG can be quantified as 400 ± 67 g CO₂eq/kWh_{el}, mainly due to CH₄ releases from the storage of digestate, that is comparable to the Italian average CO₂ emission factor for energy production (496 g CO₂/kWh_{el}): the reported figure represent the average value for three different post-methanation models. Furthermore, it should be said that the proposed balances neglect the emissions of CH₄ and N₂O from the biogas engine, as well as CO₂eq emissions relating to cultivation and transport of energy crops; these contributions would even worsen the reported GHG balances. This way, in the case energy bonus, that is strongly economically propelled, is cancelled by uncontrolled GHG released, the renewable energy mission of AD would be betrayed.

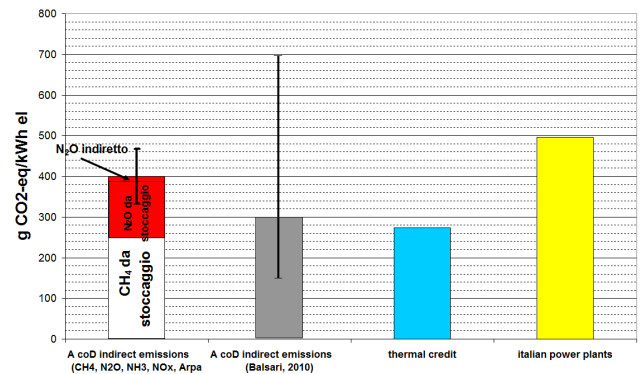


Figure 1. Indirect GHG emissions for Anaerobic coDigestion and thermal credit due to cogeneration

The negative impacts of indirect emissions from co-digestion of manure and energy crop are confirmed by some recent studies [16] and [17]; the first presentation points out a range from 150 to 700 g CO₂eq/kWh_{el} for AD (the higher value corresponds to co-digestion of manure and energy crops and it is mainly due to production and transport of biomass), while the second author reports (personal communication) that “in extreme cases (open storage of digestate and low HRT) the CO₂eq balance can reach levels of 600–700 g CO₂eq/kWh_{el}, that means: biogas production

causes the same GHG emissions as German conventional electricity production”.

As one can easily observe from the mentioned data, energy production from AD could have a negative meaning as far as sustainability aspects are concerned. As obvious, the solution can be technological as higher HRT, thermophilic digestion regimes, gas-tight storage of digestates (and combustion of released methane in the biogas engine) and thermal oxidation of waste gas from the engine can strongly reduce methane indirect emissions. Moreover, cogeneration of thermal energy can save up to 300 g CO₂eq/kWh_{th}, as showed by Figure 1, improving GHG overall balance.

V. ENERGY-CROPS AND MANURE AVAILABILITY FOR THE PROVINCE OF CUNEO, ENERGY PRODUCTION SCENARIOS

The Province of Cuneo is characterized by intensive livestock farming, more than 428.000 cattles and 824.000 swines, producing a huge amount of manure, around 8 millions tons per year. In the same area, 50.000 ha are destined to maize cultivation (173.000 in the Piedmont Region) and 30.000 ha (130.000 in the Region) to other cereals (wheat, sorghum, triticum). Based on the average producibility, the last regional planning on renewable energies (DGR 28/09/2009 n. 30-12221 “Relazione Programmatica dell’Energia della Regione Piemonte”) stated that up to 5% of cultivated fields could be used to produce energy crops, that is more or less 478.000 t/y of maize and 198.000 t/y of other cereals, still remaining within an environmentally and socio-economic sustainable context. That is to say that 200.000 t/y of energy crops could be produced in the province of Cuneo in order to improve biogas and energy production by means of anaerobic codigestion. In the following Table 1, data on manure and energy crops yearly production, dry matter and volatile solids content of materials, biogas producibility and power are reported. It is important to observe that AD of all manure produced by the province could generate 80 MW_e, that is 12% of electricity consumption of the province would be provided.

Table 1. Potential energy production from anaerobic co-digestion of all manure produced in the Province of Cuneo and energy crops from 5% of cultivated fields

	Manure/Crops (t/y)	dm (w/w)	VS/dm	Biogas (Nm ³ /tVS)	MW th IN	MW el OUT	MW th OUT
Cattle: 428.088	5.295.449	18%	75%	350	150,70	60,28	47,47
Swine: 824.663	2.944.047	10%	80%	350	49,65	19,86	15,64
maize	150.000	34%	96%	700	20,64	8,26	6,50
cereals	50.000	30%	96%	650	5,64	2,25	1,78
					90,65	71,39	

At the same time 60 MW_{th} (the thermal consumption of fermentation process, 30 % of available heat, has been already subtracted) could be produced and destined to the

substitution of existing heating plants or some industrial use (drying of digestate, wood, cereals). In the case the choice is anaerobic co-digestion of all manure and energy crops according to the regional sustainability criteria, the produced electricity would be 91 MW (13,5% of total consumption) and 71 MW of extra thermal power.

As a matter of fact, on 31th December 2010, 28 biogas plants are regularly authorized in the Province of Cuneo; on the whole, the feedstock is formed by 150.000 t/y of cattle manure, 68.000 t/y of swine manure, 114.000 t/y of maize and 43.000 t/y of other cereals, as reported by Table 2. That is to say that energy crops represents 42% of the feedstock, and they are very close to the maximum quantities admitted by regional sustainability criteria. The electricity production corresponds to 1,5% of the total consumption of the Province; unfortunately, the thermal energy at disposal, almost 9 MW (73,8 GWh/y), is dispersed for the main part, just 20-30% being use for small district heating or drying plants.

Table 2. Authorized energy production from anaerobic co-digestion of manure and energy crops

	Manure/Crops (t/y)	dm (w/w)	VS/dm	Biogas (Nm ³ /tVS)	MW th IN	MW el OUT	MW th OUT
solid cattle manure	98.531,00	0,22	0,75	350	3,66	1,46	1,15
liquid cattle manure	51.003,33	0,10	0,75	350	0,86	0,34	0,27
swine manure	68.367,92	0,07	0,8	350	0,86	0,34	0,27
maize	107.988,67	0,34	0,96	700	15,86	6,34	5,00
triticum	25.972,50	0,3	0,95	650	3,09	1,24	0,97
sorghum	15.020,83	0,26	0,96	650	1,57	0,63	0,49
ryegrass	1.750,00	0,26	0,96	650	0,18	0,07	0,06
pigswill	5.925,00	0,72	0,96	700	1,83	0,73	0,58
maize grains	341,67	0,72	0,96	700	0,11	0,04	0,03
						11,21	8,83

VI. GREENHOUSE GASES BALANCE

In order to estimate the possible CO₂ benefits arising from renewable energy plants it must be considered that, on the basis of the emission inventory for the Province of Cuneo (year 2006), agriculture and livestock farming represents 18% of total CO₂eq emissions of the Province.

In the case all manure of the Province is digested together with 200.000 t/y of energy crops (scenario in Table 1), assuming that all available thermal energy is used to displace existing heating plants (fuelled by natural gas for 70% and gasoil for 30%), that is optimal CHP, the benefit in terms of avoided CO₂ eq is quantified by Table 4. the results lies on the following assumptions:

1. electricity production: 496 g CO₂/kWh_e;
2. replaced heating plants: 55 kg CO₂/GJ for natural gas, 74 kg CO₂/GJ for gasoil;
3. 10314 t CH₄/y from traditional manure management are avoided;

4. post-methanation potential from the storage of digested materials: 5% of produced biogas (192 g CO₂ eq/kWhe);
5. GWP: 25 for methane, 298 for N₂O;
6. enhancement of ammonia volatilisation due to AD is neglected.

The reported figures comprehend the indirect N₂O emissions due to nitrogen oxides and ammonia emissions (calculated in the next chapter): if we use the overall factor suggested by Balsari [18] for AD without energy crops (250 g CO₂ eq/kWh_e), the results would be very similar (total avoided: -621.017 t CO₂ eq/y). The reported data outline that the described energy scenario would save 50% of the whole GHG emissions from agriculture, 10% of all CO₂ eq emissions of the Province. This would be an extraordinary result as far as CO₂ saving targets at 2020 are concerned (17% of final energy consumption has to be provided by renewables). The calculated CO₂ benefit could be even better (up to - 818.328 t CO₂ eq/y) in the case post-methane is recovered by means of gas-tight storage tanks.

Table 3. Avoided GHG emissions for Table 1 scenario

	t CO ₂ eq/y
avoided emission from electricity production	-393.877
avoided emission from CHP	-170.817
avoided emission from traditional manure management	-257.850
Indirect emission from anaerobic digestion	+185.299
Avoided CO₂ eq (TOTAL)	-637.245

On the contrary, the actual biogas plant authorized configuration (Table 2) would give the results showed by Table 4. In this case, the further assumptions are:

1. replaced heating plants: only 25% of the available thermal energy is used to replace natural gas and gasoil boilers (70 and 30 % respectively);
2. 258 t CH₄/y from traditional manure management are avoided;
3. indirect emissions for anaerobic co-digestion: 600 g CO₂ eq/kWhe [18];
4. enhancement of ammonia volatilisation due to AD is neglected.

In the actual conditions, biogas plant are not able to give any environmental advantage at the global scale (the balance is very close to break even) because the energy bonus due to the production of renewable energy is compensated by strong indirect GHG emissions and cogenerated thermal energy is not used in an effective way. The calculated results are confirmed by [19] that reported an indirect GHG emissions of 542 g CO₂ eq/kWh_e for a feedstock 50:50 manure/energy crops.

Table 4. Avoided GHG emissions for authorized scenario

	t CO ₂ eq/y
avoided emission from electricity production	-45.584
avoided emission from CHP	-4.942
avoided emission from traditional manure management	-6.460
Indirect emission from anaerobic digestion	+55.142
Avoided CO₂ eq (TOTAL)	-1.844

VII. ENVIRONMENTAL COMPATIBILITY AT THE LOCAL SCALE

The environmental balance carried out in the previous chapter for GHG at the global scale should be enlarged to comprehend also criteria pollutants that are very important at the local and regional extent. The following Tables 5 and 6 reports the total emissions dealing with the described energy scenarios for NO_x, PM₁₀, NH₃ and SO_x.

Table 5. Criteria pollutants balance for Table 1 scenario

	t NO _x /y	t SO _x /y	t PM ₁₀ /y	t NH ₃ /y	t N ₂ O/y
avoided emission from electricity production	-415	-532	-19	0	0
avoided emission from CHP	-155	-107	-7	0	0
avoided emission from traditional manure management	0	0	0	-12.659	-354
Indirect emission from anaerobic digestion	+953	0	0	+12.990	+362
Avoided emission (TOTAL)	+382	-639	-26	+330	+8

As one can easily observe, the emissive balance is not positive for both the analysed scenarios. In the case of the "sustainable configuration" (Table 1), NO_x emissions at the local scale (+ 953 t/y) are not totally compensated by avoided emissions due to electricity production and cogeneration and the increase of ammonia releases is around 330 t/y: the overall balance in terms of secondary particles (based on aerosol formation factors reported in the previous chapter) outlines an increase of 177 t PM₁₀/y. As far as the authorized plant configuration is concerned, the balance is even worse, + 196 t PM₁₀/y, mainly relating to additional ammonia emissions (+ 275 t/y) due to the use of large quantities of energy crops. Moreover, it should be remembered that in the latter configuration, a strong increase of nitrogen content (880 t N/y → 1.546 t N/y) has to be faced when managing digested materials, according to the limits of land spreading (170-340 kg N/ha) while in the sustainable scenario, where manure represents 98% of the feedstock, the increase of nitrogen to be managed along with digestate would be negligible (30.663 t N/y → 31.463 t N/y).

Table 6. Criteria pollutants balance for authorized scenario

	t NO _x /y	t SO _x /y	t PM ₁₀ /y	t NH ₃ /y
avoided emission from electricity production	-48	-62	-2	0

avoided emission from CHP	-4	-3	0	0
avoided emission from traditional manure management	0	0	0	-363
Indirect emission from anaerobic digestion	+118	0	0	+638
Avoided emission (TOTAL)	+65	-65	-3	+275

VIII. CONCLUSIONS

Renewable energy plants are strongly encouraged by European legislation but their effect on air quality and their sustainability in terms of CO₂ emissions, in particular for biogas plants, could be negative, specifically for compromised areas such as Northern Italy. The analysed energy scenarios for the Province of Cuneo point out that, in order to obtain benefits in terms of CO₂, energy crops should be avoided in favour of manure and agricultural waste products, thermal energy cogenerated by anaerobic digestion plants should be totally recovered to replace existing heating plants and the post-methanation production should be exploited. These conditions can help achieving CO₂ targets at 2020 but are not enough to ensure a positive or neutral emissive balance at the local scale, that is a condition of primary importance in northern Italy. To this end, NO_x emissions from the internal combustion engine should be minimized by means of SCR, cogeneration of thermal energy maximized and digestate nitrogen content should be properly treated in order to reduce ammonia emissions (covered storage tank, immediate incorporation/use of deep injectors for land-spreading) and/or produce a fertilizer (stripping-absorbing towers, dryers and/or evaporators) to be used in a more effective way if compared to traditional manure or digested materials. It is important to note that these conclusions are directed to the specific high criticality conditions of Province of Cuneo and North of Italy, but their qualitative meaning can also be extrapolated to other European situations of similar agro – industrial economy. A promising alternative solution that could ensure better environmental compatibility to AD is the production of biomethane by means of upgraded biogas. This solution could be very expensive in terms of gas purification chiefly, the advantages in terms of economic benefits from renewable energy production (green certificates) should be lost, but a better global environmental balance could be obtained, and a local emission impact should be avoided.

REFERENCES

- [1] Martina Poschl, Shane Ward, and Philip Owende, "Evaluation of energy efficiency of various biogas production and utilization pathways", *Applied Energy* 87 (2010), pp. 3305–3321;
- [2] Pal Borjesson and Maria Berglund, "Environmental systems analysis of biogas systems – Part II: The environmental impact of replacing various reference systems", *Biomass and Bioenergy* 31 (2007), pp. 326 – 344;
- [3] Colin Jury, Enrico Benetto, Daniel Koster, Bianca Schmitt, and Joelle Welfring, "Life Cycle Assessment of biogas production by monofermentation of energy crops and injection into the natural gas grid", *Biomass and Bioenergy* 34 (2010), pp. 54 – 66;
- [4] A. Lehtomaki, S. Huttunen, and J.A. Rintala, "Laboratory investigations on co-digestion of energy crops and crop residues with cow manure for methane production: Effect of crop to manure ratio", *Resources, Conservation and Recycling* 51 (2007), pp. 591 – 609;
- [5] Pornpan Panichnumsin, Anop Nopharatana, Birgitte Ahring, and Pawinee Chaiprasert, "Production of methane by co-digestion of cassava pulp with various concentrations of pig manure", *Biomass and Bioenergy* 34 (2010), pp. 1117 – 1124;
- [6] B. Schlamadinger, M. Apps, F. Bohlin, L. Gustavsson, G. Jungmeier, G. Marland, K. Pingoud, and I. Savolainen, "Towards a standard methodology for greenhouse gas balances of bioenergy systems in comparison with fossil energy systems", *Biomass and Bioenergy* 13 (1997), pp. 359 – 375;
- [7] Cinzia Buratti and Francesco Fantozzi, "Life cycle assessment of biomass production: Development of a methodology to improve the environmental indicators and testing with fiber sorghum energy crop", *Biomass and Bioenergy* 34 (2010), pp. 1513 – 1522;
- [8] Francesco Cherubini, "GHG balances of bioenergy systems – Overview of key steps in the production chain and methodological concerns", *Renewable Energy* 35 (2010), pp. 1565 – 1573;
- [9] M. Giugliano and G. Lonati, "Polveri fini in atmosfera: la componente secondaria", *Energia* 3/2005, July 2005;
- [10] F. De Leeuw, "A set of emission indicators for longrange transboundary air pollution", *Environmental Science & Policy* 5 (2002), pp. 135-145;
- [11] B. Amon, V. Kryvoruchko, and T. Amon, "Influence of different methods of covering slurry stores on greenhouse gas and ammonia emissions", *International Congress Series* 1293 (2006), pp. 315–318;
- [12] P. Weiland, "Production and energetic use of biogas from energy crops and wastes in Germany", *Applied Biochemical Biotechnology* 109 (2003), pp. 263–274;
- [13] Renewable energy from crops and agrowastes, CROPPGEN Project, D17: Database on the methane production potential from mixed digestion;
- [14] P.L.N. Kaparaju and J.A. Rintala, "Effects of temperature on postmethanation of digested dairy cow manure in a farm-scale biogas production system", *Environmental Technology* 24 (2003), pp. 1315–1321;
- [15] E. Brizio and G. Genon, Environmental compatibility of renewable energy plants, AIR POLLUTION XVIII, Wessex Institute of Technology Press, pp. 149-159;
- [16] Paolo Balsari – "incontro di lavoro sui risultati conclusivi del progetto PROBIO-BIOGAS" – 13 dicembre 2010;
- [17] A. Gronauer, Comparison of different technologies: the road to success, Conference Anaerobic Digestion: opportunities for agriculture and environment. Regione Lombardia, from the web, last access 12 January 2011;
- [18] Paolo Balsari and Simona Menardo – "Vantaggi dei pre-trattamenti delle biomasse in ingresso al digestore" – Distretto Energetica Torino, 28 aprile 2010;
- [19] Marco Cibrario final tesi – "Sostenibilità ambientale delle filiere bio-energetiche dedicate: analisi degli impatti relativi alla digestione anaerobica delle colture energetiche con metodologia LCA" – Politecnico di Torino, 2010.

Development of Complex Technologies for Biomass Processing

Konstantin Latinin
International Science and Technology Center
Moscow, Russia
e-mail: latynin@istc.ru

Vladimir Sinelshchikov, Victor Zaichenko
Joint Institute for High Temperatures of Russian
Academy of Sciences
Moscow, Russia
e-mail: zaitch@oivtran.ru

Abstract—There are presented two technologies of biomass processing. One technology is concerned with manufacture of hydrogen and pure carbon materials. It based on the process of heterogeneous pyrolysis of gaseous hydrocarbons during filtration through porous medium. As a porous material it is suggested to apply a charcoal formed as a result of thermal processing of biomass (wood, peat and agricultural waste). The advantages of this technology are the waste-less character of biomass processing and wide range of the end products. Another technology is a technology of conversion of biomass into synthesis gas. The experimental data on quantity and composition of the gaseous products formed in the process of thermal treatment of wood and peat are presented. It is shown that as a result of peat and wood pyrolysis and the subsequent cracking of emanating products at temperature 1000 °C it is possible to produce about 1.4 m³ of gas with calorific value 11.7 MJ/m³ from one kg of original raw material.

Keywords- biomass, pyrolysis, pyrocarbon, syngas, hydrogen

I. INTRODUCTION

Today utilization of biomass for power engineering in most cases is more expensive, than use of traditional fossil fuels. As a result a biomass can be competitive in the market of power resources only under the condition of state budgetary support. Under the global financial and economic crisis a budgetary support becomes problematic.

In present conditions, any scientific and technical activity in the field of energy supply should be based on two basic principles:

- full-scale mutually beneficial international cooperation;
- attractiveness of developing technologies to investors both from the economic and ecological points of view.

The first principle will provide for integration of experimental possibilities and intellectual efforts of specialists from different countries. Such integration will be the guarantor of the common successes. Practical realization of the second principle can be successful only at complex processing of a biomass with production of a wide range of the commodity output which are in popular demand in the market, namely: gaseous and liquid fuels, including hydrogen, and also carbon materials with predetermined properties – active carbon, coke, pyrocarbon.

The role of Russia in the development of the international cooperation should be considerable as there is concentrated about 42 % of peat and about 23 % of wood world reserves in Russia. Use of peat and wood waste does not demand

preliminary expenses for biomass growing, soil recultivation and other nonproduction expenses. The level of scientific and technical workings in Russia gives opportunity to hope for development of economically justified technologies of biomass utilization for power engineering. Application of biomass complex processing technologies which are developing today in Russia will allow to satisfy the requirements of Russian and partially international markets in ecologically clean fuels. Now Russia one of the main supplier of the fossil fuels on the foreign market and in the future it can make the essential contribution to formation of biofuel market and can become one of the major biofuel exporter.

Technologies of complex thermal biomass processing developed in Joint Institute for High Temperatures of Russian Academy of Sciences (JIHT) are stated below. Both technologies are based on pyrolysis of such raw materials as wood and peat and agricultural waste. Distinction between these technologies consists in the end products which can be obtained. One technology is the technology of complex processing of biomass with production of technical hydrogen and pure carbon materials [1, 2] and another is the wasteless technology of biomass processing with production of high-calorific gas fuel [3].

The main features of technologies under consideration, characteristics of end products and results of experimental investigations substantiating these technologies are presented and discussed.

II. PRODUCTION OF CARBON COMPOSITE AND TECHNICAL HYDROGEN

At the first stage of the technology for production of pure carbon materials and technical hydrogen a raw material (peat, wood or agricultural waste) are heated approximately to a temperature of 600 °C in a gas medium free of oxygen. As a result there is produced a charcoal which is a brittle porous material with the carbon content exceeding 90%. At the second stage a gaseous hydrocarbon is blown through the charcoal bed heated up to the temperature about 1000 °C. For these purpose natural gas, oil gas and waste burning gases of petrochemical manufactures can be used. Passing through the porous carbon structure formed at the first stage, gaseous hydrocarbons decompose into hydrogen and carbon which stuffs the porous carbon matrix and transforms it to a solid composite with carbon content up to 98 %. Carbon materials with such properties are in popular demand in the market.

Produced hydrogen may be used as a pure gas fuel for energy purpose. The both stages of the technology can be carried out in one device.

All methods of hydrogen production for power engineering existing now are not repaying and some financial support is need for its realization. The scheme stated above, when hydrogen production fulfilled simultaneously with the production of pure carbon materials, is paying back, as the price of produced carbon materials covers all expenses for manufacture of hydrogen and its subsequent power use.

The photo of pyrocarbon samples received with the help of the developed technology is presented in Figure 1.

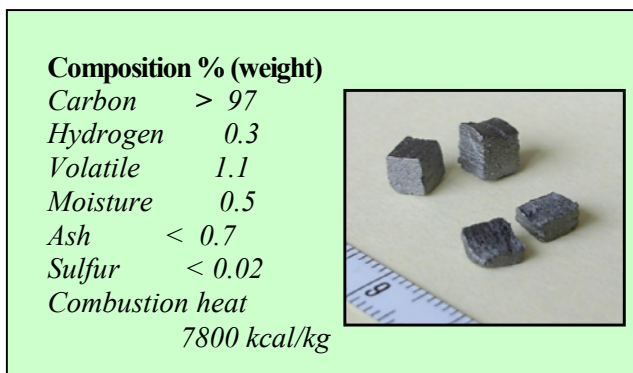


Figure 1. Samples of the carbon composite and their composition.

The results of porosity measurements give the opportunity to imagine a character of structure modification of a sample in process of the heterogeneous pyrolysis of gas hydrocarbons and its final internal structure. Figure 2 shows the time evolution of the volume fraction of open and closed pores of a charcoal sample [4]. One can see that the volume fraction of open pores decreases and the volume fraction of closed pores increases in process of the methane pyrolysis. After 100 minutes the volume fraction of closed pores is practically constant. This fact indicates that after 100 minutes pyrolysis is in progress practically only on outer surface of

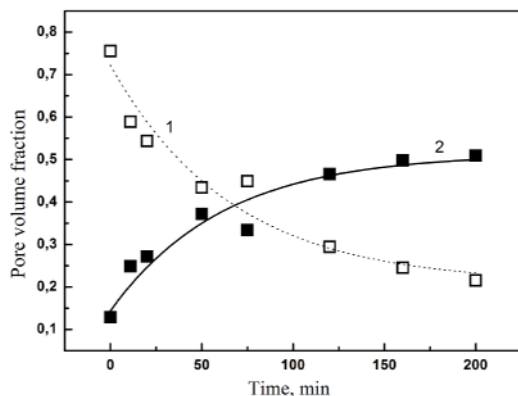


Figure 2. Change of open (1) and closed (2) pore volume fraction of wood char sample in process of methane pyrolysis.

the sample while internal pores become closed for methane diffusion though their volume fraction is about 50%.

The hydrogen content in gaseous products at the exit of reaction volume depends on the operation conditions and may reach 80 – 90 volume percents. The rest is not decomposed gaseous hydrocarbons.

III. PRODUCTION OF SYNGAS

The second technology of bioconversion is the technology of wasteless production of synthesis gas. Present day technologies of solid hydrocarbon raw materials conversion into gas can be divided on two basic groups: gasification and pyrolysis. During gasification the thermal decomposition of initial raw materials occurs in the oxidizing gas environment and the product gas contains combustion products of raw materials. At air gasification the product gas is also substantially diluted by nitrogen. As a result the combustion heat of gas mixtures produced at gasification usually does not exceed 6 MJ/m³ usually. Use of such low-calorific gas in the modern power units is ineffectively. Essential improvement of characteristics of power gas produced with the help of existing processes of biomass gasification cannot be received.

During pyrolysis the heating of initial raw materials occurs without oxidizer access. Pyrolysis products are char, noncondensable gases CO₂, CO, H₂, CH₄, C_nH_m, N₂ and volatiles. In cooling the volatiles form liquid fraction which consists of tar and pyrolyneous liquor. While pyrolysis makes it possible to produce gas mixtures with a calorific value up to 20 MJ/m³, the main demerits of the given method is the presence of the considerable carbon dioxide fraction (up to 30 % volume) in pyrolysis gases and rather low gas yield, which reaches 0.3-0.4 m³ per kg of initial raw materials at best. As a result the efficiency of energy conversion, determined as the ratio of the product gas thermal value to thermal value of initial raw materials, does not exceed 0.3. Thus, the main objective of technological advancement is an increase of conversion degree of initial raw materials into gas together with conservation of enough high specific combustion heat of product gas mixtures.

The technology of biomass (peat, wood and agricultural waste) thermal processing with production of high calorific power gas developed in the JIHT is based on high-temperature processing of the pyrolysis gases and volatiles. The method is similar to the one suggested in [5] for processing of wood sawdust and used in [3] for processing of wood waste and peat. It consists in filtration of volatiles and gases, forming by pyrolysis of initial raw materials, through the porous carbon bed kept at a fixed temperature T_f (further this regime is referred to as «pyrolysis with cracking»). As the carbon material (filter) the char obtained as a result of initial raw material carbonization was used. Due to the developed surface of the carbon filter there is a fast heating of volatiles and gases to the temperature T_f . As a result of homogeneous and heterogeneous chemical reactions in the high-temperature zone an intensive decomposition of pyrolysis gases and volatiles takes place. The conversion degree depends both on the temperature T_f and the interaction time of volatile products with heated

carbon surface. As follows from the data presented in Figure 3 the increase in the char filter temperature T_f leads to essential increase in the yield of gaseous products (T_c – current temperature of processed raw material, heating rate – $10\text{ }^\circ\text{C}/\text{min}$).

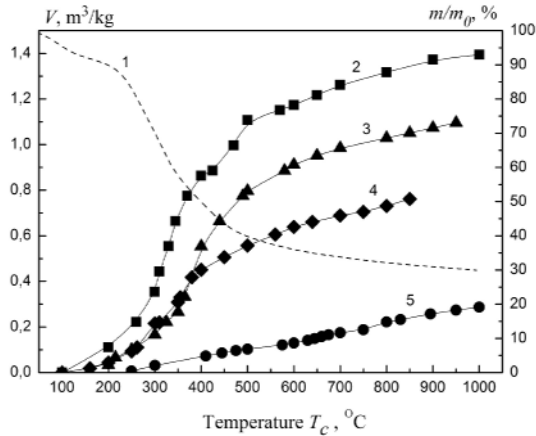


Figure 3. Change in relative mass of raw material (1) and volume gas yield per one kg of raw material (2-5) in heating of peat pellets: regime «pyrolysis with cracking» at $T_f = 1000\text{ }^\circ\text{C}$ – 2, $950\text{ }^\circ\text{C}$ – 3, $850\text{ }^\circ\text{C}$ – 4; regime «pyrolysis» – 5.

Simultaneously with the growth of gas yield the reduction of quantity of the liquid fraction in the end products is observed. For the temperature $T_f = 1000\text{ }^\circ\text{C}$ there is no liquid fraction that is evidence of full tar and pyrolygneous liquor conversion into gas. Thus during the filtration through the char filter decomposition of the volatiles, forming in process of thermal destruction of raw material and condensing as a tar, takes place. In addition interaction of pyrolytic water with char leads to generation of hydrogen and carbon monoxide.

Change of operating parameters results in change of product gas composition. From results of chromatographic analysis it is follows that carbon dioxide and methane content in the product gas decreases with the rise of the char filter temperature T_f . Composition, specific combustion heat and volume of gas mixture produced from peat and wood are presented in Table I and II. For temperature $T_f = 1000\text{ }^\circ\text{C}$ the content of carbon dioxide and methane does not exceed one percent. An increase of the char filter temperature leads to raise the rate of disoxidation of CO_2 and the rate of heterogeneous pyrolysis of methane and other paraffin hydrocarbons. As a result at $T_f = 1000\text{ }^\circ\text{C}$ the product gas mixture consists of CO and H_2 in practically equal parts.

From comparison of the Tables I and II data one can see that the specific combustion heat of gas mixtures produced at different operating conditions are rather close to each other. One of the main advantages of the «pyrolysis with cracking» regime is a considerable increase of the volume gas yield and, as a consequence, a rise in the degree of conversion of biomass into gas.

TABLE I. COMPOSITION, SPECIFIC COMBUSTION HEAT AND VOLUME OF PRODUCT GAS PRODUCED FROM ONE KG PEAT PELLETS

$T_f, \text{ }^\circ\text{C}$	Volume, m^3/kg	Volume fractions of combustible components			Combustion heat, MJ/m^3	
		H_2	CO	C_nH_m	Q_H	Q_L
850	0.76	0.40	0.27	0.08	11.7	10.6
950	1.1	0.43	0.40	0.02	11.3	10.4
1000	1.39	0.49	0.41	0.01	11.7	10.6
Pyrolysis	0.29	0.23	0.19	0.13	10.4	9.6

TABLE II. COMPOSITION, SPECIFIC COMBUSTION HEAT AND VOLUME OF PRODUCT GAS PRODUCED FROM ONE KG WOOD PELLETS

$T_f, \text{ }^\circ\text{C}$	Volume, m^3/kg	Volume fractions of combustible components			Combustion heat, MJ/m^3	
		H_2	CO	C_nH_m	Q_H	Q_L
850	0.83	0.39	0.28	0.10	12.5	11.5
950	1.24	0.47	0.41	0.01	11.5	10.6
1000	1.39	0.46	0.46	0.00	11.7	10.9
Pyrolysis	0.26	0.28	0.26	0.16	13.2	12.1

Change of the gas calorific value at reactor output in process of raw material heating (rate – $10\text{ }^\circ\text{C}/\text{min}$) is presented in Figure 4. As one can see from Figure 4, in the «pyrolysis» regime the calorific value of output gas at temperature of processed raw material above $550\text{ }^\circ\text{C}$ is higher than the calorific value of output gas in the «pyrolysis with cracking» regime. However the calorific value of output gas in the «pyrolysis» regime is strongly changes in process of raw material heating.

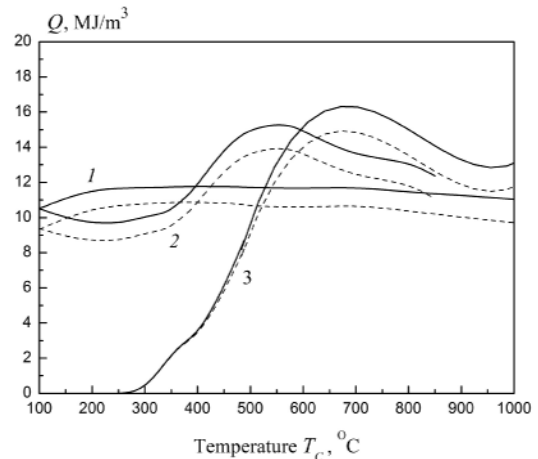


Figure 4. High (solid line) and low (dash line) calorific values of output pyrolysis gas vs. temperature of raw material (peat pellets) in different regimes of thermal processing: «pyrolysis with cracking» at $T_f = 1000\text{ }^\circ\text{C}$ – 1, $850\text{ }^\circ\text{C}$ – 2; «pyrolysis» – 3.

As appears from comparison of the dependences presented in Figure 4, in the «pyrolysis with cracking» regime an increase of the temperature T_f depresses a temperature influence on the calorific value of output gas.

As mentioned above at $T_f = 1000\text{ }^{\circ}\text{C}$ the output gas is a mixture of CO and H₂. Relation between volume fractions of this components in temperature range $T_c = 250 - 500\text{ }^{\circ}\text{C}$ (that is in the range of main gas release) does not change practically. As consequence the calorific value of output gas does not depend on the temperature of processed raw material. This circumstance is rather important from the point of view of the subsequent usage of product gas mixtures, for example, as a fuel for power plant on the base of internal combustion engine.

The ratio of thermal value of gas obtained by thermal processing of one kg of the raw material to calorific value of one kg of the utilized raw material is about 0.7 – 0.8. Significant advantage of suggested technology is the absence of liquid fraction in the end products. Such gas mixture can be used as a gas fuel for power unit on the base of gas piston engine. Burning of the gaseous fuel produced from biomass raw materials by developed technology can be carried out without reconstruction of the existing gas-fired power equipment while the direct use of wood waste or peat (for example, peat or wood pellets) requires considerable structural modifications of the existing power installations meant for electricity generation.

IV. CONCLUSION

1. The technology of manufacture of carbon materials and hydrogen based on the process of heterogeneous pyrolysis of gaseous hydrocarbons during filtration through porous structure formed as a result of thermal decomposition of biomass are presented. The carbon material produced by the developed technology may be used as a high calorific solid fuel and as a raw material for various industries, for example, metallurgy. The gaseous mixture at the exit of reaction volume contains hydrogen which concentration may be easily varied by change in operating parameters and may reach 90 volume percents. Natural gas of low-pressure gas fields, oil gas and waste hydrocarbon gases of petrochemical manufacture can be used as gaseous raw material for this technology.

2. It is shown that the mixed technology of thermal processing of different kinds of biomass, involving the stage of pyrolysis and the subsequent cracking of volatile products by their filtration through charcoal, it is possible to increase the efficiency of energy conversion of biomass into gas by several times. At the charcoal temperature $1000\text{ }^{\circ}\text{C}$ and given residence time it is possible to produce about 1.4 m^3 of gas with specific combustion heat about 11.7 MJ/m^3 per one kg of original raw material. The produced gas mixture consists generally of carbon oxide and hydrogen.

ACKNOWLEDGMENT

This work has been supported by Russian Foundation for Basic Research grant No. 10 – 08 – 005551.

REFERENCES

- [1] V.M. Zaichenko, E.E. Shpil'rain, and V.Ya. Shterenberg, "Integrated Processing of Natural Gas to Obtain Hydrogen for Power Engineering and Carbon Materials for General Use in Industry", *Thermal Engineering*, No. 3, 2006, pp. 217-223.
- [2] V.M. Zaichenko, V.V. Kosov, V.F. Kosov, V.A. Sinelshchikov, and G.F. Sokol, "Experimental Feasibility Study of Technology for Integrated Processing of Wood Waste and Natural Gas", *Thermal Engineering*, No. 7, 2008, pp. 587-593.
- [3] V.V. Kosov, V.F. Kosov, I.L. Maikov, V.A. Sinelshchikov, and V.M. Zaichenko, "High-calorific Gas Mixtures Produced by Pyrolysis of Wood and Peat", *Proc. of 17th European Biomass Conference and Exhibition*, Hamburg, Germany, 2009, pp. 1085-1088.
- [4] V.F. Kosov, V.A. Sinelshchikov, and V.M. Zaichenko, "New Technology for Integrated Processing of Biomass and Natural Gas with Production of Hydrogen and Pure Carbon Materials", *Proc. of 16th European Biomass Conference and Exhibition*, Valencia, Spain, 2008, pp. 1171 – 1175.
- [5] Snehalatha K Chembukulam, Arunkumar S. Dandge, Narasimhan L. Kovilur, Rao K. Seshagiri, and R. Vaidyeswaran, "Smokeless Fuel from Carbonized Sawdust", *Ind. Eng. Chem. Prod. Res. Dev.*, vol. 20, 1981, pp. 714-719.

CO₂ Emission Reduction from Sustainable Energy Systems: Benefits and Limits of Distributed Multi-Generation

Pierluigi Mancarella

Department of Electrical and Electronic Engineering
Imperial College London
Exhibition Road, SW7 2AZ, London, UK
e-mail: p.mancarella@imperial.ac.uk

Gianfranco Chicco

Dipartimento di Ingegneria Elettrica
Politecnico di Torino
Corso Duca degli Abruzzi 24, 10120, Torino, Italy
e-mail: gianfranco.chicco@polito.it

Abstract — The struggle to decarbonise future power systems is boosting the diffusion of high-efficiency distributed multi-generation (DMG) systems. In this respect, small-scale (below 5 MW_e) cogeneration systems for producing heat and power, as well as trigeneration systems for additional production of cooling, could play a key role. In this paper, a general analytical model for assessing the potential CO₂ emission reduction from DMG systems, in case coupled to heat/cooling networks, is presented. Different available solutions are analysed. Numerical applications make reference to typical emission intensity figures in Europe. The results show that the emission reduction potential is primarily a function of the electrical efficiency and therefore of the size, and is strongly affected by the baseline comparative references. The environmental benefits decrease if part of cogenerated heat is used to generate cooling power with single-effect absorption chillers or adsorption chillers.

Keywords - cogeneration, distributed generation, emission reduction, heat networks, trigeneration.

NOMENCLATURE

CHP	Combined Heat and Power
CCHP	Combined Cooling Heat and Power
DHN	District Heating Network
DMG	Distributed Multi-Generation
ICE	Internal Combustion Engine
MT	Microturbine
SE	Stirling Engine
SP	Separate Production
TCO _{2ER}	Trigeneration CO ₂ Emission Reduction
WAC	Water Absorption/Adsorption Chiller

I. INTRODUCTION

The evolution of power systems is being deeply influenced by the growing need for cutting CO₂ emissions from energy generation. Combined Heat and Power (CHP) plants allow more efficient fuel energy input utilization with respect to classical Separate Production (SP) means in which electricity is generated in centralized power plants and heat in traditional boilers [1]. This enhanced overall efficiency can bring along CO₂ emission reduction, also depending on the fuel carbon content and on the emission intensity of the displaced sources. In the past, economy-of-scale factors limited the adoption of CHP plants to relatively large industrial users or District Heating Networks (DHN). Conversely, today various Distributed Generation (DG)

technologies, potentially clustered within micro-grids [2] and mostly fuelled on natural gas, are available for local exploitation of cogenerated heat at different capacities. In particular, on a small-scale level (up to 5 MW_e) mature CHP prime movers include Stirling Engines (SE, available for micro-CHP applications in single dwellings, typically up to 10 kW_e) [3][4], Microturbines (MT, in the capacity range 30-300 kW_e), and Internal Combustion Engines (ICE, up to 5 MW_e) [4]. Heat networks may be needed to interconnect a set of possible users to a large prime mover, so as to establish an adequate overall thermal load.

As a further issue to be addressed, the profitability of CHP systems can be consistently affected by low thermal loads in the summertime, when the need for space heating is not present and only domestic hot water makes up the thermal demand. Hence, the CHP unit, sized on the basis of the winter thermal demand, could operate at partial load and often be switched off below a certain loading threshold, losing all or at least part of the benefits from cogeneration production. A spreading solution relies on the possibility of exploiting cogenerated heat for cooling production by means of Water Absorption or Adsorption Chillers (WAC) [5], leading to set up the so-called trigeneration or Combined Cooling Heat and Power (CCHP) plants [6]. Hence, in a CCHP plant, the CHP prime mover can be operated at high loading level also in the summertime, contributing to cover an air conditioning demand that is steadily rising even in the northern European countries. For larger plants, the DHN may be used for heat distribution and the WAC sited at the building user interfaces [5]. Smaller plants without heat networks adopt a centralized cooling plant sited close to the CHP system and to the user. Single or aggregated user typologies such as hotels, hospitals, restaurants, department stores, offices, banks, residential blocks are typical potential applications for trigeneration systems on various scales.

A CCHP plant is a particular case of the more general category of distributed multi-generation (DMG) systems [7] [8] enabling the dispatch of different types of energy and the conversion from one type of energy to another through suitably sized components, with possible other external networks for further exploitation of the energy products.

The authors have illustrated and discussed the DMG concepts and applications in recent references, following a research line developed to highlight the perspectives and assess the potential of DMG applications in terms of energy

efficiency improvement [9]-[12] and environmental impact reduction [13]-[16], up to the formulation of a unified approach to define structured indicators to quantify the technical and environmental performance of multi-generation systems [17].

The cost effectiveness of distributed CCHP systems, above all if coupled to DHN, requires thorough assessment. However, before running detailed economic analyses, simple and synthetic environmental models are needed to assess in which conditions and to which extent combined generation of multiple energy vectors can bring CO₂ emission reduction relative to the *status quo*. In this respect, in this paper the *Trigeneration CO₂ Emission Reduction (TCO₂ER)* indicator [18][19] is adopted to estimate the potential CO₂ emission saving characteristics from small-scale distributed trigeneration systems in different frameworks. The main objective is to formulate a simple analytical model, capable to highlight the parameters and variables involved in the analysis. The dependence of the emission reduction on the CCHP equipment efficiencies and on the emission intensities taken as reference for the conventional SP is investigated. Numerical applications are based on equipment currently available on the market and on the energy generation environment in Europe, with particular reference to the UK.

II. TRIGENERATION SYSTEM STRUCTURE AND PERFORMANCE INDICATORS

A. Structure, Components and Characteristics

A CCHP plant is composed of the combination of a CHP plant (with auxiliary boilers for thermal back-up and peak shaving, as well as, in case, thermal storage), and a cooling plant fed by cogenerated heat, with possible heat networks. The CCHP plant is further interconnected with the electrical distribution grid, to enable buying/selling electricity according to the rules for electricity provision (depending on the tariff system or electricity market structure).

Focusing on small-scale applications, we consider different types of technology, that is, SE, MT and ICE, all fed on natural gas. The WAC-based cooling plant can be composed of different technologies [6], to be suitably coupled to the CHP side. Single-effect absorption chillers, typically fired by hot water at around 90 °C, are considered in this paper for coupling to MT and ICE. Adsorption chillers, instead, may be fired by lower temperature sources and are available at capacities smaller than absorption chillers [5]; thus, they are adequate for combination with dwelling-sized SE. The CCHP system is usually electrically connected to the distribution network or to a microgrid.

B. Energy Performance Models for Trigeneration Equipment and Heat Networks

The energy performance of CHP prime movers can be synthetically described by means of the electrical efficiency η_w and the thermal efficiency η_Q . In addition, it is possible to characterize the CHP energy production in terms of heat-to-electricity cogeneration ratio λ_y [1]:

$$\eta_w = \frac{W_y}{F_y}, \quad \eta_Q = \frac{Q_y}{F_y}, \quad \lambda_y = \frac{Q_y}{W_y} = \frac{\eta_Q}{\eta_w} \quad (1)$$

The terms W , Q and F in (1) respectively denote electricity, heat and fuel thermal energy, while the subscript y points out cogeneration entries.

As for cooling generation equipment, the energy characteristics of a WAC are described by means of the *COP* (Coefficient Of Performance), ratio of the desired output (cooling energy R , in the form of chilled water for instance at 7 °C) to the input (heat Q_R in the form of cogenerated hot water) [5]:

$$COP = R/Q_R \quad (2)$$

All the above efficiencies depend upon the technology and upon several variables such as the loading level, the outdoor conditions, and so forth [4][5][20].

As far as heat networks are concerned, two types of losses are in general present, namely, heat losses Q_L due to heat transfer with the colder external environment, and parasitic electrical pumping losses W_L to overtake the hydraulic friction in the pipes. These loss contributions can be for instance expressed with respect to the cogenerated heat, as

$$\varepsilon_Q = Q_L/Q_y, \quad \varepsilon_W = W_L/Q_y = W_L/\lambda_y W_y \quad (3)$$

Typical values of percentage heat losses ε_Q range between 1% for small networks (few hundreds meters) to 10%-15% for large DHN (tens of kilometers). Typical percentage electrical parasitic losses ε_W due to pumping are of the order of 1% or even less for various applications [1][5].

C. CO₂ Emission Performance Models for Trigeneration Equipment

A consistent approach to evaluate the environmental performance of a trigeneration system by resorting to a system-orientated black-box representation is based on taking into account the mass of carbon dioxide involved in the exploitation of the energy system.

The mass m_X of CO₂ emitted to produce the *useful* energy output X can be worked out as $m_X = \mu_X \cdot X$, where μ_X is the CO₂ emission factor (specific emissions) related to the generic useful energy output X (e.g., electricity or heat). With very good approximation, it is possible to consider the emission factor μ_F related to the fuel thermal energy as a constant depending only upon the fuel carbon content and its Lower Heating Value (LHV). Hence, once given the fuel, the energy output-related emissions can be evaluated as a function of the device efficiency only, as [18][19]:

$$\mu_X = \mu_F / \eta_X \quad (4)$$

where η_X is the equivalent efficiency to produce the relevant energy output X from the fuel energy input F , as for instance

in (1) for CHP units. For natural gas, μ_F can be averagely assumed equal to 200 g/kWh_t, on a LHV basis [21].

III. ENVIRONMENTAL ASSESSMENT MODEL

A. General Trigeneration CO₂ Emission Reduction Assessment Model

In order to compare different energy generation alternatives, it is convenient to establish a reference scenario and to assess the various alternatives against this reference. For trigeneration systems, this can be carried out by introducing the *TCO2ER* indicator [18][19], expressing the relative reduction of the mass of carbon dioxide due to the use of a trigeneration system to displace the energy production needed to serve a certain energy output in the combined production of multiple energy vectors. From the conceptual framework used in cogeneration system analysis, the SP of electricity and heat comes from classical and standardized references (power generation system and boilers). It is however less immediate to identify the reference technology for SP of cooling. The authors in [9] introduced the assumption that the baseline technology reference for cooling power generation is an electric chiller, in turn supplied by the electrical network. Under this assumption, the *TCO2ER* indicator is expressed as

$$\begin{aligned} TCO2ER &= \frac{m_F^{SP} - m_F}{m_F^{SP}} = \\ &= 1 - \frac{\mu_F \cdot F_z}{\mu_W^{SP} \cdot (W_z + R_z / COP^{SP}) + \mu_Q^{SP} \cdot Q_z} \end{aligned} \quad (5)$$

The expression (5) applies to a general trigeneration plant with F_z as the energy fuel input and electricity W_z , heat Q_z , and cooling energy R_z as the threefold useful energy output. The subscript z points out net input-output entries for the overall plant. Setting $R_z = 0$ in (5) leads to cogeneration assessment as a sub-case. In terms of emission mass, m_F^{SP} is the CO₂ mass emitted by combustion of the fuel thermal input F^{SP} in order to produce the same amount of trigenerated energy in SP, while m_F is the CO₂ mass emitted by combustion of the CCHP fuel thermal input. The model (5) can also be extended to entail the presence of distribution

networks; in this case, the output entries are considered net of the distribution and parasitic losses. In terms of baseline references, the specific emissions μ_W^{SP} and μ_Q^{SP} represent the equivalent emission factors for SP, while μ_F refers to the CCHP fuel thermal input. Emissions from cooling generation are assessed through the reference electricity emissions, and considering an electric chiller with cooling-to-electricity efficiency equal to COP^{SP} . The emission factors and the chiller efficiency for SP are evaluated as conventional values. As such, they may be related to the underlying assumptions of the study, as illustrated in Section IV.

Positive *TCO2ER* values represent the existing convenience of adopting trigeneration to displace conventional energy generation in the supply of the corresponding energy demands. The maximum positive value of *TCO2ER* is unity (or 100%), ideally representing the adoption of a trigeneration system supplied by carbon dioxide-free fuel. Negative *TCO2ER* values (not limited in amplitude) indicate that introducing trigeneration to displace SP is not convenient.

B. Specific Energy System Model for CHP-WAC Trigeneration and Heat Network

A more specific formulation of the expression (5) is derived here for the CHP-DHN-WAC energy system under analysis. In this respect, let us consider the plant model in Figure 1, in which all the equipment and the relevant efficiencies are schematized as black-boxes. All the energy produced is assumed to be utilized. More specifically, the cogenerated electricity W_y coincides, net of the pumping losses for heat distribution, with the overall trigenerated electricity W_z , and goes to supply the local user or is injected into a local microgrid or the distribution network. The cogenerated heat Q_y , net of heat distribution losses, splits into two components, namely, Q_z corresponding to the net trigenerated heat output for direct thermal purposes (for instance, domestic hot water generation and space heating), and the other one to fire a WAC for generating the trigenerated cooling energy R_z . The “splitting variable” is indicated as α_R , and corresponds to the relative amount of cogenerated heat going to feed the WAC.

With reference to Figure 1, taking into account the

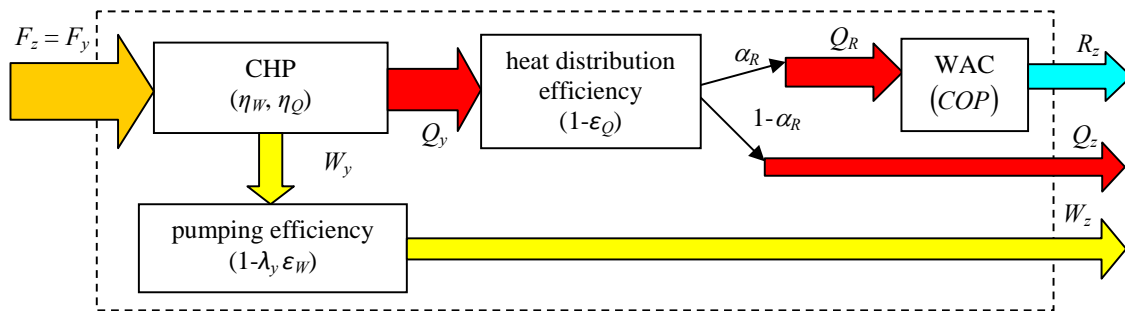


Figure 1. Energy flow model in a distributed trigeneration plant with CHP, DHN and WAC.

thermal losses due to the heat network, it can be written:

$$\begin{aligned} Q_y (1 - \varepsilon_Q) &= Q_R + Q_z = \\ &= \alpha_R (1 - \varepsilon_Q) Q_y + (1 - \alpha_R) (1 - \varepsilon_Q) Q_y \end{aligned} \quad (6)$$

Then, on the basis of the definition of the cogeneration efficiencies in (1), the fuel thermal input $F_z = F_y$ can be expressed in different forms, looking at the output-to-input paths connecting each one of the three energy outputs from the trigeneration system to the unique fuel input, namely:

$$F_z = \frac{Q_y}{\eta_Q} = \frac{Q_z}{(1 - \alpha_R)(1 - \varepsilon_Q)\eta_Q} \quad (7)$$

$$F_z = \frac{W_y}{\eta_W} = \frac{W_z}{\eta_W - \varepsilon_W \eta_Q} \quad (8)$$

$$F_z = \frac{R_z}{\alpha_R COP (1 - \varepsilon_Q) \eta_Q} \quad (9)$$

On these bases, the $TCO2ER$ indicator (5) becomes:

$$TCO2ER = 1 - \frac{\mu_F}{\mu_W^{SP} \cdot \xi + \mu_Q^{SP} \cdot \eta_Q (1 - \alpha_R) (1 - \varepsilon_Q)} \quad (10)$$

where $\xi = (\eta_W - \varepsilon_W \eta_Q) + \alpha_R \frac{COP}{COP^{SP}} (1 - \varepsilon_Q) \eta_Q$.

The $TCO2ER$ model in (10) yields an analytical formulation of the potential emission reduction in trigeneration as a function of the plant component and network-related efficiencies, the splitting factor, and the emission factors for the input fuel and the SP references. Therefore, it is possible to run various analyses to highlight the role played by the specific entries involved in the study, as shown in the following section.

IV. NUMERICAL APPLICATIONS

A. Energy System Description

Different equipment typologies available for small-scale applications are considered, namely, an SE coupled to an adsorption chiller, and a MT and two ICE coupled to a single-effect absorption chiller. The average performance characteristics (assumed to be constant and equal to nominal values, for the sake of simplicity) and typical capacities for the equipment analysed are shown in Table I. In addition, also average energy penalties due to heat networks are considered, with heat losses increasing with the CHP typology and size, assuming that larger heat networks are subsequently needed. The pumping electrical parasitic losses are instead assumed equal to 1% in all cases. For SE, no DHN connection is considered. All CHP systems are natural gas-fuelled.

The $TCO2ER$ indicator is plotted in Figure 2 assuming α_R as the independent variable. Two cases are analysed:

- Case 1): The SP emission factor for electricity refer to average emissions in UK ($\mu_W^{SP} = 430$ g/kWh_e) [3], while the heat-related emission factor is calculated assuming average boilers with efficiency $\eta_Q^{SP} = 0.8$, fed on natural

gas, thus obtaining $\mu_Q^{SP} = \mu_F / \eta_Q^{SP} = 250$; finally, for the reference chiller $COP^{SP} = 3$; the results are shown in Figure 2a.

- Case 2): peak ("marginal plant") emissions for the UK power system (570 g/kWh_e) [3] are considered, also introducing lower (with respect to case 1) average efficiency values for boilers (0.7) and chillers (2.5); the results are reported in Figure 2b.

TABLE I. AVERAGE CAPACITY AND EFFICIENCY VALUES FOR SMALL-SCALE DISTRIBUTED TRIGENERATION SYSTEM EQUIPMENT

	capacity [kW _e]	η_W	η_Q	COP	ε_Q	ε_W
SE	3	0.1	0.75	0.4	0	0
MT	100	0.3	0.5	0.7	0.01	0.01
ICE	1000	0.35	0.5	0.7	0.03	0.01
ICE2	5000	0.4	0.45	0.7	0.05	0.01

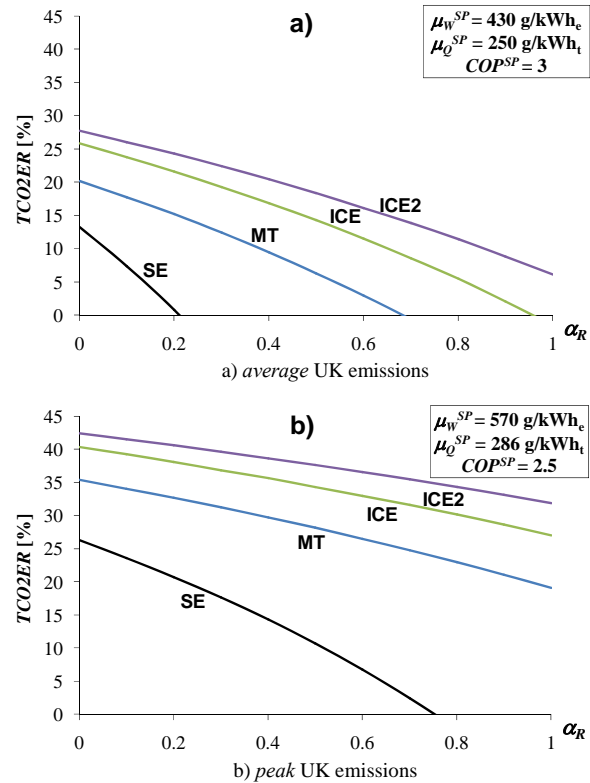


Figure 2. CO₂ emission reduction for small-scale trigeneration systems.

B. Discussion and Comments on the Numerical Results

The analysis presented has been carried out by using only the parameters of the CCHP systems and of the SP equivalents, with no need to specify the amount of electricity, heat and cooling involved. The rationale of this procedure is that the emissions reduction depends only on the contribution of the trigeneration systems in efficiently displacing SP of the various energy vectors needed. In the energy system, the possible excess of demand of any energy vector is covered by external supply coming from the additional components in place (that is, the electricity

distribution grid for electricity, boilers for heat and electric chiller for cooling; these components are not explicitly shown in Figure 1), whose characteristics are the same as the ones assumed for the corresponding separate production equivalents. The analysis based on the *TCO2ER* indicator then refers to the effectiveness of displacing part of the SP with trigeneration, for the same amount of the energy demand supplied through the trigeneration chain shown in Figure 1. For instance, when $\alpha_R = 0$ there is no cooling demand supplied through the trigeneration chain, meaning that any cooling demand is covered by electric chillers with parameter COP^{SP} supplied by the electrical network with equivalent emission factor μ_W^{SP} . Likewise, for $\alpha_R = 1$ there is no trigenerated heat, and the entire heat demand is conventionally covered by boilers with equivalent emission factor μ_Q^{SP} . The amounts of energy not provided by the trigeneration system are then excluded from the analysis.

From Figure 2, when operating in electricity and heat cogeneration mode ($\alpha_R = 0$), all the technologies considered bring CO₂ emission reduction with respect to the base case references, increasing with the electrical efficiency (and size). The emission reduction potential for CCHP systems decreases with increasing α_R . The cooling production through thermal power in a WAC, in fact, although from wasted heat, is energetically inefficient compared with a relatively higher-efficiency reference electric chiller. Thus, it is more environment-effective to cogenerate heat and electricity ($\alpha_R = 0$) than cogenerating cooling and electricity ($\alpha_R = 1$). In particular, considering *average* UK emission intensities (Figure 2a), the emission reduction becomes negative beyond a certain α_R , whose values increases with the CHP electrical efficiency (and size). More specifically, an SE coupled to an adsorption chiller proves to be ineffective in terms of CO₂ emission reduction already for α_R above 0.2. The environmental performance is instead much better if the CCHP systems are compared to *peak* UK emissions (Figure 2b: for the various technologies, the emission reduction almost doubles for $\alpha_R = 0$ and even triplicates for $\alpha_R = 1$ with respect to the average baseline reference. In this case, the MT and the two ICE, coupled to absorption chillers, could bring emission reductions of the order of 20% to 40% in the whole range of α_R , while the SE would bring benefits for $\alpha_R < 0.75$.

The environmental evaluation of CCHP systems is strongly affected by the selection of the *reference* scenario. What rationale is more correct to adopt in terms of baseline reference may be policy matter. In particular, it is possible to argue that DG is likely to displace marginal plant operation [3], since renewables and nuclear plants are usually operated with the flattest possible profile. In addition, in a deregulated environment it is often tough to figure out what plants are being offset, with older coal plants that may be preferred to newer gas plants on the basis of economic reasons. In any case, marginal power plants are the most likely to be displaced by CCHP systems producing cooling power in the summer peak hours. In addition, the actual efficiency of boilers may be much less than the rated one, above all in the

summertime, as assumed when drawing the picture in Figure 2b. On the other hand, an average generation mix reflects, somehow, the more decarbonised future UK and several European countries are committed to. However, in the next years also CCHP efficiencies are expected to improve, so that again the overall emission reduction resulted from distributed trigeneration could be of the order of magnitude of the ones obtained for marginal plant operation.

In order to highlight the effectiveness of CCHP introduction in various countries, a further analysis has been made by considering the potential emission reductions an ICE2 (the technology leading to the highest CO₂ emission reduction among the ones tested above) could bring in different jurisdictions or national contexts, considering the emission factors referring to average specific emissions. For this analysis the *TCO2ER* equation (10) has been used by changing the value of average specific emissions μ_W^{SP} and maintaining the same values for μ_Q^{SP} and COP^{SP} . In addition to the UK case already shown (with $\mu_W^{SP} = 430$ g/kWh_e), the values considered, taken from [19][22], refer to Norway ($\mu_W^{SP} = 3$ g/kWh_e), France ($\mu_W^{SP} = 78$ g/kWh_e), the former EU15 ($\mu_W^{SP} = 362$ g/kWh_e), and Italy ($\mu_W^{SP} = 525$ g/kWh_e). Figure 3 shows the relevant results.

It is conceptually evident that trigeneration can be more effective in jurisdictions with higher electricity-related specific emissions. However, *TCO2ER* analysis provides clear emission reduction quantification in the various contexts. The application of the same technology (ICE2) with the purpose of reducing CO₂ appears to be effective in Italy and UK for every usage (*i.e.*, for any value of α_R), while it would never be effective in Norway or France. The results for EU15 are of course of an intermediate nature. However, EU15 specific emissions are obtained by averaging out values referring to very different jurisdictions. The use of an overall value masks the possible benefits in jurisdictions with prevailing fossil fuels, as well as the total inadequacy of putting natural gas-supplied trigeneration systems in other jurisdictions with almost CO₂ emission-free electricity production. This confirms how making global averages in very heterogeneous contexts can lead to results that are not useful for any of the individual communities.

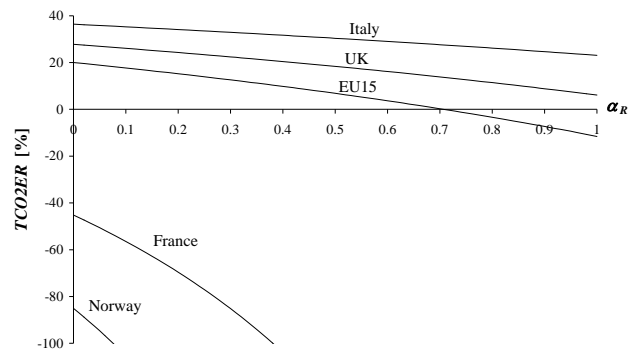


Figure 3. Effectiveness of CO₂ emission reduction by using ICE2 in different national contexts.

V. FINAL REMARKS AND FUTURE WORKS

In the development of energy systems with enhanced energy efficiency and environmental performance, the exploitation of distributed multi-generation systems based on combined generation of multiple energy vectors is a particularly significant and promising option.

This paper has introduced a general analytical model based on black-box representations for CO₂ emission reduction assessment from distributed trigeneration (as well as cogeneration) systems, in case coupled to heat networks. Dedicated assessment of the carbon dioxide reductions that can be obtained from the deployment of such trigeneration systems has been performed by comparing the trigeneration systems outcomes that satisfy the energy demand of different energy vectors with the separate production baseline references to supply the same demand of the corresponding energy vectors. In particular, the numerical analyses have been focused on small-scale energy systems currently available in the market.

The results show that consistent benefits can be obtained when the reference case points to marginal generation in UK, that is, the one most likely to be displaced by DG systems. Electrical efficiency, which is also a function of the plant size, plays a key role in the overall assessment, while the losses due to heat network affect marginally the results. Hence, micro-CHP Stirling engines prove to be the least effective, mainly due to their low electrical efficiency. The emission reduction performance is also a function of the quota of cogenerated heat feeding the chillers. With the cooling equipment considered here, in general the emission reduction decreases if the cogenerated heat firing the chiller increases. Although trigeneration allows for potential recovery of otherwise wasted heat, negative emission reduction (i.e., emission increase) could arise in certain operation points, also depending on the baseline reference. This assessment should be carried out at the planning stage, in order to avoid the setup of environmentally inefficient solutions.

The analysis has then been extended to show that the same trigeneration technology can be effective in certain jurisdictions characterized by fossil fuels in the energy mix used to supply the national electricity generation system, while it may exhibit total inadequacy of being adopted in other jurisdictions in which fossil fuels are almost unused.

The analyses presented here are meant to be a preliminary assessment of the potential emission reduction from distributed multi-generation systems. In particular, further analyses are in progress, including more detailed models of heat networks, and based on time-domain simulations that take into account load variations and actual operating conditions for all the equipment. In addition, the environmental benefits of different distributed energy solutions are to be assessed against their cost effectiveness and their impact on the electrical network. This may also require sensitivity studies on the underlying economic assumptions, such as the fuel and electricity rates, as well as analysing the possibility of operating CCHP systems within microgrids.

REFERENCES

- [1] J.H. Horlock, *Cogeneration-Combined Heat and Power*, Krieger, Malabar, FL, 1997.
- [2] N. Hatzigiorgiou, N. Jenkins, G. Strbac, J.A. Peças Lopes, J. Ruela, et al., "Microgrids - Large Scale Integration of Microgeneration to Low Voltage Grids", *CIGRE 2006*, Paris, France.
- [3] Carbon Trust, "Micro-CHP Accelerator – Interim report", Carbon Trust, UK, November 2007.
- [4] A.M. Borbely and J.F. Kreider (ed.), *Distributed generation: the power paradigm of the new millennium*, CRC Press, Boca Raton, Florida, USA, 2001.
- [5] L.D. Danny Harvey, *A handbook on low energy buildings and district energy systems*, Quicksilver Drive, Sterling, USA, 2006.
- [6] G. Chicco and P. Mancarella, "From cogeneration to trigeneration: profitable alternatives in a competitive market", *IEEE Transactions on Energy Conversion*, Vol.21 (1), March 2006, pp. 265-272.
- [7] G. Chicco and P. Mancarella, "Distributed Multi-Generation: a Comprehensive View", *Renewable and Sustainable Energy Reviews*, Vol. 13 (3), April 2009, pp. 535-551.
- [8] P. Mancarella and G. Chicco, *Distributed multi-generation systems: energy models and analyses* (ISBN: 978-1-60456-688-8), Nova Science Publishers, New York, 2009.
- [9] G. Chicco and P. Mancarella, "Trigeneration Primary Energy Saving Evaluation for Energy Planning and Policy Development", *Energy Policy*, Vol.35 (12), 2007, pp. 6132-6144.
- [10] G. Chicco and P. Mancarella, "Evaluation of multi-generation alternatives: an approach based on load transformations", *Proc. IEEE PES GM 2008*, Pittsburgh, PA, 20-24 July 2008, paper 08GM1283.
- [11] P. Mancarella, "Cogeneration systems with electric heat pumps: energy-shifting properties and equivalent plant modelling", *Energy Conversion and Management*, Vol.50, 2009, pp. 1991-1999.
- [12] G. Chicco and P. Mancarella, "Matrix modelling of small-scale trigeneration systems and application to operational optimization", *Energy*, Vol. 34 (3), March 2009, pp. 261-273.
- [13] G. Chicco and P. Mancarella, "Environmental Sustainability of Distributed Cogeneration Systems", *Proc. IEEE Melecon 2008*, Ajaccio, France, May 5-7, 2008, pp. 514-519.
- [14] P. Mancarella and G. Chicco, "CO₂ emission reduction from multi-generation systems: evaluation of combined cooling heat and power scenarios", *Energetica*, Vol.56 (8), August 2008, pp. 326-333.
- [15] P. Mancarella and G. Chicco, "Global and Local Emission Impact Assessment of Distributed Cogeneration Systems with Partial-load Models", *Applied Energy*, Vol.86 (10), October 2009, pp. 2096-2106.
- [16] P. Mancarella and G. Chicco, "Distributed cogeneration: modeling of environmental benefits and impact", Chapter 1 in D.N. Gaonkar (ed.) *Distributed generation* (ISBN 978-953-307-046-9), In-Teh, Vukovar, Croatia, February 2010, pp. 1-26.
- [17] G. Chicco and P. Mancarella, "A unified model for energy and environmental performance assessment of natural gas-fueled poly-generation systems", *Energy Conversion and Management*, Vol. 49 (8), August 2008, pp. 2069-2077.
- [18] G. Chicco and P. Mancarella, "Assessment of the greenhouse gas emissions from cogeneration and trigeneration systems. Part I: Models and Indicators", *Energy*, Vol. 33 (3), Mar. 2008, pp. 410-417.
- [19] P. Mancarella and G. Chicco, "Assessment of the greenhouse gas emissions from cogeneration and trigeneration systems. Part II: analysis techniques and application cases", *Energy*, Vol. 33 (3), March 2008, pp. 418-430.
- [20] US Environmental Protection Agency, Catalogue of CHP Technologies, www.epa.gov.
- [21] EDUCOGEN, The European Educational Tool on Cogeneration, December 2001, www.cogen.org/projects/educogen.htm.
- [22] Intergovernmental Panel on Climate Change, Working Group III, "Data on carbon dioxide intensities", http://arch.rivm.nl/env/int/ipcc/pages_media/SROC-final/Tables/t0305.pdf.

Application of Sulfated tin oxide in Transesterification of Waste Cooking oil: An Optimization Study

Man Kee Lam

School of Chemical Engineering,
Universiti Sains Malaysia, Engineering Campus,
14300 Nibong Tebal, Pulau Pinang, Malaysia.
Email: mk_lam11@yahoo.com

Keat Teong Lee

School of Chemical Engineering,
Universiti Sains Malaysia, Engineering Campus,
14300 Nibong Tebal, Pulau Pinang, Malaysia.
Email: chktlee@eng.usm.my

Abstract— Biodiesel is a biodegradable and non-toxic fuel which can be produced through transesterification reaction. However, it is impractical to use the refined vegetable oils as the feedstock for biodiesel production due to its high production cost and priority for food products. Thus, low-grade oil with high free fatty acids (FFA) content, typically waste cooking oil has been a promising choice to improve the economical feasibility of biodiesel. In the present study, superacid sulfated tin oxide catalyst, $\text{SO}_4^{2-}/\text{SnO}_2$ has been successfully prepared through impregnation method. Bimetallic effect was also studied at which SnO_2 mixed with SiO_2 and Al_2O_3 , respectively at different weight ratio in order to enhance the catalytic activity of SnO_2 . The effect of different reaction parameters such as calcinations temperature and period, reaction temperature, catalyst loading, methanol to oil ratio and reaction time were studied to optimize the reaction conditions. It was found that $\text{SO}_4^{2-}/\text{SnO}_2\text{-SiO}_2$ with weight ratio 3 exhibited an exceptional high activity with optimum yield 92.3% at reaction temperature 150°C, catalyst loading 3 wt%, methanol to oil ratio 15 and reaction time 3 hours.

Keywords- solid acid catalys; sulfated tin oxide; biodiesel; waste cooking oil

I. INTRODUCTION

Rapid diminishing of energy reserves and fluctuating petroleum prices has intensified the search for renewable energy sources, globally. Fatty acid methyl ester (FAME) or better known as biodiesel can be a potential renewable energy re-placing petroleum-derived diesel [1-4]. Biodiesel can be easily synthesized through transesterification of virgin vegetable oils, animal fats or even recycled grease from the food industry [1, 5-6] in the presence of short chain alcohol and catalyst. However, high cost of the most common biodiesel feedstock, virgin vegetable oil, has hindered wider utilization and commercialization of future biodiesel plant [7]. Therefore, to overcome this limitation, cheaper feedstock such as low-grade oil, typically waste cooking oil can be a better option as this can reduce the overall biodiesel production cost significantly.

Recently, researchers in this field are focusing on developing solid acid catalyst for heterogeneous transesterification reaction, typically from low-grade oil [2, 6-7]. The advantages of solid acid instead of liquid acid catalyst are; (1) the catalyst is insensitive to FFA content, (2)

can simultaneously catalyze esterification and transesterification reactions, (3) easier catalyst separation and (4) easily incorporated into a packed bed reactor for continuous production of biodiesel [1,7]. Among various solid acid catalysts available, many studies have highlighted the application of sulfated metal oxides in biodiesel production, especially sulfated zirconia ($\text{SO}_4^{2-}/\text{ZrO}_2$) due to its high catalytic activity [1, 6, 8, 9]. Sulfated tin oxide ($\text{SO}_4^{2-}/\text{SnO}_2$) is another potential catalyst for transesterification reaction due to its strong surface acidity that is reported to be stronger than $\text{SO}_4^{2-}/\text{ZrO}_2$ [10-12]. Nevertheless, study concerning the usage of $\text{SO}_4^{2-}/\text{SnO}_2$ catalyst in biodiesel production is still very limited.

Thus, this study is aimed to provide supplement technical information on the application of $\text{SO}_4^{2-}/\text{SnO}_2$ catalyst for transesterification reaction. Firstly, the effects of calcination temperature and calcination period towards the reaction performance were studied. This is followed by optimizing transesterification process variables including reaction temperature, catalyst loading, alcohol to oil ratio and reaction period. The effect of using mixed-metal was also investigated.

II. EXPERIMENTAL

A. Materials

Waste cooking oil was collected from cafeteria of Engineering Campus, Universiti Sains Malaysia, Penang. Methanol (purity 99.8%) and n-hexane (purity 99%) were purchased from Medina Jaya Sdn. Bhd. Methyl heptadecanoate which was used as internal standard for gas chromatography (GC) and sulfuric acid with purity 95-97% was purchased from Fluka Chemie, Germany. Pure methyl esters (references for GC analysis) such as methyl myristate, methyl palmitate, methyl stearate, methyl oleate and methyl linoleate with purity more than 99%, tin (IV) oxide (SnO_2) with purity 99.9%, quartzsand (SiO_2) with purity 99.8% and alumina oxide (Al_2O_3) with purity 98% were purchased from Sigma Aldrich, Malaysia.

B. Transesterification reaction

50 ml of waste cooking oil and a pre-determined amount of catalyst and methanol (parameters to be varied) were charged into a 300 ml stainless steel batch reactor equipped with thermocouple and magnetic stirrer. The reactor was then pressurized to 10 bars to ensure that all reactants remain in liquid phase for the entire duration of reaction. The reactants were stirred at 350 rpm in order to maintain uniform temperature and suspension. The reactor temperature was controlled by a heater with a programmable PID temperature controller. After running the reaction for a desired duration, the reactor was cooled to room temperature. After cooling, the product was discharged out and filtered using filter paper to separate the solid catalyst from the mixture of FAME-glycerol.

C. Method of analysis

The identity and relative composition of fatty acids present in the methyl ester product were analyzed by Perkin-Elmer Clarus 500 gas chromatograph equipped with flame ionization detector (FID) and Nukol™ column (15 m × 0.53 mm × 0.5 μm). Helium was used as carrier gas. Oven temperature were held at 110 °C (0.5 minutes) and was then heated at a rate of 10°C/min to 220°C (8 minutes). The temperature of injector and detector were set at 220°C and 250°C, respectively.

III. RESEULT AND DISCUSSION

A. Effect of reaction temperature and mixed metal oxide

Fig. 1 shows the effect of transesterification reaction temperature (100 to 200°C) on the yield of FAME using various bi-metallic catalysts at different weight ratio. When the reaction was increased from 100 to 150°C, there is a significant increase in the yield of FAME for all types of catalyst. However, beyond 150°C, except for bi-metallic catalyst prepared with ratio 1, the yield of FAME seems to level off as the batch of reactants had reached its equilibrium conversion. On the other hand, the increase in yield when reaction temperature increased from 100 to 150°C could be justified as follows. Waste cooking oil and methanol are immiscible, therefore reaction with heterogeneous catalyst would create a 3-phase system at which the mass transfer rate of reactant molecules between the three phases is very limited [13]. As the reaction temperature is increased, all reactant molecules will gain more kinetic energy that will eventually accelerated the mass transfer rate between the oil-methanol-catalyst phases that resulted in the formation of more FAME in a shorter time.

The effect of mixed metal oxide (bi-metal oxide) on the yield of FAME was also studied and the results are given in Fig. 1. SiO₂ and Al₂O₃ were chosen to mix with SnO₂ at different weight ratio as both metal oxides were reported to

be able to stabilize the crystalline structure of SnO₂ [14, 15]. The weight ratio of SnO₂:SiO₂ and SnO₂:Al₂O₃ were varied at 1:1, 3:1 and 5:1 (hereafter refer to as 1, 3 and 5) and impregnated with 2.0 M H₂SO₄ to become sulfated mixed metal oxide. Since 150°C was found to be the minimum temperature to achieve equilibrium conversion, discussion in this section will focus on the data trend for reaction temperature above 150°C. Furthermore, when the reaction temperature was below 150°C, no significant data trend can be observed. From Fig. 1, it is obvious that the weight ratio between the bi-metal affect the yield of FAME significantly. For all sulfated mixed metal with ratio 1, the yield of FAME was even lower than SO₄²⁻/SnO₂ with exceptional at the extreme end of higher reaction temperature. However for sulfated mixed metal with ratio 3 and 5, the yield was significantly higher than SO₄²⁻/SnO₂ with ratio 3 giving higher yield. These results showed that with appropriate amount of SiO₂ and Al₂O₃, acid sites on the surface of SnO₂ can be enhanced and therefore increases its contact with reactants that led to higher reactivity [16]. The optimum yield for SO₄²⁻/SnO₂-SiO₂ (3) and SO₄²⁻/SnO₂-Al₂O₃ (3) was 82.1% and 79.6%, respectively at 150°C.

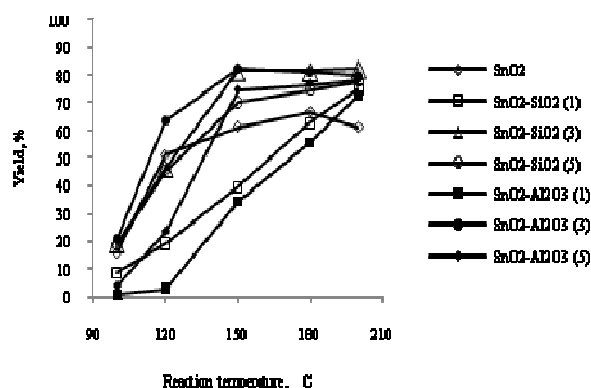


Figure 1. Effect of reaction temperature on FAME yield using SO₄²⁻/SnO₂ and its sulfated mixed metal oxide. Reaction condition: methanol:oil ratio 10, catalyst loading 3 wt %, reaction time 3 hours. All samples were calcined at 300 °C for 2 hours.

B. Effect of catalyst loading

Catalyst loading is an important parameter that needs to be optimized to increase the FAME yield. Fig. 2 shows the effect of catalyst loading on the yield of FAME. The value of catalyst loaded into the reaction mixture was varied from 1 to 8 wt% (based on weight of waste cooking oil). From the figure, it can be noted that the yield of FAME increased with higher catalyst loading up until a value in which higher increment no longer increase the yield of FAME. This is because with more catalyst addition, the total number of available active sites increased resulted in faster reaction rate to reach reaction equilibrium [17]. However, further increase in catalyst loading beyond its optimum value will have negligible increase in FAME yield. This might be due to the immiscibility of waste cooking oil and methanol, which causes the reaction to be rate limiting step at the beginning of the reaction. However, as catalyst is introduced in the

reaction mixture, it provides an external contact surface area that facilitates the formation of FAME. As more FAME is produced, it eventually acted as co-solvent, by dissolving both reactants to become a single phase reaction system. Subsequently, the reaction rate is being controlled by the diffusion of the reactants to the active sites, instead of catalyst loading. Hence, increasing the dosage of catalyst in the reaction mixture will have an insignificant effect on the yield of FAME. The optimum catalyst loading for $\text{SO}_4^{2-}/\text{SnO}_2$, $\text{SO}_4^{2-}/\text{SnO}_2\text{-SiO}_2$ (3), and $\text{SO}_4^{2-}/\text{SnO}_2\text{-Al}_2\text{O}_3$ (3) are 6, 3 and 3 wt %, respectively.

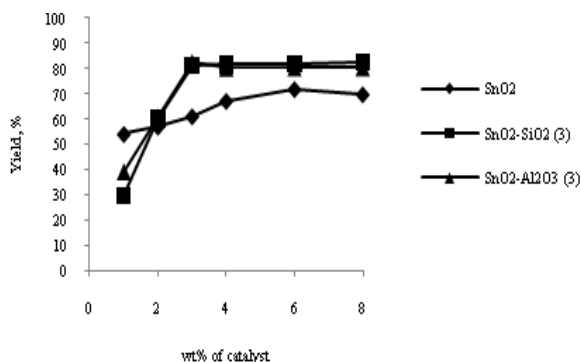


Figure 2. Effect of catalyst loading on FAME yield using $\text{SO}_4^{2-}/\text{SnO}_2$ and its sulfated mixed metal oxide. Reaction condition: reaction temperature 150°C, methanol:oil ratio 10, reaction time 3 hours.

C. Effect of methanol:oil ratio

Basically, for a reversible reaction like transesterification [1], reactants (methanol) are normally used in excess to push the reaction forward for formation of products (FAME). However, care must be taken as to how much excess methanol is to be used because too much methanol may dilute the system and eventually cause a drop in the yield of FAME due to slower reaction [18]. Fig. 3 shows the effect of methanol to oil ratio on the yield of FAME using three types of catalyst. In the present work, methanol to oil ratio were set at 5, 10, 15, 20, 25 and 30 in order to optimize the transesterification reaction as shown in Fig. 5. From the figure, the yield of FAME catalyzed by $\text{SO}_4^{2-}/\text{SnO}_2$ increased abruptly from 69.0% to 91.5% as the methanol to oil ratio increased from 5 to 30. Nevertheless, the observation for transesterification reaction catalyzed by $\text{SO}_4^{2-}/\text{SnO}_2\text{-SiO}_2$ (3) and $\text{SO}_4^{2-}/\text{SnO}_2\text{-Al}_2\text{O}_3$ (3) showed a different pathway as the yield of FAME decreased at a certain ratio, indicating an optimum value. The maximum yield obtained by $\text{SO}_4^{2-}/\text{SnO}_2\text{-SiO}_2$ (3) was 92.3% at ratio 15 whereas for $\text{SO}_4^{2-}/\text{SnO}_2\text{-Al}_2\text{O}_3$ (3) was 82.3% at ratio 10. It can be clearly seen that due to the high reactivity of sulfated $\text{SnO}_2\text{-SiO}_2$ catalyst, methanol to oil of 15 is sufficient to achieve a high yield as compared to the original sulfated SnO_2 whereby this can only be achieved at a ratio of more than 30.

D. Effect of reaction time

Fig. 4. shows that the yield of FAME increased steadily as the reaction time was increase from 1 to 3 hrs of reaction time. After 3 hrs., the yield level off as near-equilibrium composition was achieved. This shows that sulfated SnO_2 is a very suitable solid catalyst that has a very high reactivity to catalyze transesterification reaction as typical solid catalyst requires more than 10 hrs. of reaction time. The optimum yield obtained for reaction catalyzed by $\text{SO}_4^{2-}/\text{SnO}_2$, $\text{SO}_4^{2-}/\text{SnO}_2\text{-SiO}_2$ (3) and $\text{SO}_4^{2-}/\text{SnO}_2\text{-Al}_2\text{O}_3$ (3) was 91.5%, 92.3% and 87.4%, respectively corresponding to their optimum reaction time.

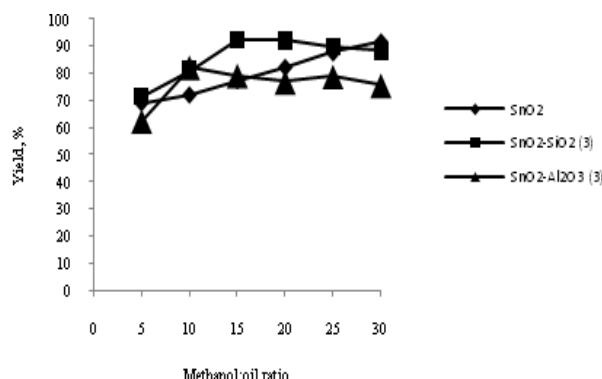


Figure 3. Effect of methanol to oil ratio on FAME yield using $\text{SO}_4^{2-}/\text{SnO}_2$ and its sulfated mixed metal oxide. Reaction condition: reaction temperature 150°C, catalyst loading 6 wt % for $\text{SO}_4^{2-}/\text{SnO}_2$ and 3 wt % for $\text{SO}_4^{2-}/\text{SnO}_2\text{-SiO}_2$ (3) and $\text{SO}_4^{2-}/\text{SnO}_2\text{-Al}_2\text{O}_3$ (3), reaction time 3 hours.

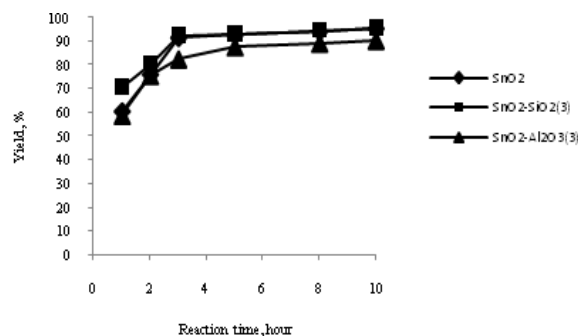


Figure 4. Effect of reaction time on FAME yield using $\text{SO}_4^{2-}/\text{SnO}_2$ and its mixed metal oxide. Reaction condition: reaction temperature 150°C, methanol:oil ratio 10 for $\text{SO}_4^{2-}/\text{SnO}_2\text{-Al}_2\text{O}_3$ (3), 15 for $\text{SO}_4^{2-}/\text{SnO}_2\text{-SiO}_2$ (3) and 30 for $\text{SO}_4^{2-}/\text{SnO}_2$, catalyst loading 6 wt % for $\text{SO}_4^{2-}/\text{SnO}_2$ and 3 wt % for $\text{SO}_4^{2-}/\text{SnO}_2\text{-SiO}_2$ (3) and 30 for $\text{SO}_4^{2-}/\text{SnO}_2\text{-Al}_2\text{O}_3$ (3).

E. FAME Properties

Table 2 summarized some of the FAME properties produced from $\text{SO}_4^{2-}/\text{SnO}_2\text{-SiO}_2$ (3) catalyst. From the table, it was found that all the listed properties met the specification of standard En 14214.

TABLE I. FAME PROPERTIES

Property	Unit	Value	EN 14214
Density at 15°C	Kg/m ³	885.5	860-900
Viscosity at 40°C	mm ² /s	4.08	3.5-5.0
Flash point	°C	201	>101
Sulfur	mg/kg	0.5	<10
Sulfated ash	% mass	0.01	<0.02
Iodine value	-	70.9	<120
Methanol content	% mass	0.1	<0.2

IV. CONCLUSION

The present study had open a new synthetic route in application of modified SO₄²⁻/SnO₂ as a promising catalyst in biodiesel production, typically from low grade oil with high free fatty acid content. It was found that adding appropriate amount of SiO₂ or Al₂O₃ to SO₄²⁻/SnO₂ will eventually enhance the catalytic activity of the catalyst leading to higher yield of FAME with minimum catalyst loading and methanol to oil molar ratio. The highest FAME yield of 92.3 % was obtained by using SO₄²⁻/SnO₂-SiO₂ (3) catalyst in which the catalyst was calcined at 300°C for 2 hours, while the optimum transesterification reaction condition was at 150°C, 3 wt% catalyst, 15:1 methanol to oil ratio and 3 hours reaction time.

ACKNOWLEDGEMENT

The authors would like to acknowledge the funding given by Universiti Sains Malaysia (Research University Grant, Short Term Grant and USM Fellowship) for this project.

REFERENCES

- [1] E. Lotero, Y. Liu, D.E. Lopez, K. Suwannakarn, D.A. Bruce, and J.G. Goodwin, "Synthesis of biodiesel via acid catalysis," *Jr. Ind. Eng. Chem. Res.*, vol. 44, 2005, pp. 5353-5363.
- [2] A.A. Kiss, A.C. Dimian, and G. Rothenberg, "Solid acid catalysts for biodiesel production-towards sustainable energy," *Adv. Synth. Catal.*, vol. 348, 2006, pp. 75-81
- [3] T.F. Dossin, M.-. Reyniers, R.J. Berger, and G.B. Marin, "Simulation of heterogeneously MgO-catalyzed transesterification for fine-chemical and biodiesel industrial production," *Appl. Catal., B*, vol. 67, 2006, pp. 136-148.
- [4] E. Li, Z.P. Xu, and V. Rudolph, "MgCoAl-LDH derived heterogeneous catalysts for the ethanol transesterification of canola oil to biodiesel," *Appl. Catal., B*, vol. 88, 2009, pp. 42-49.
- [5] N. Boz, N. Degirmenbasi, and D.M. Kalyon, "Conversion of biomass to fuel: Transesterification of vegetable oil to biodiesel using KF loaded nano- γ -Al₂O₃ as catalyst," *Appl. Catal., B*, vol. 89, 2009, pp. 590-596.
- [6] K. Jacobson, R. Gopinath, L.C. Meher and, A.K. Dalai, "Solid acid catalyzed biodiesel production from waste cooking oil," *Appl. Catal., B*, vol 85, pp. 86-91.
- [7] M.G. Kulkarni and A.K. Dalai, "Waste Cooking Oil — An Economical Source for Biodiesel: A Review," *Ind. Eng. Chem. Res.*, vol. 45, 2006, pp. 2901-2913.
- [8] S. Furuta, H. Matsushashi, and K. Arata, Catal. "Biodiesel fuel production with solid superacid catalysis in fixed bed reactor under atmospheric pressure," *Catal. Commun.*, vol. 5, 2004, pp. 721-723.
- [9] J. Jitputti, B. Kitiyanan, P. Rangsunvigit, K. Bunyakiat, L. Attanatho, and P. Jenvanitpanjakul, "Transesterification of crude palm kernel oil and crude coconut oil by different solid catalysts," *Chem. Eng. J.* vol. 116, 2006, pp. 61-66.
- [10] H. Matsushashi, M. Hino, and K. Arata, "Solid catalyst treated with anion: XIX. Synthesis of the solid superacid catalyst of tin oxide treated with sulfate ion," *Appl. Catal.*, vol. 59, 1990, pp. 205-212.
- [11] G. Wang, H. Hattori, and K. Tanabe, "Acid-Base and Catalytic Properties of ZrO₂-SnO₂," *Bull. Chem. Soc. Jpn.* vol. 56, 1983, pp. 2407-2410.
- [12] S. Furuta, H. Matsushashi, and K. Arata, *Appl. Catal., A* "Catalytic action of sulfated tin oxide for etherification and esterification in comparison with sulfated zirconia," vol. 269, 2004, pp. 187-191.
- [13] Z. Yang and W. Xie, "Soybean oil transesterification over zinc oxide modified with alkali earth metals," *Fuel Process. Technol.* vol. 88, 2007, pp. 631-638.
- [14] Y. Du, S. Liu, Y. Ji, Y. Zhang, S. Wei, and F. Liu, "Synthesis of Sulfated Silica-Doped Tin Oxides and Their High Activities in Transesterification," *Catal. Lett.*, vol. 124, 2008, pp. 133-138.
- [15] H. Guo, P. Yan, X. Hao, and Z. Wang, "Influences of introducing Al on the solid super acid SO₄²⁻/SnO₂," *Mater. Chem. Phys.* vol. 112, 2008, pp. 1065-1068.
- [16] A. Kawashima, K. Matsubara, and K. Honda, "Development of heterogeneous base catalysts for biodiesel production," *Bioresour. Technol.* vol. 99, 2008, pp. 3439-3443.
- [17] X. Liu, X. Piao, Y. Wang, S. Zhu, and H. He, "Calcium methoxide as a solid base catalyst for the transesterification of soybean oil to biodiesel with methanol," *Fuel* vol. 87, 2008, pp. 1076-1082.
- [18] L. Gao, B. Xu, G. Xiao, and J. Lv, "Transesterification of Palm Oil with Methanol to Biodiesel over a KF/Hydrotalcite Solid Catalyst," *Energy Fuels* vol. 22, 2008, pp. 3531-3535.

Analysing the effect of Renewable Energy Sources on Electricity Prices in Spain. A Maximum Entropy Econometric Approach.

Blanca Moreno
Department of Applied Economics
University of Oviedo
Oviedo, Spain
e-mail: morenob@uniovi.es

María Teresa García-Álvarez
Department of Economic Analysis and Business
Administration
University of La Coruna
La Coruna, Spain
e-mail: mtgarcia@udc.es

Abstract— There is a controversial debate about the effects of the promotion of renewable energy and electric power sector reforms on electricity prices. This paper explores the impact of renewable energies and other environmental and economic variables on electricity prices in Spain. However, information available regarding renewable energies is scarce so when trying to estimate the electricity price model through regression procedures a dimensionality problem arises. Therefore we use a Maximum Entropy Econometric approach which allows estimating models when information is limited.

Keywords— electricity price, renewable energy, Entropy measures

I. INTRODUCTION

The promotion of renewable energies is a key concept in European Union by environmental and economic reasons. This type of energy contributes to obtain the objectives established by Kyoto Protocol. Besides, it allows the obtaining of various social-economic advantages, such as the diversification of energy offer, the improvement of opportunities in regional and local development, and the creation of a domestic industry and employment¹.

In contrast, the renewable energies also have some costs related to the adjustments in production, prices and transportation systems.

Regarding the price effects, since the majority of renewable energy technologies are not profitable at current energy prices, they are expected to increase energy costs. In order to make them profitable, there are several public supports. The support scheme used in Spain is the feed-in tariffs. This system requires that distributors acquire, in first place, the energy produced by renewable energy sources at a determined price established by regulator during a specific time period (generally, around fifteen years). From generator view point, it operates as a subsidy.

¹ Several studies have reviewed the effects of the introduction of renewable energies at EU country levels. This is the case of [1] for United Kingdom or [2] for Germany. Other studies as [3] have analysed the macroeconomic impact of renewable energy at local level.

In addition, environmental costs related to CO₂ emissions in electricity generation in general have a significant negative effect on energy costs as a CO₂ emission trading scheme exists [4]. The substitution of conventional electricity generation by renewable energies could reduce the cost derived from environmental emissions and the electricity price. Besides, it is necessary to consider that a higher use of renewable energies could reduce even the final electricity prices because its promotion stimulates the generation of renewable energy which is characterized by variable costs lower than fossil conventional technologies [5].

Therefore the cost disadvantage of renewable compared to conventional energies is crucially dependent on future prices of energies used in power plants as well as on the amount of CO₂ emission permits. The expansion of renewable energy could affect electricity price.

Moreover, the regulatory reforms in the Spanish Electricity Market also could have its effect on electricity prices. In fact, the introduction of liberalization in the retailing activity could reduce electricity price as a consequence of the competition system.

Since in Spain there is a part of the electricity price paid by the government, it could be interesting to study the effect of the general economic activity on electricity price.

Therefore, there are several variables affecting electricity prices.

In this paper, we explore the effect of electricity generated by renewable energy and other factors (matrix X) on household electricity prices in Spain (y). Our data sets are provided by Eurostat during the period 2002-2007.

During the last years, several studies have been developed using cross-sectional or temporal data to explain the effect of several variables on electricity price. Some of them include explanatory variables related to energy use or technology [6][7] or market liberalization [8][9]. Our empirical study takes into consideration all effects together.

Traditional parametric methods require an elevated sample size for the efficient estimation of the coefficients in the models. Thus, $y = X\beta + u$ its estimation by regression

techniques requires that the number of observations was superior to the number of independent variables.

However, information available regarding renewable energy and electricity market liberalization is scarce so it limits the sample date. Therefore, when trying to estimate the electricity price model through regression procedures a dimensionality problem arises.

As an alternative to estimate the model, when a dimensionality problem arises, we propose a Maximum Entropy Econometric approach, which has been defined by [10] as “a sub-discipline of processing information from limited and noisy data with minimal a priori information on the data-generating process”. This approach has its roots in Information Theory and builds on the entropy-information measure [11], the classical maximum entropy principle [12],[13], which was developed to recover information from underdetermined models, and the Generalized Maximum Entropy Theory [14].

The maximum entropy Econometric approach was developed to estimate models using limited or incomplete data. Therefore, we investigate its possibilities in the estimation of household electricity price.

This paper is divided into two more sections. The first of them (Section II) makes a revision of the functioning of Spanish electricity market and analyzes the important role of the renewable energies in such electricity system.

The next section (Section III) assesses the problem of electricity price model estimation through regression-based procedures when a dimensionality problem arises. It also contains a brief description of some of the uncertainty measures provided by the Information Theory and the requirements to optimize their values. Furthermore, we describe the Maximum Entropy Econometric procedure in order to estimate the model. Moreover, we present an empirical application of the proposed method to Spanish household electricity prices over the period 2002-2007. Some concluding remarks complete the paper.

II. ELECTRICITY MARKET IN SPAIN. AN OVERVIEW

In this section, we analyze the characteristics of the Spanish electricity market after the liberalization process and the role of renewable energies in such market.

Liberalization of the Spanish electricity system is begun with Law 54/1997 [15] where the key element is the creation of the wholesale electricity market (pool²).

In daily market, electricity companies determine, for every generation unit, the offered amount and price. In parallel, electricity consumers establish the demanded

² Spanish electricity market is structured on various markets where electricity demand and offer is adjusted. Daily market is emphasized because the electricity price shaped in it supposes around the 89% of final electricity price. In this market, electricity energy is negotiated for every one of the twenty-four hours of the following day.

amount and the maximum prices that they are ready to pay. In this context, the use of an algorithm based on auctions of first price establishes the wholesale electricity price (see Fig.1).

On the other hand, liberalization of Spanish electricity system entails too the creation of a retail electricity market. In this market, consumer can choose distributor freely and negotiate with them the price and the conditions of the electricity supply. Therefore, consumers have two options of supply: regulated (by means of the payment of a “integral” tariff where all supply costs are included) and competitive or of market (by means of the payment of an access tariff to the networks plus the energy contracting costs and other services).

Regarding the role of renewable energies in the electricity generation the European Community Directives 2001/77/EC [16] and 2009/28/EC [17] give freedom to each member state for choosing the support mechanism of renewable resources.

In the case of Spain, the current legal framework of renewable energy is the Royal Decree 661/2007 [18] whose aim is to minimize the environmental impact of electricity supply. Like that, the basic instrument introduced is feed-in tariff. This mechanism entails two possibilities in the sale of electricity, generated by renewable energies: a) to sell the electricity to distributor at a regulated tariff or b) to sell the electricity directly in the market where the remuneration is given by the negotiated price in the market plus a feed-in tariff.

This legal framework has allowed that Spain was a pioneering and leader country in the integration of renewable energies as the wind or solar energy in the electricity system (Spain is the second European country in terms of installed capacity and production of these types of energy, only behind Germany).

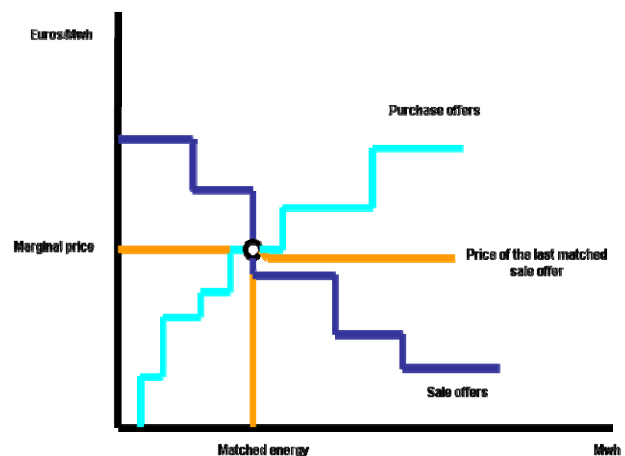


Fig. 1. Establishment of Wholesale electricity prices €/MWh

III. MODELLING THE IMPACT OF RENEWABLES ON ELECTRICITY PRICES. A MAXIMUM ENTROPY ECONOMETRIC APPROACH.

Our goal is to estimate the effect of several variables (m) on electricity prices (y) by using data of several years (T).

$y = X\beta + u$, being X a matrix $T \times m$, y a matrix $T \times 1$, β the vector of coefficients to be estimated (vector $m \times 1$) and vector of disturbances u.

A. Maximum Entropy Econometric Approach.

The estimation of $y = X\beta + u$ by regression techniques requires that the number of observations (T) has to be superior to the number of independent variables (m).

Nevertheless, information available regarding renewable energy and electric liberalization market is scarce. Therefore, in a situation of limited sample data the estimation of the model by regression procedures (OLS) is not possible as the problem is undetermined or ill-posed.

However, when these circumstances of small amount of information available make it unfeasible to combine forecasts through OLS procedures the Maximum Entropy Econometric approach allows us to recover the estimates of $\beta_1, \beta_2, \dots, \beta_m$ in the corresponding parameterized model without making distributional assumptions. The approach consists of developing a non-linear inversion procedure [14] which requires the application of the tools provided by the Information Theory ([11], [12], [13]).

Consider a regression-based method: $y = X\beta + u$ in a situation of limited sample data where $m > T$. A probability distribution should be used in order to represent partial and limited information regarding the individual observations so they are consistent with the observed sample data. Therefore, following [14] it is possible to define an inverse general problem for recovering β defined as: $y = X\beta + u = XP + u$, where $P: (p_1, \dots, p_m)'$ is a m-dimensional vector of unknown terms related to the probability distribution. The main objective is to estimate a probability distribution P given the limited information and minimal distributional assumptions and therefore recover β as $\hat{P} = \hat{\beta}$.

However, as the number of observations (T) is smaller than the number of independent variables (m), if we attempt to recover P by using traditional procedures of mathematical inversion, there is more than one vector P making the solution feasible. Therefore the problem is ill-posed and we have no basis for picking a particular solution vector for P from the feasible set. Thus, if we ask for a particular set of probabilities considered as most likely, it seems reasonable to favour the one that could have been generated in the greatest number of ways given the available data.

The definition of the entropy measure H(P) and the formulation of the Entropy Maximization problem can help us to estimate a unique P distribution since the principle of

Maximum Entropy provides a basis for transforming the sample information into a probability distribution that reflects our uncertainty about the individual outcomes.

The measures of entropy H(P) quantify the uncertainty associated with a random experiment. In particular, given a random variable X with values x_i and probability distribution

$$P = (p_1, \dots, p_n) \text{ with } p_i \geq 0 \text{ (i=1, \dots, n) and } \sum_{i=1}^n p_i = 1,$$

Shannon's measure of entropy ([11]) is defined as:

$$H_s(P) = H_s(p_1, \dots, p_n) = -\sum_{i=1}^n p_i \log p_i.$$

The value of the entropy is maximum when all the values x_i have the same probability (and then P is a uniform distribution). This situation would be justified by the Laplace Indifference Principle, according to which the uniform distribution is the most suitable representation of our knowledge when the random variable is completely unknown. Nevertheless, sometimes the ignorance of the probability distribution of X is not absolute and we have some partial information on the distribution such as the mean, variance, moments or some characteristics which can be formulated as equality constraints. In such a case, it is possible to estimate the probability distribution through the application of the Maximum Entropy principle ([12], [13]) choosing the distribution for which the available information is just sufficient to obtain the probability assignment.

Thus, if we know certain values a_r ($r=1, \dots, s$) associated with functions $g_r(X)$ of the values of X but we do not know its distribution, the problem consists of estimating a nonnegative distribution that fulfils the conditions $p_i \geq 0$ for $i=1, \dots, n$ and $\sum_{i=1}^n p_i = 1$, maximizing the value of the entropy.

By solving the maximization problem we can obtain the estimated probabilities $\hat{P} = \{\hat{p}_1, \dots, \hat{p}_n\}$. We pointed out that the maximum entropy distribution does not have a closed-form solution and therefore numerical optimization techniques must be used to compute the probabilities.

Working towards a criterion for recovering the parameters of the regression model related to electricity price in the general inverse problem $y = X\beta + u = XP + u$, if there is no evidence that a specific independent variable is more significant than others, the related probability distribution (P) would be the uniform (according to Laplace Indifference Principle). However, the principle of maximum entropy provides a basis for using the sample information in a probability distribution P that reflects our uncertainty about the individual independent variable. Therefore, the problem consists of estimating a nonnegative distribution P by maximizing the value of the entropy H(P) subject to the available information. By solving the optimization problem the estimated probability distribution \hat{P} is obtained.

We consider a general inverse problem $y = X\beta + u = XP + u$ where we wish to determine the unknown and unobservable frequencies $P = (p_1, \dots, p_m)'$, representing the data generating process. Then, within the possible sets of probabilities fulfilling $\sum_{i=1}^m p_i = 1, p_i \geq 0$, we must choose to assign a single vector. Through the application of the principle of maximum entropy we maximize $H(P)$ under the restrictions of information consistency $y = X\beta + u$, and the adding up-normalization constraint for P: $P'\ell = 1$.

If the vector of disturbances, u , is assumed to be a random vector with finite location and scale parameters, we can represent our uncertainty about it by treating each u_t ($t=1, \dots, T$) as a finite and discrete random variable with $2 \leq J \leq \infty$ possible outcomes.

Thus, it is assumed that each u_t is limited by an interval (v_{t1}, v_{tJ}) , whose probability, $\Pr(v_{t1} < u_t < v_{tJ})$, can become as small as we want. For example, for $J=2$, the error can be defined as: $u_t = w_t v_{t1} + (1 - w_t) v_{tJ}$ where each $w_t \in [0, 1]$ is a vector of error weights. Furthermore, $J \geq 2$ can be used to assume certain characteristics of symmetry and kurtosis about the error distribution.

Because there may be different levels of uncertainty underlying each β_i , for more general inferential purposes, point estimates may be limiting and unrealistic. Consequently, it is possible to generalize the maximum entropy problem to permit a discrete probability distribution to be specified and obtained for each β_i . Rather than search for the point estimates of β , each β_i is viewed as the mean value of some well defined random variable z .

Then, for each β_i , we assume there exists a discrete probability distribution that is defined over a parameter space \mathbb{R}^K by a set of equally distanced discrete points $z_i = [z_{i1}, \dots, z_{iK}]'$ with corresponding probabilities $p_i = [p_{i1}, \dots, p_{iK}]'$ and with $K \geq 2$. Therefore: $\beta_i = E_{p_i} [z_i]$ or $\beta = E_p [z]$.

Using the Maximum entropy econometric approach, one investigates how “far” the data pull the estimates away from a state of complete ignorance (uniform distribution). In order to measure the reduction in the initial uncertainty, the information index entropy measure R is defined ([19], [20], [21]) and where $R \in [0, 1]$. A high value of R implies the data tell us something about the estimates, or similarly, there is valuable information in the data.

Moreover, we can define measures to evaluate the information in each one of the variables $i = 1, 2, \dots, m$ as the normalized entropy: $S(\hat{p}_i)$.

These variable-specific information measures reflect the relative contribution (of explaining the dependent variable) to the independent variable. Where $S(\hat{p}_i) \in [0, 1]$, zero reflects no uncertainty while one reflects total uncertainty in the sense that P is uniformly distributed.

B. Estimated Models.

The basic time series data for the period 2002–2007 were taken from Eurostat (available at the web site <http://epp.eurostat.ec.europa.eu>):

Dependent variable y:

Electricity prices for household consumers: This indicator presents electricity prices charged to final consumers. Electricity prices for household consumers are defined as follows: Average national price in Euro per miles kWh without taxes applicable for the first semester of each year for medium size household consumers (Consumption Band Dc with annual consumption between 2500 and 5000 kWh).

Independent variables, m:

Electricity generated from renewable sources (% of gross electricity consumption): This indicator is the ratio between the electricity produced from renewable energy sources and the gross national electricity consumption for a given calendar year. It measures the contribution of electricity produced from renewable energy sources to the national electricity consumption. Electricity produced from renewable energy sources comprises the electricity generation from hydro plants (excluding pumping), wind, solar, geothermal and electricity from biomass/wastes. We also have information about *Electricity generated from wind power* and *Electricity generated from hydroelectricity* as % of gross electricity consumption)

Electricity generated from nuclear- % Total gross electricity generation

Electricity generated from natural gas- % Total gross electricity generation

Electricity generated from petroleum - % Total gross electricity generation

Electricity generated from hard coal- % Total gross electricity generation.

These two last variables are used also as proxy of the effects of GHG emissions on prices as electricity generated from petroleum or coal (thermal power stations) are the energy industries with more GHG emissions. We also have considered the variable *Greenhouse gas emissions by Energy industries* (-% total Greenhouse gas emissions).

As variables related to electricity market and its liberalization we consider:

Number of enterprises dedicated to generation of electricity

Number of enterprises dedicated to distribution and trade of electricity

GDP per capita (thousands of euros): Since in Spain there is a part of the electricity price paid by the government, it could be interesting to study the effect of the general economic activity on electricity price.

Moreover as Spain has a high level of *energy dependency* (around 80% levels) we also have into consideration this fact. The most imported energy is gas and petroleum so petroleum prices could have some impacts on electricity price. We use the *brent crude petroleum price* by barrel (in dollars).

For the solution of the optimization the GAMS program version 21.3 (*General Algebraic Modeling System*) is used. This is a programming language which allows diverse optimization problems to be solved.

We first deal with a general maximum entropy model with a reparameterized error. We establish an a priori range for the possible values that may be assumed by error u in the model, which may be employed to assume certain characteristics of its distribution: V . Since this decision is arbitrary, we have assigned a support vector for the errors: $(-v, -v/2, 0, v/2, v)$ for $v > 0$, which guarantees its symmetry around zero. The decision regarding the amplitude of the range of values which it may assume is arbitrary. According with [22] support vector v can be assessed if we perfect knew the variability presented on y and we can use the *three standard deviation rule* as estimation for v . In fact we follow the proposal of [23] who use the sample variance of y (5,38 miles de euros and then $v=16.15$) as an estimate for v . However, as a widening of the error bound by increasing v the estimated weights converge on the uniform distribution (the difference between the weights of the variables is reduced) we have used the most reduced v that makes the solution feasible ($v=7$).

Moreover, we establish an a priori range for the possible values that may be assumed by β in the model. Thus, we should choose the support space Z , and then use the data to estimate the P which in turn yields β . The restrictions imposed on the parameter space through Z should reflect our prior knowledge about the unknown parameters. However, such knowledge is not available as the estimated models are scarce, and we may want to entertain a variety plausible bound on β . However, we have considered a vector support symmetrical and centered on zero and in accordance with the value ranking that the independent variables may take. Moreover, as an initial approximation, we have calculated a covariate matrix finding negative values in β . So, we consider $Z = (-z, 0, z)$ for $z > 0$, which guarantees its symmetry around zero. We consider the same z for all coefficients ($z=0.7$). It implies that we have to be very cautious in the interpretation of the estimated $\hat{\beta}$. As we report $S(\hat{\beta}_i)$ and $S(\hat{\beta}_i) \cong 1$ implies $\hat{\beta}_i \cong 0$ a natural criterion for identification of the information content of a given x_i is just the normalized entropy.

Table I shows our estimated weights for the electricity price (β) under the reparameterized system. We report the estimated coefficients for the model with highest R obtained. The results are those obtained under the narrowest V vector.

The estimated information index $R=0.722$ indicates a reduction of the uncertainty by using the maximization entropy approach, however, the findings yield that the variable *Electricity generated from renewable energies (RES)* does not have sense to explain electricity prices as $S(\hat{\beta}_i) \cong 1$.

Therefore, we tried to study separately the renewable energy sources. In Spain, the largest part of the electricity generation by RES is devoted to wind power and hydro, so we estimate the model with *Electricity generated from wind power* and *Electricity generated from hydroelectricity* variables. Table II shows our new estimated weights for the electricity price (β).

TABLE I. HOUSEHOLD ELECTRICITY PRICE. A MAXIMUM ENTROPY ECONOMETRIC ESTIMATED MODEL.

Variables	$\hat{\beta}_i$	$S(\hat{\beta}_i)$
Electricity generated from RES	0.193	0.833
Electricity generated from nuclear	0.388	0.127
Electricity generated from natural gas	-0.398	0.021
Electricity generated from petroleum	-0.396	0.048
Electricity generated from hard coal	0.399	0.443
Nº enterprises electricity generation	-0.007	1.000
Nº enterprises distribution and trade of electricity	0.399	0.014
GDP per capita	-0.307	0.537
Energy dependency	0.399	0.014
Petroleum price	0.331	0.113
Support vector for the errors $(-v, -v/2, 0, v/2, v)$ $v=7$		
Support space for coefficients $(-z, 0, z)$ $z=0.7$		
Estimated information index $R=0.722$		

TABLE II. HOUSEHOLD ELECTRICITY PRICE . A MAXIMUM ENTROPY ECONOMETRIC ESTIMATED MODEL.

Variables	$\hat{\beta}_i$	$S(\hat{\beta}_i)$
Electricity generated from wind	-0.391	0.095
Electricity generated from hydro	0.116	0.942
Electricity generated from nuclear	0.380	0.183
Electricity generated from natural gas	-0.372	0.234
Electricity generated from petroleum	-0.306	0.540
Electricity generated from hard coal	0.397	0.035
Nº enterprises electricity generation	-0.006	1
Nº enterprises distribution and trade of electricity	0.361	0.298
GDP per capita	0.062	0.984
Energy dependency	0.399	0.014
Petroleum price	0.361	0.299
Support vector for the errors $(-v, -v/2, 0, v/2, v)$ $v=7$		
Support space for coefficients $(-z, 0, z)$ $z=0.7$		
Estimated information index $R=0.58$		

The results give us additional information with respect to the first model about the direction in which the RES affect the dependent variable. *Electricity generated from wind* is a very important variable ($S(\hat{\rho}_1) = 0.095$) which contributes to reduce electricity prices. Moreover, when *electricity generated from hard coal* increases the electricity prices, these increases could be in part due by the cost of the GHG emissions which have to be paid by hard coal based energy industries. Energy dependence has also an important effect.

Regarding to the electricity market liberalization variables, the *number of enterprises dedicated to electricity generation* does not have sense to explain electricity prices. However, the *Number of enterprises dedicated to distribution and trade of electricity* gives more information to explain y as $S(\hat{\rho}_1) = 0.298$, nevertheless it has a positive effect on electricity prices. Electricity market opening does not necessarily imply effective competition and competitive prices. Achieving competitive prices depends on the number of the players and the nature of consumer demand as consumers could be resistant to switching.

IV. MAIN FINDINGS AND CONCLUDING REMARKS

We have analyzed the role of some economic and environmental variables on electricity price in Spain for the time period 2002-2007, applying Theory Information Approach due the small sample size.

By applying the General Maximum Entropy Estimation Approach, it becomes possible to estimate a model bearing in mind all, and only, the limited information available which would not be possible with more traditional estimation methods.

Regarding the price effects of renewable energies, since the majority of renewable energy technologies are not profitable at current energy prices, they are expected to increase energy costs.

In addition, environmental costs related to CO₂ emissions in electricity generation in general have a significant negative effect on energy costs. Moreover, the regulatory reforms in the Spanish Electricity Market also could have its effect on electricity prices.

The results showed that electricity generated from wind contributes to reduce electricity prices. Moreover, when electricity generated from hard coal increases the electricity prices, these increases could be in part due by the cost of the GHG emissions which have to be paid by hard coal based energy industries. Energy dependence has also an important effect on electricity prices in Spain.

The liberalization of electricity industry, in retail activities, has a positive effect on electricity prices. Electricity market opening does not necessarily imply effective competition and competitive prices. Achieving competitive prices depends on the number of the players and the nature of consumer demand as consumers could be resistant to switching.

REFERENCES

- [1] P.M. Connor, "UK renewable energy policy: a Review", *Renewable and Sustainable Energy Reviews*, n°7, 2003, pp. 65-82.
- [2] B. Hillebrand, H.G. Buttermann, J.M. Behringer, J.M. and M. Bleuel, "The expansion of renewable energies and employment effects in Germany", *Energy Policy*, vol. 34, 2006, pp. 3484-3494.
- [3] B. Moreno and A.J. López, "The effect of renewable energy on employment: The case of Asturias (Spain)", *Renewable and Sustainable Energy Reviews*, vol. 12, 2008, pp. 732-751
- [4] M. Rathmann, "Do support systems for RES-E reduce EU-ETS-driven electricity prices?", *Energy Policy*, vol. 35, 2007, pp. 342-349.
- [5] S. Jensen and K. Skytte, "Simultaneous attainment of energy goals by means of green certificates and emission permits", *Energy Policy*, vol. 31, 2003, pp. 63-71.
- [6] D.J. Swider, L. Beurskens, S. Davidson, J. Twidell, J. Pyrko, W. Prügler, H. Auer, K. Vertin and R. Skema, "Conditions and costs for renewables electricity grid connection: Examples in Europe", *Renewable Energy*, vol. 33, 2008, pp. 1832-1842.
- [7] L. Dale, D. Milborrow, R. Slark and G. Strbac, "Total cost estimates for large-scale wind scenarios in UK," *Energy Policy*, vol. 32, 2004, pp. 1949-1956.
- [8] H. Nagayama, "Effects of regulatory reforms in the electricity supply industry on electricity prices in developing countries", *Energy Policy* vol. 35, 2007, pp. 3440-3462.
- [9] H. Nagayama, "Electric power sector reform liberalization models and electric power prices in developing countries. An empirical analysis using international panel data", *Energy Economics*, vol. 31, 2009, pp. 463-472.
- [10] A. Golan, "Information and entropy econometrics –Editor's view", *Journal of Econometrics*, vol. 107, 2002, pp. 1-15.
- [11] C.E. Shannon, "A Mathematical Theory of Communication", *Bell System Technology Journal*, vol. 27, pp. 379-423.
- [12] E.T. Jaynes, "Information Theory and Statistical Mechanics I", *Physics Review*, vol. 196, 1957, pp. 620-630.
- [13] E.T. Jaynes, "Information Theory and Statistical Mechanics II", *Physics Review*, vol. 108, 1957, pp.171-190.
- [14] A. Golan, G. Judge and D. Miller, *Maximum Entropy Econometrics: robust estimation with limited data*. John Wiley & Sons Ltd: London, 1996.
- [15] Law 54/1997, of 27 of November, of Electricity Industry.
- [16] Directive 2001/77/EC of the European Parliament and of the Council of 27 September 2001 on the promotion of electricity produced from renewable energy sources in the internal electricity.
- [17] Directive 2009/28/EC of the European Parliament and of the Council of 23 April 2009 on the promotion of the use of energy from renewable sources and amending and subsequently repealing Directives 2001/77/EC and 2003/30/EC.
- [18] Royal Decree 661/2007, BOE 178, 26/07/2007.
- [19] A. Golan, "A multi-variable stochastic theory size distribution of firms with empirical evidence", *Advances in Econometrics*, vol. 10, 1994, pp.1-46.
- [20] E.S. Soofi, "A generalizable formulation of conditional logit with diagnostics", *Journal of the American Statistical Association*, vol. 89, 1992, pp.1243-1254.
- [21] E.S. Soofi, "Capturing the intangible concept of information", *Journal of the American Statistical Association*, vol. 89, 1994, pp. 1243-1254.
- [22] F. Pukelsheim, "The three sigma rule", *The American Statistician*, vol. 48, n° 2, 1994, pp. 88-91
- [23] A. Golan, G. Judge and D. Perloff, "Estimation and inference with censored and ordered multinomial response data", *Journal of Econometrics*, vol. 79, 1997, pp. 23-51.

The Impact of Renewable Energies and Electric Market Liberalization on Electrical Prices in the European Union. An Econometric Panel Data Model.

Blanca Moreno
Department of Applied Economics
University of Oviedo
Oviedo, Spain
e-mail: morenob@uniovi.es

Ana Jesús López
Department of Applied Economics
University of Oviedo
Oviedo, Spain
e-mail: anaj@uniovi.es

Abstract— A controversial debate has arisen about the effects on household electricity prices of electricity generation from Renewable Energy Sources and regulatory reforms in the European Union Electricity Market. In this paper we propose to use panel data models with the aim of explaining the household electricity prices as a function of several economic variables related to renewable energy sources and electricity market regulation. More specifically we use a panel data set provided by Eurostat and covering 27 European Union countries during the period 1998–2009. Our results suggest that electricity prices increase with the deployment of Electricity from Renewable Energy Sources.

Keywords—renewable energy, electricity market, panel data model.

I. INTRODUCTION

There is a controversial debate about the effects of the promotion of renewable energy and electric power sector reforms on electricity prices.

The European Union has emphasized the need to control climate change and then it has assumed a binding unilateral greenhouse gas emission reduction target for 2020, according to which the EU is committed to reducing emissions to at least 20% below 1990 levels. In order to achieve this target the European Union is working on the development of renewable energy industries, the implementation of energy efficiency measures and saving energy technologies.

More specifically, the Community Directive 2009/28/EC [1] on the promotion of the use of energy from renewable sources has agreed European targets for 2020: European Union should achieve by 2020 a 20% share of Renewable Energy Sources (RES) in the Community's gross final consumption of energy and a 10% share of energy from renewable sources in transport energy consumption.

The EU sustainable development strategy [2] recognises that environmental investments as well as technological innovation are the prerequisites for long-term competitiveness and better environmental protection.

Therefore, the development of renewable energy industries and energy-saving technologies provides several

positive effects, mainly with reference to the expected increase in energy self-sufficiency, employment, investment and production¹, but it also has some costs related to the adjustments in production, prices and transportation systems

Regarding the effects on prices, the majority of renewable energy technologies increase electricity generation costs with regard to conventional generation so they are expected to increase the electricity price paid by final consumers. In fact, there are three principal components of extra costs: the generation costs, the costs of distribution and transmission system reinforcements and, in the case of the intermittent renewals, the extra balancing costs.

In the European Union the largest part of the investments for electricity production was devoted to new wind power stations and Photovoltaic and Solar thermal systems as we can see in Table I.

The generation of Electricity from Renewable Energy Sources (RES-E) especially from wind and photovoltaic power, can increase generation costs when compared with conventional generation. A number of recent studies have sought to quantify the costs associated with large-scale renewable generation by wind ([6], [7] and [8] among others).

Moreover, the majority of renewable energy technologies are not profitable at current energy prices so their development is mainly driven by different public renewable support schemes: feed in tariffs, quota obligations, green-certificate trading, fiscal measures as tax benefits, investment grants, etc. Some important classification criteria are whether policy instruments address to price or quantity, and whether they support investment or generation. A classification of the existing promotion strategies for renewals is provided in [9].

¹ Several studies have reviewed the effects of the introduction of renewable energies at EU country level. This is the case of [3] for the United Kingdom or [4] for Germany. Other studies as [5] have analysed the macroeconomic RES impact at local level.

TABLE I. EU INFRASTRUCTURE FOR ELECTRICITY PRODUCTION. NET INSTALLED CAPACITY (MEGAWATT)

Infrastructures	Percentage of change 2000-2007
Thermal power stations	10.31
Nuclear power stations	-3.25
Hydro power stations	2.08
Pumped storage plants	5.10
Wind-turbines	339.75
Geothermal plants	15.56
Steam turbine power plants	:
Gas turbine power plants	:
Combined cycle power plants	:
Internal combustion engine plants	:
Public power plants	12.18
Autoproducer power plants	24.65
Photovoltaic systems	2540.56
Solar thermal systems	1200.00
Municipal solid wastes	141.13
Biogas	218.22
Industrial wastes	-20.79

Source of data: Eurostat, http://epp.eurostat.ec.europa.eu/portal/page/portal/statistics/search_database: Statistics data base/Energy Statistics/infrastructure/electrical infrastructure.

Most RES-E support systems are financed via the electricity market, which increases the retail electricity price. Therefore promotion systems have costs for the final consumers. For example, [10] shows that Quota-based Tradable Guarantee-of-Origin Certificates systems as well as Feed-in tariff systems create an artificial market and cause policy costs (¼ additional costs to be usually paid by electricity customers).

In Table II we summarise the main promotion mechanism implemented in specific EU countries. Quota-based systems are now in place in the UK, Sweden, Italy, Belgium, and Poland. Moreover, as each country has different targets set in Directive 2009/28/EC [12], the dimension of policy support can be different thus following in different effects on electricity prices.

In addition, environmental costs related to CO₂ emissions in electricity generation usually have a significant negative effect on energy costs as a CO₂ emission trading scheme (ETS) exists. The substitution of conventional electricity generation by renewable energies could reduce the cost derived from environmental emissions and the electricity price. Support systems for Electricity from Renewable Energy Sources (RES-E) can reduce electricity prices that have also been influenced by a CO₂ Emission Trading Scheme (ETS): Additional RES-E substitute electricity from fossil fuels, and thus CO₂-emissions are reduced. The demand for emission reductions is lowered; as a result the CO₂ price is also reduced and consequently the wholesale price for electricity decreases [13].

TABLE II. RES-E PROMOTION MECHANISM IMPLEMENTED IN EUROPEAN UNION COUNTRIES

EU members	Feed in Tariff	Quota-based Tradable Guarantee-of-Origin Certificates	Fiscal incentives
Austria	X		
Belgium		X	
Bulgaria	X		X
Cyprus	X		
Czech Republic	X		
Denmark	X		
Estonia	X		
Finland			X
France	X		
Germany	X		
Greece	X		
Hungary	X		
Ireland	X		
Italy		X	
Latvia	X		
Lithuania	X		
Luxembourg	X		
Malta	X		
Netherlands		X	
Poland		X	
Portugal	X		
Romania			
Slovak Republic	X		
Slovenia	X		
Spain	X		
Sweden		X	
United Kingdom		X	

Source [11]

It is also necessary to consider that a higher use of renewable energies could reduce even the electricity final prices because its promotion stimulates the generation of renewable energy which is characterized by variable costs lower than fossil conventional technologies [14].

Regarding the legislative aspects, the regulatory reforms in the EU Electricity Market could also have effects on electricity prices. In fact the liberalization of generating and retailing activities could increase competition thus reducing electricity prices.

Following the EU Directives 96/92/EC [15] and 2003/54/EC [16] the electricity markets in Europe were fully liberalized the 1st of July 2007. Since then all electricity users are able to choose their own suppliers, and electricity network service providers are separated from generating and/or supply companies.

This liberalization of the European electricity markets aims to increase efficiency by competition, thus decreasing electricity prices for final consumers.

However, as [17] points out, market liberalization does not necessarily imply effective competition and competitive prices. Achieving competitive prices depends on the number

of enterprises and the nature of consumer to switch. The combination of low elasticity to prices and a small number of competitors means that market prices can easily deviate from competitive levels.

Regarding the production market structure, the liberalization in many of the EU countries in the generation sector has not provided a less concentrated market structure.

In Figure 1 we can see that the market share of the largest generator in the electricity market has not a significant decrease for the majority of the EU countries from 1999 to 2008. This lack of competition may allow electricity prices on the wholesale markets to increase, thus leading to higher retail electricity prices, especially for household consumers.

Therefore, there are several economic variables related to renewable energy sources and electricity market regulation affecting the electricity prices. During the last years several studies have been developed in order to explain the effect of several variables on electricity prices using cross-sectional, temporal or panel data. Some of them include explanatory variables related to energy use or technology [18] and [19] or liberalization market [20] [21]. In this paper we propose an empirical study including all the potential effects together and therefore we propose panel data models with the aim of explaining the household electricity prices as a function of variables related to renewable energy sources and electricity market regulation. The main objective of our empirical work is to explain some differential aspects of the European Union member countries in the electricity prices.

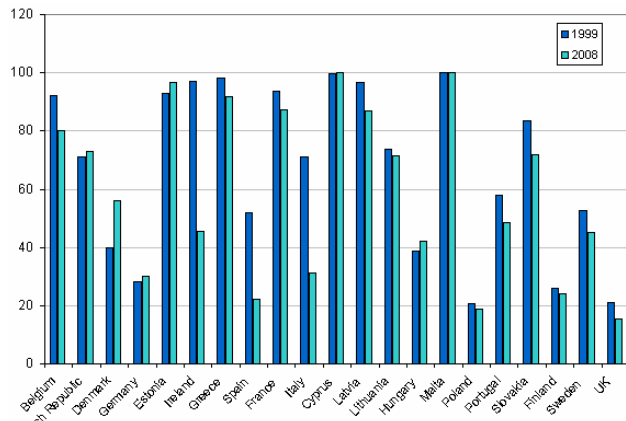


Figure 1. Market share of the largest generator in the electricity market. Percentage of the total generation. Source of data: Eurostat.

http://epp.eurostat.ec.europa.eu/portal/page/portal/statistics/search_database

II. MODELLING THE IMPACT OF RENEWABLES ON ELECTRICITY PRICES. PANEL DATA MODELS

The European Union is working in the development of renewable energy industries, the implementation of energy efficiency measures and saving energy technologies. Within this framework countries pledge to make substantial efforts in their energy policy. However, each country tries to effectively implement renewable energies according to its own characteristics such as energy consumption, energy diversity or composition of electricity generation.

Moreover, the RES-E policy support and dimension of each EU member can vary, leading to different effects in electricity prices. With regard to the market liberalization each country has particularities in its market structure, size (number of enterprises) and consumer demand.

All these differences lead to a wide range of household electricity prices in the EU countries as we can see in Figure 2.

In this section we propose panel data models with the aim of explaining the household electricity prices as a function of several economic variables related to renewable energy sources and electricity market regulation. More specifically we use a panel data set provided by Eurostat and covering 27 countries of the EU during the time period 1998–2009.

The basic country-level time series data for the period 1998–2009 were taken from Eurostat (available at the web site <http://epp.eurostat.ec.europa.eu>).

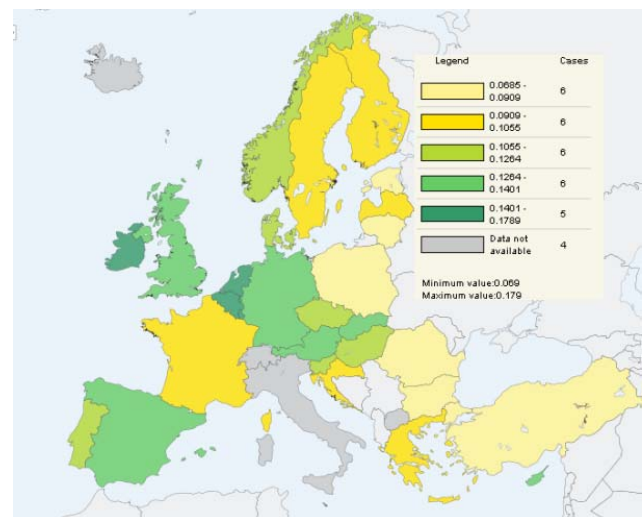


Fig. 2. Electricity prices for household consumers €/kWh (year 2009). Source of data: Eurostat.

http://epp.eurostat.ec.europa.eu/portal/page/portal/statistics/search_database

The considered dependent variable is *Electricity prices for household consumers*. This indicator measures electricity prices charged to final consumers, which are defined as follows: Average national price in Euro per kwh without taxes applicable for the first semester of each year for medium size household consumers (Consumption Band Dc with annual consumption between 2500 and 5000 kwh). Until 2007 the prices are referring to the status on the 1st of January for medium size consumers.

We propose the following explanatory variables related to renewable energy sources and electricity market regulation:

- Electricity generated from renewable sources - % of gross electricity consumption (RES-E). This indicator is computed as the ratio between the electricity produced from renewable energy sources and the gross national electricity consumption for a given year. Electricity produced from renewable energy sources comprises the electricity generation from hydro plants (excluding pumping), wind, solar, geothermal and electricity from biomass/wastes. We expect a positive estimated effect of this variable on electricity prices as the generation of Electricity from Renewable Energy Sources (RES-E) increases generation costs and their development is mainly driven by different public renewable support schemes.
- Percentage of Greenhouse gas emissions (GHG) by Energy industries as a total of Greenhouse gas emissions (Energy Industries Emissions). We expect a positive estimated effect of this variable on prices as emission trading schemes exist.
- Market share of the largest generator in the electricity market- Percentage of the total generation (Electricity Generation Competition-ECG). This indicator shows the market share of the largest electricity generator in each country. To compute this variable, the total net electricity production during each reference year is considered, meaning that the electricity used by generators for their own consumption is not taken into account. Then, the net production of each generator during the same year is considered in order to calculate the corresponding market shares, and only the largest market share is reported under this indicator. As a result a positive effect of this variable on electricity prices is expected, since market share increases also increment the market power thus leading to higher electricity prices.
- Gross Domestic Product, GDP per capita, measured in Purchasing Power Standards PPS- (GDPpps). This variable aims to study the effect of the general economic activity on electricity prices. Besides the convenience of considering the general economic context, the inclusion of this indicator is particularly interesting in some European Countries (as in Spain) where part of the electricity price is paid by the government through state budgets.

In the described situation the use of panel data techniques could be advisable if significant country effects exist, allowing us to determine if there are differences at country-level among the European Union member states.

We specify the following panel regression model:

$$y_{i,t} = \alpha_i + \beta_1 R ESE_{it} + \beta_2 EGC_{it} + \dots + \beta_4 GDPpps_{it} + u_{it}$$
 where $i=1, \dots, 27$, $t=1998, \dots, 2009$.

Parameters α_i denote country effects and they are included in the model with the aim of capturing the specific effects related to the different EU countries, since the omission of these terms might lead to biased estimates. The disturbances of this model are denoted by u_{it} and are assumed to be independently and identically distributed random variables with mean zero and variance σ_u^2 .

In order to identify the most suitable specification, the proposed model has been estimated considering both fixed and random effects². According to the fixed effects model α_i is considered as a regression parameter while the random effects model treats it as a component of the random disturbance. In order to establish whether the fixed or the random effects estimator is more appropriate a Hausman test is performed [26].

If the effects α_i are correlated with the explanatory variables, then the random effects model cannot be consistently estimated, and the Hausman test can be used to test for inconsistency in the random effects estimation by comparing the fixed-effects and random-effects estimated coefficients (a significant difference indicates that the random effects model is estimated inconsistently). In other words, the null hypothesis of the Hausman test is that individual country effects are uncorrelated with the other explanatory variables and thus the random-effects model is the most appropriate estimator.

The obtained value for the Hausman test statistic is 39.81 and the related p -value (approximately 0) leads to a rejection of the null hypothesis of strict exogeneity. Therefore, we conclude that the fixed effects model is better than the random effects option.

Further, the existence of country specific effects has been checked through the F test (whose null hypothesis is the existence of equal α_i for all the countries). If the individual country effect α_i is assumed to be equal across all countries, then the pooled Ordinary Least Square are consistent and efficient.

The obtained results are summarized in Table III confirming the existence of country-specific effects (The F test statistic leads to the rejection of the null hypothesis at the 1% level). As a result, different α_i are assumed in order to control for unobserved heterogeneity of EU-27 members as significant differences between countries in electricity prices exist.

² The details about panel data econometrics can be seen in [22], [23], [24] and [25], amongst others.

TABLE III. ESTIMATED FIXED PANEL DATA MODEL FOR HOUSEHOLD ELECTRICITY PRICES (PANEL DATA SET COVERING 27 EU COUNTRIES DURING THE PERIOD 1998–2009).

Explanatory Variables	Estimated parameters
RES-E (%)	0.00167 ^{***}
Electricity Generation Competition (%)	-0.000559 ^{**}
Energy Industries Emissions (%)	0.00181 ^{**}
GDPpps	0.001 ^{**}
R ²	0.80
Hausman test	39.81 ^{***}
F test (country-specific effects)	24,175 ^{***}

(1) **significant at 5%; ***significant at 1%.

(2) Robust regression is used to adjust the results for heterokedasticity

The fixed effects estimated model has a good explanatory power (the overall goodness of fit is 80%).

The panel regression results indicate that, according to the t-test, the overall considered variables are statistically significant at 5% level. The variable Electricity generated from RES has a positive estimated coefficient, showing that a 1% increasing in RES-E, holding constant all other explanatory variables, causes an increase of 0.00167 Euro per kwh in the household electricity prices.

Moreover, Energy Industries Emissions and GDPpps have also estimated positive effects on electricity prices. More specifically, by increasing 1% the Green Gas Emissions produced by Energy Industries the electricity price would increase in 0.00181 Euros per kwh (holding constant all other variables). The positive estimated effect of the GDP per capita on electricity prices could indicate that the RES-E promotion expenditures in countries with higher income are usually supported by increasing electricity prices paid at the end by the consumers (in stead of state budgets).

Lastly, the variable related to the liberalization of electricity generation (Electricity Generation Competition) has a negative impact on household electricity prices. This result does not fulfil our initial expectations as it is generally expected that liberalization of generating activities increase competition thus reducing electricity prices.

In fact, when market share of the largest generator in the electricity market decreases 1% (holding constant all other variables) the household electricity prices are expected to increase in 0,00056 Euro per kwh. Therefore, Electricity market liberalization does not necessarily imply effective competition and competitive prices. Achieving competitive prices depends on the number of players, the nature of electricity supply and the nature of consumer demand.

Since the largest part of the EU electricity generation by RES is devoted to wind power and hydro, we estimate the model including the explanatory variables *Electricity generated from wind power* and *Electricity generated from hydroelectricity*, obtaining the results summarized in Table IV. In this new model, the Hausman test for the null of random effects versus fixed effects leads to a chi-squared statistic with a value of 10,56 and therefore random components can not to be rejected at 5% of significance.

TABLE IV. ESTIMATED RANDOM PANEL DATA MODEL FOR HOUSEHOLD ELECTRICITY PRICES (PANEL DATA SET COVERING 27 EU COUNTRIES DURING THE PERIOD 1998–2009).

Explanatory Variables	Estimated parameters
RES-E from Wind (%)	0.0025 ^{***}
RES-E from Hydro (%)	-0.0001
Electricity Generation Competition (%)	-0.0003 ^{***}
Energy Industries ´ Emissions (%)	-0.0004
GDPpps	0.0003 ^{**}
Log-likelihood	400.74
Hausman test	10.56 [*]
Breusch-Pagan test (country-specific effects)	354.96 ^{***}

(1) **significant at 5%; ***significant at 1%.

(2) Robust regression is used to adjust the results for heterokedasticity

According to the estimated t statistics, the RES-E for hydro and Energy Industries ´ Emissions are not significant explanatory variables.

Regarding Electricity generated from wind, the estimated coefficient suggests that an 1% increasing in this variable (holding constant all other variables) leads to an increase of 0.0025 euros per kwh in household electricity prices.

III. MAIN FINDINGS AND CONCLUDING REMARKS

The liberalization of electricity markets in Europe aims to increase competition, thus decreasing electricity prices for the final consumers. However, the promotion of European electricity generation from renewable energy (RES-E) could have an opposite effect on electricity prices.

In the framework of a controversial debate about the effects of RES-E on household electricity prices, this paper explores the impact of several economic variables on household electricity prices in the European Union.

With this aim, panel data models are estimated trying to explain the household electricity prices as a function of several economic variables related to renewable energy sources and electricity market regulation: Electricity generated from renewable sources, Greenhouse gas emissions produced by Energy industries and Market share of the largest generator in the electricity market. The panel data set is provided by Eurostat covering 27 EU countries during the period 1998–2009 and the obtained results indicate that electricity prices increase with the deployment of RES-E and also with the increased emissions of energy industries.

Regarding the liberalization of electricity generation, our findings suggest that when the market share of the largest generator in the electricity market decreases 1% the household electricity prices increases in 0,00056 euro per kwh. Therefore, the liberalization of Electricity markets does not necessarily imply effective competition and competitive prices.

REFERENCES

- [1] European Parliament & European Council. Directive 2009/28/EC of the European Parliament and of the Council of 23 April 2009 on the promotion of the use of energy from renewable sources and amending and subsequently repealing Directives 2001/77/EC and 2003/30/EC. 2009. Brussels.
- [2] European Council. Renewed EU sustainable development strategy. European Council on 15/16 June 2006 DOC 10917/06. DOC 10917/06: 2006. Brussels.
- [3] P.M. Connor, "UK renewable energy policy: a Review", *Renewable and Sustainable Energy Reviews*, n^o7, 2003, pp. 65-82.
- [4] B. Hillebrand, H.G. Buttermann, J.M. Behringer, J.M. and M. Bleuel, "The expansion of renewable energies and employment effects in Germany", *Energy Policy*, vol. 34, 2006, pp. 3484-3494.
- [5] B. Moreno and A.J. López, "The effect of renewable energy on employment: The case of Asturias (Spain)", *Renewable and Sustainable Energy Reviews*, Vol. 12, 2008, pp. 732-751
- [6] L. Dale, D. Milborrow, R. Slark and G. Strbac, "Total cost estimates for large-scale wind scenarios in UK," *Energy Policy*, vol. 32, 2004, pp. 1949-1956.
- [7] A. Demireren and U. Yilmaz, "Analysis of change in electric energy cost with using renewable energy sources in Gökceada, Turkey: An island example", *Renewable and Sustainable Energy Reviews*, Vol. 14, 2010, pp. 323-333.
- [8] D.J. Swider, L. Beurskens, S. Davidson, J. Twidell, J. Pyrko, W. Prügler, H. Auer, K. Vertin and R. Skema, "Conditions and costs for renewables electricity grid connection: Examples in Europe", *Renewable Energy*, Vol. 33, 2008, pp. 1832-1842.
- [9] R. Haas, C. Panzer, G. Resch, M. Ragwitz, G. Reece and A. Held, "A historical review of promotion strategies for electricity from renewable energy sources in EU countries", *Renewable and Sustainable Energy Reviews*, Vol. 15, 2011, pp. 1003-1034.
- [10] R. Haas, G. Resch, C. Panzer, S. Busch, M. Ragwitz and A. Held, "Efficiency and effectiveness of promotion systems for electricity generation from renewable energy sources: Lessons from EU countries", *Energy*, 2008., in press.
- [11] European Commission: The Support of Electricity from Renewable Energy Sources Accompanying Document to the Proposal for a Directive of the European Parliament and of the Council on the Promotion of the Use of Energy from Renewable Sources., COM(2008) 19. Brussels, 2008, SEC(2008) 57.
- [12] European Parliament & European Council, Directive 2009/28/EC of the European Parliament and of the Council of 23 April 2009 on the promotion of the use of energy from renewable sources and amending and subsequently repealing Directives 2001/77/EC and 2003/30/EC: 2009. Brussels.
- [13] M. Rathmann, "Do support systems for RES-E reduce EU-ETS-driven electricity prices?", *Energy Policy*, vol. 35, 2007, pp. 342-349.
- [14] S. Jensen and K. Skytte, "Simultaneous attainment of energy goals by means of green certificates and emission permits", *Energy Policy*, vol. 31, 2003, pp. 63-71.
- [15] European Parliament & European Council, Directive 96/92/EC of the European Parliament and of the Council of 19 December 1996 concerning common rules for the internal market in electricity: 1996, Brussels.
- [16] European Parliament & European Council, Directive 2003/54/EC of the European Parliament and of the Council of 26 June 2003 concerning common rules for the internal market in electricity and repealing Directive 96/92/EC: 2003. Brussels
- [17] T. Jamasb, M. Pollitt(2005). *Electricity Market Reform in the European Union: Review of Progress towards Liberalisation and Integration*. Cambridge Working Papers in Economics CWPE 0471.
- [18] D.J. Swider, L. Beurskens, S. Davidson, J. Twidell, J. Pyrko, W. Prügler, H. Auer, K. Vertin and R. Skema, "Conditions and costs for renewables electricity grid connection: Examples in Europe", *Renewable Energy*, vol. 33, 2008, pp. 1832-1842.
- [19] L. Dale, D. Milborrow, R. Slark and G. Strbac, "Total cost estimates for large-scale wind scenarios in UK," *Energy Policy*, vol. 32, 2004, pp. 1949-1956.
- [20] H. Nagayama, "Effects of regulatory reforms in the electricity supply industry on electricity prices in developing countries", *Energy Policy* vol. 35, 2007, pp. 3440-3462.
- [21] H. Nagayama, "Electric power sector reform liberalization models and electric power prices in developing countries. An empirical analysis using international panel data", *Energy Economics*, vol. 31, 2009, pp. 463-472.
- [22] J. M. Wooldridge, *Econometric Analysis of Cross Section and Panel Data*. MIT Press, 2001.
- [23] C. Hsiao, *Analysis of panel data*. Cambridge. Cambridge: University Press, 1990.
- [24] Y. Mundlak, "On the pooling of time series and cross section data," *Econometrica*, vol. 46, 1978, pp. 69-85.
- [25] B.H. Baltagi, *Econometric Analysis of Panel Data*. Wiley, 1995.
- [26] J. A. Hausman, "Specification Tests in Econometrics," *Econometrica*, vol. 46, 1978, pp. 1251-1271.

Interactions Between BTEX, TPH, and TCE During Their bio-removal from the Artificially Contaminated Water

Yiqin Chen, Junhui Li, Chengkeng Lei, and Hojae Shim
 Department of Civil and Environmental Engineering
 Faculty of Science and Technology, University of Macau
 Taipa, Macau SAR, China
 Yiqin CHEN: celerychenyiqin@gmail.com
 Junhui LI: Lee.environmentalist@gmail.com
 Chengkeng LEI: ma86563@umac.mo
 Hojae SHIM: hjshim@umac.mo

Abstract— Many environmental sites are becoming contaminated by mixed wastes, including such organic compounds as BTEX (benzene, toluene, ethylbenzene, and three isomers of xylene), TPH (total petroleum hydrocarbons), and CAHs (chlorinated aliphatic hydrocarbons) including TCE (trichloroethylene). TCE, as a representative CAH, has been widely used in various industrial processes and is among the most prevalent hazardous organic compounds present in the environment. In this study, a microbial pure culture enriched and isolated from a heavily oil-contaminated site in Xiamen, China, was used to remove mixtures of BTEX, TPH, and TCE under different pHs (5, 7, and 9) at 25°C, from the artificially contaminated water and to assess the interactions between those compounds during their bio-removal. The mixtures of BTEX (BTE_oX, BTE_mX, and BTE_pX) and TPH showed different trends when TCE added to the mixture. TCE showed an inhibitory effect on bio-removal of *o*-xylene in BTE_oX mixture, while it showed a stimulatory effect on the overall removal efficiencies for BTE_mX and BTE_pX mixtures. On the other hand, TCE was the most efficiently removed when mixed with BTE_oX and TPH, except at pH 5, while less removed in other mixtures at almost similar amounts, regardless of pH. The highest removal of BTEX and TPH occurred at pH 7 or 9, while the highest removal of TCE occurred at pH 7, regardless of mixtures.

Keywords – BTEX; interaction; mixture; pH; TCE; TPH

I. INTRODUCTION

Due to the industrialization, petroleum production is not only the primary source of fuel but also the contamination source of soil and groundwater [1]. Besides of basic usage of these productions, lots of them are lost by leakage. Major causes of crude oil-contaminated soil include leaking storage tanks and pipelines, land disposal of petroleum waste, and accidental or intentional spills [2]. There are many compounds in petroleum. Benzene, toluene, ethylbenzene, and three isomers (*ortho*-, *meta*-, and *para*-) of xylene, collectively known as BTEX, are among these compounds, which are also widely used as industrial solvents for organic synthesis and equipment cleansing [3]. Trichloroethylene (TCE) is widely used in various industrial processes, such as industrial dry cleaning, textile manufacturing, etc. It is among the most prevalent hazardous organic compounds

present in the environment [4]. TCE is also carcinogenic and would cause other serious health effects on humans [5].

There have been lots of studies focused on removing these contaminants. Among all the current technologies, biological treatment is regarded as the most economical and environmentally sound approach [6]. However, no microorganism capable of growing on TCE as a sole carbon or energy source has yet been isolated [7]. Instead, several anaerobic and aerobic bacteria are known to degrade TCE by the co-metabolic transformation. Hence, a non-growth-supporting substrate is transformed through the catalysis of non-specific enzymes synthesized by bacteria in the presence of a growth substrate [8].

Many studies have proved that TCE has an inhibitory effect to other compounds during the bio-removal process. TCE significantly inhibited phenol degradation during the degradation of phenol and trichloroethylene by *Pseudomonas cepacia* G4 [9]. TCE was regarded an inhibitor to 1,1-dichloroethylene bio-removal [10] and also showed an inhibitory effect to isopropyl alcohol [11]. On the other hand, the efficacy of TCE biodegradation varies with different compounds under different conditions. The combination of BTEX, TPH, and TCE can be frequently found in the environment.

The efficacy of biodegradation is also influenced by a number of factors including bioavailability, quality and quantity of contaminants, temperature, pH, and oxygen. These factors are essential for formulating successful bioremediation strategies [8]. In this study, one indigenous microorganism isolated from a heavily oil-contaminated site in Xiamen, China was used to remove mixtures of BTE_om/pX (350 mg/L), TPH (1,000 mg/L), and TCE (15 mg/L) under three different pH values (5, 7, and 9) at 25°C, from the synthetic contaminated water. Indigenous microorganisms were first enriched and isolated from the contaminated soil. The interaction between BTEX, TPH, and TCE during their bio-removal from the artificially contaminated water under different pH conditions was evaluated. Results would help find out the interactions and the most appropriate combination of contaminants and environmental conditions when the bioremediation technology applied to the mixed wastes contaminated sites.

II. MATERIALS AND METHODS

A. Chemicals

Benzene (purity, 99.7%), toluene (purity, 99%), ethylbenzene (purity, 99%), *ortho*-xylene (purity, 99%), *meta*-xylene (purity, 99%), and *para*-xylene (purity, 99%) were purchased from the International Laboratory (USA). TCE (purity, 99%) was purchased from Da Mao Chemical Manufacture in Tianjin, China. TPH were purchased from the Caltex Company in Macau Special Administrative Region (SAR), China, and the TPH stock solution was prepared using the 1:1 ratio (v/v) of unleaded gasoline and diesel mixed with [dimethylformamide](#) (DMF).

B. Soil sample collection

Indigenous microorganisms were isolated from the soil samples, potentially contaminated with petroleum compounds and obtained from a site near a gas station in Xiamen, China. Soil samples were stored in a freezer until use.

C. Enrichment and isolation

The microbial pure cultures were enriched and isolated from the soil sample. Soil sample (5%, w/w) was first added into the nutrient broth (contained 3.0 g/L beef extract and 5.0 g/L peptone) in a serum bottle, and then 150 mg/L of toluene was added as a substrate for the microbial growth. After the serum bottles were covered with stoppers (90% teflon/10% silicone) and aluminum crimp sealed, they were inverted and placed on an orbital shaker (IKA) at 150 rpm and 25°C. Then, 10% (v/v) inocula from these bottles were aseptically inoculated into the mineral salts medium (MSM contained KH_2PO_4 1.0 g/L; K_2HPO_4 1.0 g/L; NH_4NO_3 1.0 g/L; $\text{MgSO}_4 \cdot 7\text{H}_2\text{O}$ 0.2 g/L; $\text{Fe}_2(\text{SO}_4)_3$ 0.5 g/L; and CaCO_3 0.02 g/L) containing 150 mg/L of toluene as a sole substrate. After several weeks of subculturing, pure cultures were isolated from the bottles by using nutrient agar (NA) plates. The pH of medium was adjusted by adding HNO_3 (1.0 mol/L) or NaOH (1.0 mol/L) solution. All the apparatus and media were autoclaved (HIRAYAMA) for 20 min at 121°C, under 15 psi (103.5 kPa) in advance.

Several microbial colonies with different morphologies were chosen from the NA plates and aseptically transferred to test tubes containing MSM with 150 mg/L of toluene. After the tubes were incubated on the shaker at 150 rpm and 25°C, one microbial pure culture from the soil sample, which showed higher turbidities by measuring optical density (OD) at 600 nm and higher toluene removal efficiencies, was chosen for further experiments. The selected pure culture was further transferred, 10% (v/v), into the newly prepared MSM containing mixtures of BTEX and TPH.

D. Analytical methods

The concentrations of BTEX, TPH, and TCE were measured using a gas chromatograph (Agilent, 6890N, Agilent Technologies Co., Ltd, China) equipped with a flame ionization detector (FID) and a capillary column (HP-5; 30 m \times 0.53 μm I.D. with a stationary-phase film thickness of

0.88 μm). One microliter of liquid samples was injected by the autosampler injector (7638 Series, Agilent Technologies Co., Ltd, China) equipped with a tapered microsyringe (5181-1267, Hamilton Company, USA). Nitrogen was used as a carrier gas. The inlet and detector temperatures were 280°C and 300°C, respectively. The column temperature was programmed as initial temperature, 40°C (hold for 2 min), then incrementally increased at 12°C/min to 300°C (hold for 10 min).

E. Bio-removal of mixtures

After several weeks of subculturing, the pure cultures (10%, v/v) were added into the fresh MSM which contained different concentrations of BTEo/m/pX/TPH/TCE mixtures at different pH values (5, 7, and 9) at 25°C.

After the serum bottles were sealed with stoppers and aluminum crimps, they were inverted to minimize the volatilization of these compounds, then incubated on the shaker at 150 rpm. Bottles containing MSM with these compounds but without microorganisms served as controls. Sample aliquots of 2 mL were periodically withdrawn from the bottles and analyzed for the concentrations of BTEX, TPH, and TCE.

III. RESULTS AND DISCUSSION

The experimental results for the interactions between BTEX (350 mg/L for BTEo/m/pX), TPH (1,000 mg/L), and TCE (15 mg/L) in the artificially contaminated water at different pH values at 25°C are shown below.

A. Removal of BTEoX and TPH

The removal efficiencies for benzene, toluene, ethylbenzene, *ortho*-xylene, and TPH in BTEoX/TPH mixture without and with TCE after 144 hours of incubation are shown in Figure 1 and 2, respectively. For the mixture without TCE, the highest total removal efficiencies for BTEoX mixture and TPH were 84.7% at pH 7 and 63.7% at pH 9, respectively, and the lowest total removal efficiencies were 29.1% at pH 5 and 34.5% at pH 5, respectively (data not shown). On the other hand, for the mixture with TCE, the highest removal efficiencies for BTEoX mixture and TPH were 74.5% at pH 9 and 61.5% at pH 7, respectively, and the lowest total removal efficiencies were 28.9% at pH 5 and 35.8% at pH 5, respectively (data not shown). These results suggested the inhibitory effect of TCE on the removal of BTEoX mixture and TPH. The removal efficiency for *o*-xylene in BTEoX/TPH mixture was most affected by the presence of TCE, regardless of environmental conditions. After TCE was added into the mixture of BTEoX (350 mg/L) and TPH (1,000 mg/L) at 25°C, the removal efficiency for *o*-xylene dropped rapidly from 17.6% to 9.9%, from 82.3% to 13.8%, from 83.2% to 10.3% at pH 5, 7, and 9, respectively.

B. Removal of BTEmX and TPH

The removal efficiencies of benzene, toluene,

ethylbenzene, *meta*-xylene, and TPH in BTE_mX/TPH mixture without and with TCE after 144 hours of incubation are shown in Figure 3 and 4, respectively. For the mixture of BTE_mX and TPH without TCE, the highest removal efficiencies for BTE_mX mixture and TPH were 82.4% at pH 7 and 70.4% at pH 7, respectively, while the lowest removal efficiencies were 39.2% at pH 5 and 36.7% at pH 5, respectively (data not shown). On the other hand, for the mixture with TCE, the highest removal efficiencies for BTE_mX mixture and TPH were 85.5% at pH 9 and 64.0% at pH 7, respectively, while the lowest removal efficiencies were 49.4% at pH 5 and 28.1% at pH 5, respectively (data not shown). Overall, these results indicated a slightly stimulatory effect of TCE towards the removal of BTE_mX mixture. However, as shown in Figures 3 and 4, the removal efficiencies for individual compound in BTE_mX mixture and TPH were not significantly affected by the presence of TCE, regardless of pH.

C. Removal of BTE_pX and TPH

The removal efficiencies for benzene, toluene, ethylbenzene, *para*-xylene, and TPH in mixture of BTE_pX and TPH without and with TCE after 144 hours of incubation are shown in Figure 5 and 6, respectively. For the mixture without TCE, the highest removal efficiencies for BTE_pX mixture and TPH were 82.6% at pH 9 and 60.7% at pH 7, respectively, while the lowest removal efficiencies 42.0% at pH 5 and 30.5% at pH 5, respectively (data not shown). On the other hand, for the mixture with TCE, the highest removal efficiencies for BTE_pX mixture and TPH were 85.0% at pH 9 and 61.9% at pH 9, respectively, while the lowest removal efficiencies were 49.0% at pH 5 and 26.1% at pH 5, respectively (data not shown). As for the BTE_mX/TPH mixture, TCE showed a slightly stimulatory effect on the removal of BTE_pX mixture and TPH. The removal efficiencies for BTE_pX mixture with TCE compared to without TCE were 49.0% vs. 42.0% at pH 5, 85.5% vs. 82.6% at pH 9, while there was about 0.5% difference at pH 7. As shown, the removal efficiency for TPH in the mixture was most significantly stimulated by the presence of TCE at pH 9.

D. Removal of TCE

Table 1 shows the removal efficiencies for TCE (15 mg/L) at different pH values at 25°C when mixed with BTE_oX (350 mg/L)/TPH (1,000 mg/L), BTE_mX (350 mg/L)/TPH (1,000 mg/L), or BTE_pX (350 mg/L)/TPH (1,000 mg/L) mixtures. TCE was the most efficiently removed when mixed with BTE_oX and TPH at pH 7 or 9, while less removed in other mixtures at almost similar amounts regardless of pH. The highest removal of TCE occurred at pH 7, regardless of mixtures. The amounts of chloride generated from the co-metabolism/mineralization of TCE at each pH are stoichiometrically equivalent to the bio-removal efficiencies except when mixed with the BTE_mX/TPH mixture at pH 7 and 9.

IV. CONCLUSION

This study evaluated those interactions among the most frequently found organic environmental contaminants (BTEX, TPH, and TCE) when they existed in mixtures at different pH values at 25°C. The highest removal efficiencies for the mixtures of BTEX and TPH were at pH 7 or 9, while the lowest were at pH 5, regardless of the presence of TCE, implying the isolate (indigenous microorganism) preferring neutral or slightly alkaline condition. When the removal efficiencies for BTE_oX, BTE_mX, or BTE_pX mixed with TPH were compared with or without TCE, TCE showed an inhibitory effect on the *o*-xylene removal in BTE_oX mixture, while it showed a slightly stimulatory effect on the overall removal efficiencies for BTE_mX and BTE_pX mixtures. On the other hand, TCE was the most efficiently removed when mixed with BTE_oX and TPH at pH 7 or 9, while less removed in other mixtures regardless of pH, and the highest TCE removal occurred at pH 7 regardless of mixtures. Even though this study warrants more works, such as effects of different temperatures and dissolved oxygen levels and contaminants concentrations, to further evaluate the contaminants' interactions in mixtures, these preliminary results would still help improve the applicability of bioremediation technology to the mixed wastes contaminated sites.

TABLE I. BIO-REMOVAL EFFICIENCIES (%) FOR TCE, MIXED WITH BTEX/TPH, UNDER DIFFERENT PH CONDITIONS (MEAN ± SD FOR DUPLICATES) (CHLORIDE IN MG/L)

pH	Removal Efficiency	BTE _o X/TPH TCE	BTE _m X/TPH TCE	BTE _p X/TPH TCE
5	Biotic	12.8	17.2	14.1
	Abiotic	6.1	7.5	10.2
	Total	18.9±7.2	24.7±10.2	24.3±12.7
	Chloride	2.1±1.0	3.8±0.4	2.0±0.3
7	Biotic	31.6	19	20.8
	Abiotic	8.5	10.9	5.3
	Total	40.1±6.2	29.9±8.4	26.1±8.3
	Chloride	4.0±1.2	2.2±0.9	3.1±1.2
9	Biotic	25.8	14.1	12.2
	Abiotic	10.3	7.1	8.6
	Total	36.1±7.0	21.2±13.4	20.8±8.5
	Chloride	2.9±0.5	2.6±1.1	1.9±0.3

ACKNOWLEDGMENT

This study was supported by a research grant from the

University of Macau Research Committee and the Macau Science and Technology Development Fund.

REFERENCES

[1] M. Paul, J. R. White, D. C. Wolf, G. J. Thoma, and C. M. Reynolds, "Phytoremediation of Alkylated Polycyclic Aromatic Hydrocarbons in a Crude Oil-Contaminated Soil". *Water, Air, and Soil Pollution*, 2006, 169, pp. 207-220.

[2] I. Bossert and R. Bartha, "The fate of petroleum in soil ecosystems". *Petroleum Microbiology*, 1984, pp. 434-476.

[3] H. Shim, B. H. wang, S. S. Lee, and S. H. Kong, "Kinetics of BTEX biodegradation by a coculture of *Pseudomonas putida* and *Pseudomonas fluorescens* under hypoxic conditions". *Biodegradation*, 2005, 16, pp. 319-327.

[4] H. Shim, W. Ma, A. Lin, and K. Chan, "Bio-removal of mixture of benzene, toluene, ethylbenzene, and xylenes/total petroleum hydrocarbons/trichloroethylene from contaminated water". *Journal of Environmental Sciences*, 2008, 21, pp. 758-763.

[5] ATSDR (Agency for Toxic Substances and Disease Registry), *Toxicology Profile for Trichloroethylene*, Atlanta, Georgia, USA, 1997.

[6] S. Kota, M. A. Barlaz, and R. C. Borden, "Spatial Heterogeneity of Microbial and Geochemical Parameters in Gasoline Contaminated

Aquifers". *Practice Periodical of Hazardous, Toxic, and Radioactive Waste Management*, 2004, 8(2), pp. 105-118.

[7] M. R. Hyman, S. A. Russell, R. L. Ely, K. J. Williamson, and D. J. Arp, "Inhibition, inactivation, and recovery of ammonia oxidizing activity in cometabolism of trichloroethylene by *Nitrosomonas europaea*". *Applied and Environmental Microbiology*, 1995, 61(4), pp. 1480-1487.

[8] B. A. Kocameci and F. Cecen, "Kinetic analysis of the inhibitory effect of trichloroethylene (TCE) on nitrification in cometabolic degradation". *Biodegradation*, 2007, 18, pp. 71-81.

[9] B. R. Folsom, P. J. Chapman, and P. H. Pritchard, "Phenol and trichloroethylene degradation by *Pseudomonas cepacia* G4: kinetics and interactions between substrates". *Applied and Environmental Microbiology*, 1990, 56(5), pp. 1279-1285.

[10] M. E. Andersen, M. L. Gargas, H. J. Clewell, and K. M. Severyn, "Quantitative evaluation of the metabolic interactions between trichloroethylene and 1,1-dichloroethylene in vivo using gas uptake methods". *Toxicology and Applied Pharmacology*, 1987, 89, pp. 149-157.

[11] G. Z. Wang, T. Takano, K. Tomita, K. Nakata, and K. Nakamura, "Interaction of trichloroethylene and isopropyl alcohol in the perfused rat liver". *Nippon Eiseigaku Zasshi*, 1993, 48(5), pp. 1000-1005.

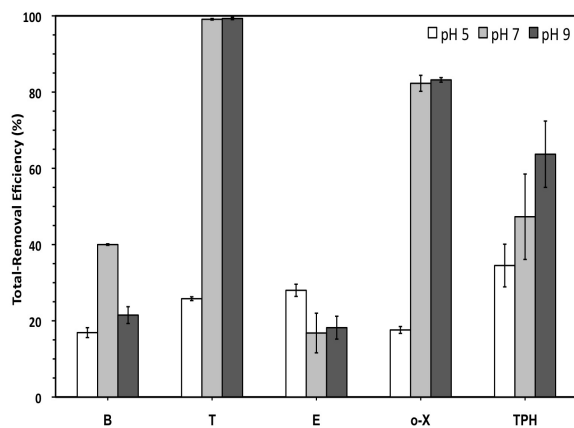


Figure 1. Removal efficiencies (%; average of replicates) for benzene, toluene, ethylbenzene, ortho-xylene, and TPH in BTEoX/TPH mixture after 144 hours of incubation in MSM at different pHs at 25°C.

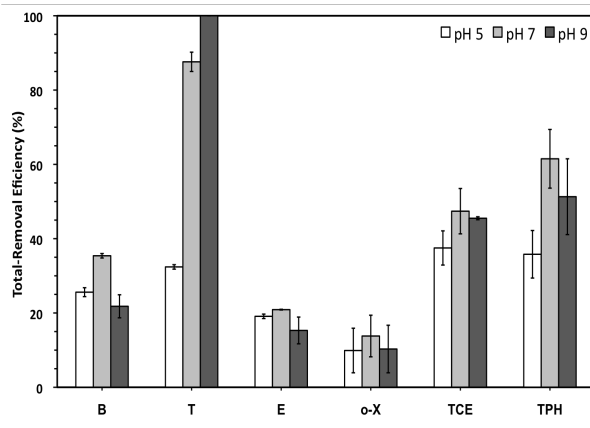


Figure 2. Removal efficiencies (%; average of replicates) for benzene, toluene, ethylbenzene, ortho-xylene, TPH, and TCE in BTEoX/TPH/TCE mixture after 144 hours of incubation in MSM at different pHs at 25°C.

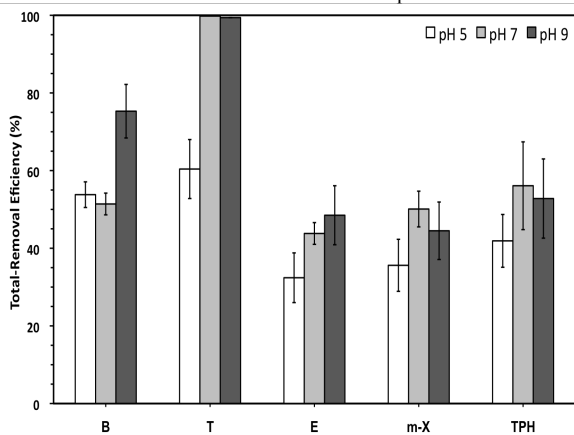


Figure 3. Removal efficiencies (%; average of replicates) for benzene, toluene, ethylbenzene, meta-xylene, and TPH in BTEmX/TPH mixture after 144 hours of incubation in MSM at different pHs at 25°C.

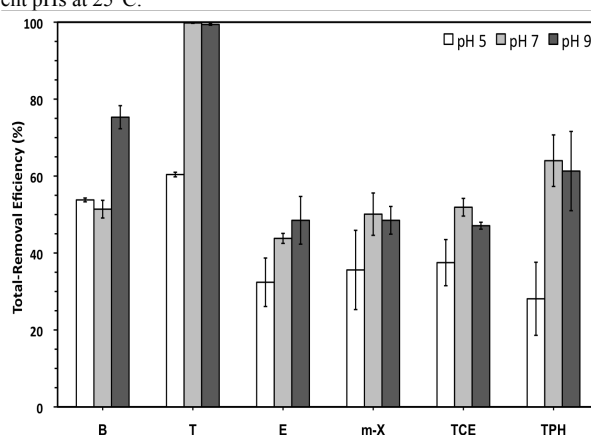


Figure 4. Removal efficiencies (%; average of replicates) for benzene, toluene, ethylbenzene, meta-xylene, and TPH in BTEmX/TPH/TCE mixture after 144 hours of incubation in MSM at different pHs at 25°C.

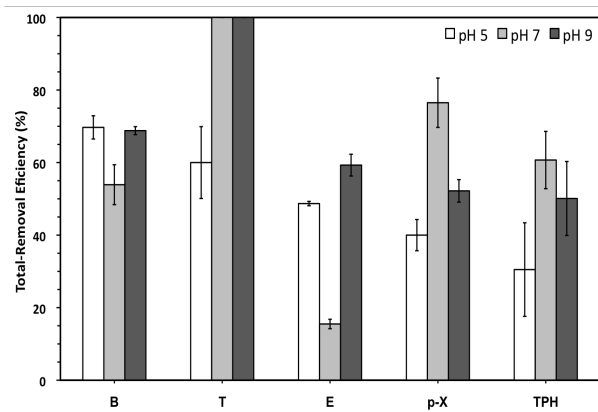


Figure 5. Removal efficiencies (%; average of replicates) for benzene, toluene, ethylbenzene, *para*-xylene, and TPH in BTEpX/TPH mixture after 144 hours of incubation in MSM at different pHs at 25°C.

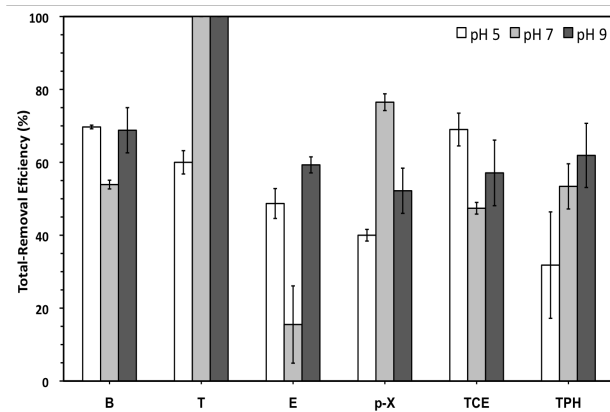


Figure 6. Removal efficiencies (%; average of replicates) for benzene, toluene, ethylbenzene, *para*-xylene, and TPH in BTEpX/TPH/TCE mixture after 144 hours of incubation in MSM at different pHs at 25°C.

Arctic Perennial Sea Ice Crash of the 2000s and its Impacts

Son V. Nghiem and Gregory Neumann

Jet Propulsion Laboratory
California Institute of Technology
Pasadena, California, U.S.A.
Son.V.Nghiem@jpl.nasa.gov
Gregory.Neumann@jpl.nasa.gov

Ignatius G. Rigor

Applied Physics Laboratory
University of Washington
Seattle, Washington, U.S.A.
ignatius@apl.washington.edu

Pablo Clemente-Colón

National Ice Center
National Oceanic and Atmospheric Administration
Washington, District of Columbia, U.S.A.
Pablo.Clemente-Colon@noaa.gov

Donald K. Perovich

Cold Regions Research and Engineering Laboratory
US Army Corps of Engineers
Hanover, New Hampshire, U.S.A.
Donald.K.Perovich@usace.army.mil

Abstract—Satellite and surface observations show that half of the extent of perennial sea ice in the Arctic Ocean has been lost in the decade of 2000s. Perennial sea ice is the class of old and thick ice important for the stability of the Arctic environment. Perennial ice extent set the record low in 2008 and has remained low as seen in updated satellite scatterometer data and surface drifting buoy measurements in 2011. The drastic decline of Arctic sea ice is far exceeding the worst-case projections from climate models of the Intergovernmental Panel on Climate Change Fourth Assessment Report. The important role of the Polar Express phenomenon has been identified, indicating dynamic and thermodynamic effects are combined to expedite the loss of perennial sea ice. Consequently, major impacts include decreases in Arctic surface albedo, increases in absorbed insolation, facilitation of sea-route opening, and changes in tropospheric chemical processes such as bromine explosion, ozone depletion, and mercury deposition that impact the biosphere.

Keywords—Perennial sea ice loss, Polar Express, albedo, insolation, Arctic passages, tropospheric chemical changes.

I. INTRODUCTION

The Arctic sea ice cover consists of two major synoptic ice classes: seasonal or first-year sea ice that grows and melts in a seasonal cycle, and perennial or multi-year sea ice that survives at least a summer melt season and can last for multiple years. At their boundary, these sea ice classes can be mixed together to form an area of mixed ice. Perennial sea ice is older, thicker, and more massive than seasonal sea ice, and its presence is critical to the stability of the Arctic environment. The total sea ice extent (S_T), encompassing both perennial and seasonal ice, typically reaches a minimum in late summer or early fall. Setting a record low in 2007, S_T has been reduced far beyond the worst-case projections from climate models of the Intergovernmental Panel on Climate Change Fourth Assessment Report (IPCC-AR4) [1-2], which are in dire need for improvements in the next IPCC assessment. While the 2007 record minimum of S_T in summer has been widely reported [3-5], the partition between perennial and seasonal ice within the total ice extent

in springtime is crucial to assess the overall change in sea ice and its resulting impacts. Much attention has been on increased heating as a thermodynamic cause of sea ice loss by melting within the Arctic Ocean [3-5]. In this paper, we review the extreme loss of Arctic perennial ice in the decade of 2000s with respect to a half-century record, present the latest update on the state of Arctic sea ice in 2011, highlight the role of the Polar Express phenomenon as an important dynamic mechanism for perennial ice loss by ice transport out of the Arctic Ocean, and discuss impacts of the precipitous loss of Arctic perennial ice. Observations of perennial sea ice are presented in Section II, impacts of perennial ice loss are discussed in Section III, and finally the conclusions and future perspectives are noted in Section IV.

II. OBSERVATIONS OF ARCTIC PERENNIAL SEA ICE

A decadal record of backscatter data has been obtained globally throughout the lifetime of the National Aeronautics and Space Administration (NASA) SeaWinds scatterometer, a stable and accurate radar aboard the QuikSCAT satellite from 1999 to 2009. QuikSCAT Ku-band backscatter (QS) is sensitive to different sea ice classes with a large dynamic range of signatures, providing an excellent capability to accurately delineate and map Arctic perennial and seasonal ice [6-8]. We review the recent state of Arctic sea ice including observations from QS data in the 2000s in a multi-decadal context.

Perennial sea ice extent (S_P) during the transition period between winter and spring (March) is an important parameter since it represents the amount of older and thicker ice that preconditions the summer melt of the Arctic sea ice cover and thus the minimum S_T . Furthermore, this transition period is the time of polar sunrise that affects chemical photolysis processes in the Arctic troposphere depending on the relative composition of perennial and seasonal sea ice. A new record has been set in the reduction of March S_P in 2008, while the total sea ice extent has been stable compared to the average over the previous nine years as observed in QS data. In March 2008, QS-measured S_P was reduced by one million km² compared to that in March 2007.

Beyond the QS satellite data time-series, the perennial sea ice pattern change has been deduced by using surface observations from buoys and manned ice camps to track sea ice movement around the Arctic Ocean beginning in 1955. The surface-based S_p is obtained from the Drift-Age Model (DM) [9]. The combination of the satellite and surface data records confirms that the reduction of winter perennial ice extent broke the record in 2008 compared to data over the last half century. Another historical fact is that the boundary of perennial sea ice already crossed the North Pole (NP) in February 2008, leaving the area around the NP occupied by seasonal sea ice. This is the first time, not only from the satellite data record but also in the history of sea ice charting at the National Ice Center since the 1970's, that observations indicate the seasonal ice migration into the NP area so early in winter.

In the context of a half century change, perennial sea ice has been declining precipitously in this decade. Perennial ice extent declines at rate of 0.5 million km² per decade in the 1970s-1990s while there is no discernable trend in the 1950s-1960s. Abruptly, the rate of decrease has tripled to 1.5 million km² per decade in the 2000s. This crashing rate of S_p is cross-validated by both satellite sensor and surface buoy measurements [10-11].

In November 2009, QS antenna was stuck in one azimuth direction due to a malfunction in the antenna rotary joint after more than 10 years in orbit. Nevertheless, the scatterometer is still working to collect good global backscatter data albeit a much reduced swath and a longer time for a full Arctic coverage. New results from QS show that S_p remained low in March 2010. Thus, the climatic data record of Arctic perennial ice extent in the 2000s (2000-2009) can be continued if QS is kept in continuous operation.

While QS can still map perennial sea ice well, the rotary problem reduces the capability of QS to delineate seasonal sea ice. To supplement this deficiency, we utilized a new daily sea ice analysis product called the Multisensor Analyzed Sea Ice Extent – Northern Hemisphere (MASIE-NH) [12], which is an Arctic-wide sea ice extent analysis produced by the National Ice Center (NIC) using a multitude of data sources. Different formats of MASIE-NH are derived and distributed by the National Snow and Ice Data Center. Since QS can detect perennial sea ice, the remainder of the total sea ice extent identified by MASIE-NH consists of seasonal as well as a mixed ice class. Thus, the QS/MASIE-NH composite product can map both perennial and non-perennial sea ice (seasonal and mixed ice) [13]. Moreover, DM results are used in conjunction with QS/MASIE-NH observations of ice to explain ice dynamics. To illustrate the drastic reduction of S_p , Figure 1 compares the extensive extent of perennial sea ice in 2001 with the much smaller perennial ice cover in 2011.

Although considerable efforts were made to investigate thermodynamics effects on sea ice melt in the last several decades, the importance of dynamic effects as a significant sea ice reduction mechanism was noted in recent years [9, 10, 14]. In the 2000s, a record low of S_7 first occurred in summer 2005, which was broken again in 2007. While the ice extent had been decreasing throughout the summer 2005

significantly by melting, an important contribution to this minimum extent was from dynamic effects due to wind forcing. Data from the National Centers for Environmental Prediction/National Center for Atmospheric Research (NCEP/NCAR) reanalysis in July-September 2005 reveal a dipole anomaly pattern (DAP) of the surface level pressure (SLP) with a coexistence of a pronounced atmospheric low pressure over the Barents Sea together with a strong high pressure over the Canadian Basin. Clockwise winds around the high SLP merged together with counterclockwise winds around the low SLP to set up the strong wind anomaly along the Transpolar Drift Stream (TDS) that enhanced the ice transport out of the Arctic via the Fram Strait [15].

This phenomenon, called the Polar Express (PE) [10], forces the ice extent loss by these processes: (1) compressing sea ice from both sides of the TDS, (2) pushing sea ice from the Russian Arctic toward Greenland while accelerating the TDS, (3) transporting of sea ice by the TDS out of the Arctic, and (4) melting of the exported sea ice in the Greenland Sea by warm Atlantic waters originated from the south [10, 15]. It was not until 2007 that the PE occurred again. The 2007 PE was strong, and together with feedback effects on the lighter sea ice cover due to the loss of massive perennial ice in 2005, leading to another record low of S_7 after the 2007 summer melt, and subsequently contributing to the record low of S_p in 2008.

III. IMPACTS OF PERENNIAL ICE LOSS

The crash of perennial sea ice extent in the 2000s has profound impacts on the Arctic environment. Here, we review several results including changes in surface albedo, absorbed radiation, Arctic sea routes, and tropospheric chemical processes.

The different classes of sea ice partition solar energy differently, with the perennial ice having a larger albedo and thereby transmitting less solar radiation to the ocean [16]. The shift in the Arctic Ocean from perennial to thinner seasonal ice thus suggests a coincident decrease in surface albedo and more solar energy absorbed in the ice ocean system during summer melt [16-17]. To investigate changes in albedo and insolation, a synthetic approach was used to combine satellite-derived ice concentrations, incident irradiances determined from reanalysis products, and field observations of ocean albedo over the Arctic Ocean and the adjacent seas. Results show an increase in the solar energy deposited in the upper ocean over the past few decades in 89% of the studied region spanning across Chukchi Sea, Beaufort Sea, and East Siberian Sea, and the largest anomaly of solar heat input occurred in the 2000s [18]. As the Arctic becomes more dominated by seasonal sea ice with a lower overall albedo and lower ice mass, melting will become much more effective in causing sea ice loss.

Less perennial sea ice and more seasonal ice, which is thinner and requires less energy to melt, may facilitate the summer opening of Arctic sea routes such as the Northwest Passage (NWP) along the North American side or the Northern Sea Route (NSR) along the Siberian side. In winter 2007 and 2008, S_p loss was driven by winds that compressed the ice and transported it out of Fram Strait (east of

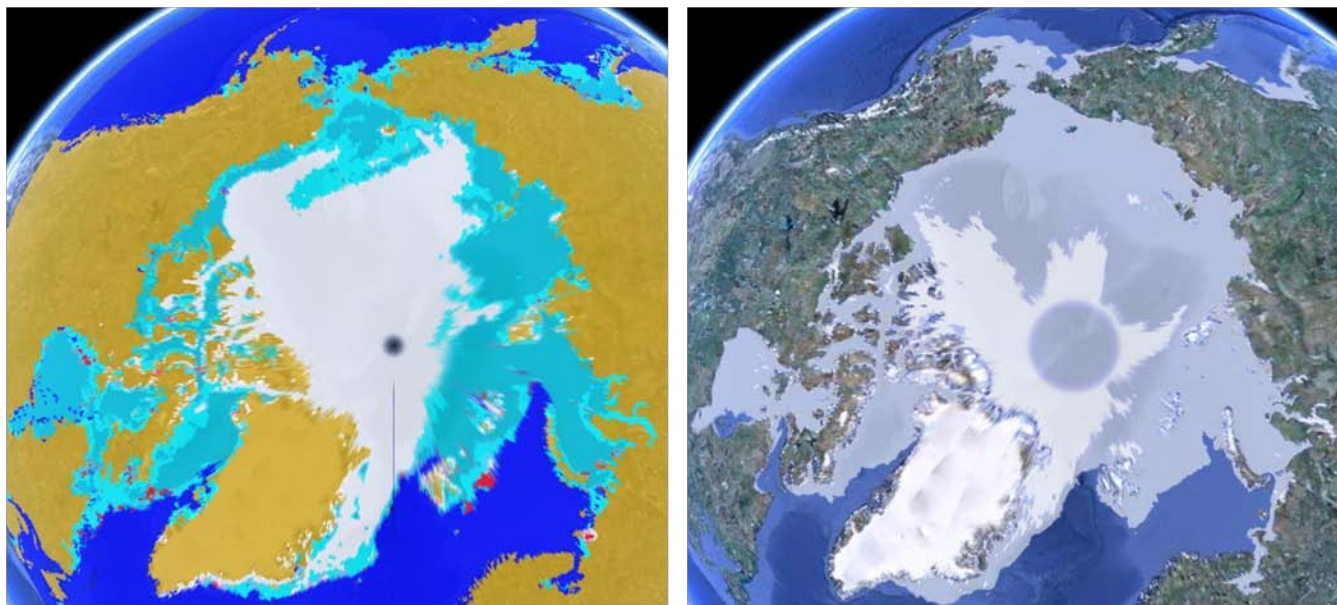


Figure 1. Comparison of Arctic sea ice maps showing the loss of half of perennial ice extent. Left panel is QS sea ice map for 6 January 2001: grayish white for perennial sea ice, aqua for seasonal ice, cyan for mixed ice, blue for open water, brown for land, and a dark disc around the North Pole for QS missing data. Right panel is QS/MASIE-NH composite sea ice map with bluish white for perennial sea ice from 3 weeks of QS data ending on 6 January 2011, light blue for non-perennial sea ice consisting of mixed ice and seasonal ice from MASIE-NH on 6 January 2011, and a large blue disc around the North Pole for QS missing data. The QS/MASIE-NH sea ice map is translucently overlaid on a bathymetric chart of the Arctic Ocean.

Greenland) and Nares Strait (west of Greenland) as observed by QS [19]. By March 2008, QS sea ice maps revealed that seasonal ice occupied the NSR, a vast region from Kara Sea and Laptev Sea to the North Pole, and most of two branches of the NWP north and south of Victoria Island [19]. In a news release in October 2008 [20], the International Ice Charting Working Group (IICWG) issued the statement “For the first time in recorded history, national ice charts showed that both the Northwest Passage and the Northern Sea Route were simultaneously open water for a brief period in September 2008” and also warned that “At lower concentrations, hazardous ice floes and icebergs are more mobile and less easily detected by mariners. Sustained monitoring with high resolution satellite sensors combined with surface and aerial reports is essential for safe navigation.” In 2009, perennial ice remained low [21], and the IICWG reported a record number of pleasure craft transited the NWP although ice conditions were more difficult for shipping than in the three previous years [22]. In January 2011, little perennial ice was seen in the NWP and seasonal ice dominated the NSR (right panel in Figure 1).

As perennial sea ice diminished, the Arctic Ocean becomes dominated by seasonal ice, consisting of salty ice together with more leads, polynyas, and frost flowers. The high salinity in these ice conditions affects the release of bromine monoxide (BrO), a catalyst for depletions of ozone (O_3) [23] and gaseous element mercury (GEM) [24]. These changes may have significant implications on chemical fluxes in the Arctic biosphere [25-26], where ozone and mercury are toxic to people and wildlife. During polar sunrise, oxidation from bromide activates photochemically reactive forms, which are photo-disassociated into Br atoms that destroy O_3 and oxidize GEM. The Br atoms are

regenerated to repeat this autocatalytic process. Subsequent reactions further multiply available bromine, which is called “bromine explosion” [27]. In 2007, the acceleration of the Transpolar Drift (TD), due to the Polar Express phenomenon excessively transported sea ice toward the Atlantic sector and finally out of the Arctic across Fram Strait. The 2007 TD acceleration was actually verified by a vessel drift during the TARA expedition [28]. Consequently, from QS observations, a polynya as large as the country of Austria was created with an extensive frost flower cover near the Taymyr Peninsula, and ozone depletion events were observed far down wind [29]. While S_p was low during the 2008 spring transition, bromine enhancement was observed across the Beaufort Sea to the Amundsen Gulf [30]. In March-May of 2009 and 2010 with low S_p , strong bromine explosion events were detected by satellite sensors [31].

IV. CONCLUSIONS AND FUTURE PERSPECTIVES

As observed from decadal satellite and surface data across the Arctic, half of the perennial sea ice extent was lost in the decade of 2000s when the ice-loss rate was the most precipitous in the last half century. The role of dynamic mechanisms, such as the PE, has been identified as an important factor in causing the drastic sea ice loss, which is accelerated by the combination of dynamic and thermodynamic effects. Without appropriately accounting for these effects, many projections from IPCC-AR4 climate models underestimated the Arctic sea ice loss by far. Recently, Zhang et al. [32] conducted a model study to show that preconditioning, anomalous wind forcing, and ice-albedo feedback are the main contributors responsible for sea ice loss in 2007, and that the Arctic has become vulnerable to the anomalous atmospheric forcing. Later, Wang et al. [33]

examined the DAP and used a coupled ice-ocean model to explain the low extents of sea ice including the records in 2005 and in 2007. What causes the change between the typical Arctic Oscillation pattern and the anomalous DAP, how such change can be related to global temperature change, and whether the impacts can be amplified or suppressed by positive or negative feedbacks remain to be investigated in future research.

Given the 2000s crash of perennial sea ice, it is critical to closely monitor the sea ice change with both surface and satellite measurements. For surface measurements, the International Arctic Buoy Programme has been enhanced with a larger number of buoys during the International Polar Years 2007-2008. The need for the buoy program to sustain ocean observations has been articulated [34]. Regarding satellite scatterometer observations, QS unfortunately suffered from the rotary malfunction that has reduced its capability for sea ice mapping. Sea ice maps derived from the limited QS data after the rotary incident still need to be improved with better calibration and geolocation efforts. Launched in September 2009, the Indian Oceansat-2 satellite [35], carrying a sensor similar to QS, is currently operating and collecting global Ku-band backscatter data. Access to fully calibrated and validated data will be useful. Planned for a launch later in 2011, the Chinese Haiyan-2 satellite [36] will also have a Ku-band scatterometer. The U.S. National Research Council Decadal Survey recommends the development of another advanced satellite scatterometer [37]. All of these international satellite missions will potentially contribute to sea ice monitoring in the long term.

While important advances have been made for understanding sea ice changes and environmental impacts, many science questions as well as practical issues still need to be addressed. Sea ice-albedo feedback processes are complex, which demands interdisciplinary research involving all components including air, ice, ocean, and land to determine various inter-related positive and negative mechanisms in the overall feedback process of the Earth system. Either from satellite and surface observations or from model estimates, diverse and extensive temporal and spatial scales should be considered since results for a given area or a time period will likely lead to inconclusive or even erroneous projections from a series of non-physical numerical correlations, interpolations, and extrapolations. In any case, reducing potential causes, which would further decrease the albedo such as dust or black carbon deposition in the Arctic, may help to mitigate albedo feedback effects.

With the prospect of a more navigable Arctic, new issues have emerged and necessitated the need for high-resolution operational satellite sensors to monitor ice in polar sea routes, more accurate and complete bathymetry measurements, and consensus on international agreements such as the United Nations Convention on the Law of the Sea or the Arctic Council Memorandum on Search and Rescue. New bathymetry data are critical to avoid or reduce the threat of navigation hazards that may lead to environmental disasters such as oil spills. Although much attention has been paid to Arctic sea-route shortcuts and resource exploitation, it is important to consider the impact

to the Arctic biosphere by changes in chemical processes, transport, and distribution that may adversely affect the well being of people and wildlife. There is a general understanding that a saltier snow and ice cover may exacerbate bromine explosions, ozone depletions, and mercury depositions. Reducing mercury emission into the atmosphere, under the auspices of the United Nations Environment Programme (UNEP) [38], may diminish the mercury source and thus decrease the mercury deposition in the Arctic environment. Nevertheless, exact contributions from different components such as seasonal ice, snow on sea ice, frost flowers in leads and polynyas, high salinity expulsion on ice surface, aerosols in the atmosphere, and chemical composition and exchange in the troposphere and stratosphere are not well understood. In this respect, more intensive interdisciplinary research is underway [31].

ACKNOWLEDGMENT

The research carried out at the Jet Propulsion Laboratory (JPL), California Institute of Technology, was supported by the National Aeronautics and Space Administration (NASA) Cryospheric Sciences Program. The statements, findings, conclusions, and recommendations in this paper are those of the author(s) and do not necessarily reflect the views of the National Oceanic and Atmospheric Administration or the Department of Commerce.

REFERENCES

- [1] I. N. Allison, L. Bindoff, R. A. Bindshadler, P. M. Cox, N. de Noblet, M. H. England, J. E. Francis, N. Gruber, A. M. Haywood, D. J. Karoly, G. Kaser, C. Le Quéré, T. M. Lenton, M. E. Mann, B. I. McNeil, A. J. Pitman, S. Rahmstorf, E. Rignot, H. J. Schellnhuber, S. H. Schneider, S. C. Sherwood, R. C. J. Somerville, K. Steffen, E. J. Steig, M. Visbeck, and A. J. Weaver, *The Copenhagen Diagnosis, 2009: Updating the World on the Latest Climate Science*, The University of New South Wales Climate Change Research Centre (CCRC), Sydney, Australia, 60 pp., 2009.
- [2] J. Stroeve, M. M. Holland, W. Meier, T. Scambos, and M. Serreze, "Arctic sea ice decline: Faster than forecast," *Geophys. Res. Lett.*, vol. 34, L09501, doi:10.1029/2007/GL029703, 2007.
- [3] J. A. Maslanik, C. Fowler, J. Stroeve, S. Drobot, J. Zwally, D. Yi, and W. Emery, "A younger, thinner Arctic ice cover: Increase potential for rapid, extensive sea-ice loss," *Geophys. Res. Lett.*, vol. 34, no. 24, L24501, doi:10.1029/2007GL032043, 2007.
- [4] D. K. Perovich, J. Richter-Menge, K. F. Jones, and B. Light, "Sunlight, water, and ice: Extreme Arctic sea ice melt during summer 2007," *Geophys. Res. Lett.*, vol. 35, no. 11, L11501, doi:10.1029/2008GL034007, 2008.
- [5] J. Richter-Menge, J. Comiso, W. Meier, S. Nghiem, and D. Perovich, "Sea Ice Cover," in *State of the Climate in 2007*, *Bull. Amer. Meteorol. Soc.*, vol. 89, no. 7, pp. S1-S179, 2008.
- [6] S. V. Nghiem, M. L. Van Woert, and G. Neumann, Rapid formation of a sea ice barrier east of Svalbard, *J. Geophys. Res.*, vol. 110, doi:10.1029/2004JC002654, 2005.
- [7] S. V. Nghiem and G. Neumann, "Arctic Sea-Ice Monitoring," in 2007 McGraw-Hill Yearbook of Science and Technology, pp. 12-15, McGraw-Hill, New York, 2007.
- [8] F. Girard-Ardhuin, R. Ezraty, D. Croizé-Fillon, "ASCAT/MetOp scatterometer data: First results for sea ice study," *Acte Coll., Archimer, Arch. Inst. Ifremer, Plouzané, France*, 2009.
- [9] I. G. Rigor and J. M. Wallace, Variations in the age of Arctic sea-ice and summer sea-ice extent, *Geophys. Res. Lett.*, vol. 31, L09401, doi:10.1029/2004GL019492, 2004.

- [10] S. V. Nghiem, I. G. Rigor, D. K. Perovich, P. Clemente-Colon, J. W. Weatherly, and G. Neumann, "Rapid reduction of Arctic perennial sea ice," *Geophys. Res. Lett.*, vol. 34, L19504, doi:10.1029/2007GL031138, 2007.
- [11] S. V. Nghiem, I. G. Rigor, P. Clemente-Colón, D. K. Perovich, and J. E. Overland, "Triple Loss Rate of Arctic Perennial Sea Ice Extent in the Decade of 2000s," International Polar Year Oslo Science Conference, Oslo, Norway, 8-12 June 2010.
- [12] P. Clemente-Colón, S. R. Helfrich, M. Vancas, F. Fetterer, and M. Savoie, "A New Role for a NIC Product: the Multisensor Analyzed Sea Ice Extent (MASIE)," submitted to IEEE Int. Geosci. and Remote Sens. Symp. (IGARSS), 2011.
- [13] S. V. Nghiem, P. Clemente-Colón, I. G. Rigor, and G. Neumann, "Remote sensing of Arctic perennial sea ice reduction and its impact on tropospheric chemical processes," submitted to IEEE Int. Geosci. and Remote Sens. Symp. (IGARSS), 2011.
- [14] S. V. Nghiem, Y. Chao, G. Neumann, P. Li, D. K. Perovich, T. Street, and P. Clemente-Colon, "Depletion of perennial sea ice in the East Arctic ocean," *Geophys. Res. Lett.*, vol. 33, L17501, doi:10.1029/2006GL027198, 2006.
- [15] S. V. Nghiem, Y. Chao, G. Neumann, P. Li, D. K. Perovich, T. Street, and P. Clemente-Colón, "Significant reduction in Arctic perennial sea ice," *EOS Trans., AGU*, vol. 87, no. 52, Fall Meet. Suppl., Abst. C33B-1265, 2006.
- [16] D. K. Perovich, T. C. Grenfell, B. Light, and P.V. Hobbs, "The seasonal evolution of Arctic sea ice-albedo," *J. Geophys. Res.*, doi:10.1029/2000JC000438, 2002.
- [17] D. K. Perovich, S. V. Nghiem, T. Markus, and A. Schweiger, "Seasonal evolution and interannual variability of the solar energy absorbed by the Arctic sea ice-ocean system," *J. Geophys. Res.*, vol. 112, C03005, doi:10.1029/2006JC003558, 2007.
- [18] D. K. Perovich, B. Light, H. Eicken, K. F. Jones, K. Runciman, S. V. Nghiem, "Increasing solar heating of the Arctic Ocean and adjacent seas, 1979–2005: Attribution and role in the ice-albedo feedback," *Geophys. Res. Lett.*, vol. 34, L19505, doi:10.1029/2007GL031480, 2007.
- [19] S. V. Nghiem, I. G. Rigor, P. Clemente-colón, D. K. Perovich, and G. Neumann, "New record reduction of Arctic perennial sea ice in winter 2008," *Sci. Res. Article*, JPL D-44233, Jet Prop. Lab., California Institute of Technology, Mar. 13, 2008.
- [20] International Ice Charting Working Group, "National Ice Services Advise of Continuing Navigation Hazards," news release, Luleå, Sweden, Oct. 24, 2008.
- [21] S. V. Nghiem, I. G. Rigor, P. Clemente-Colón, D. K. Perovich, H. Eicken, J. E. Overland, T. Markus, D. G. Barber, and G. Neumann, "Observing the State of Arctic Sea Ice," *State of the Arctic Conference*, Miami, Florida, Mar. 16-19, 2010.
- [22] International Ice Charting Working Group, "National Ice Services Advise of Continuing Navigation Hazards," news release, Geneva, Switzerland, Oct. 16, 2009.
- [23] L. A. Barrie, J. W. Bottenheim, R. C. Schnell, P. J. Crutzen, and R. A. Rasmussen, "Ozone destruction and photo-chemical reactions at polar sunrise in the lower Arctic atmosphere," *Nature*, vol. 334, pp. 138-141, 1988.
- [24] W. H. Schroeder, K. G. Anlauf, L. A. Barrie, J. Y. Lu, A. Steffen, D. R. Schneeberger, and T. Berg, "Arctic springtime depletion of mercury," *Nature*, vol. 394, pp. 331-332, 1998.
- [25] J. Y. Lu, W. H. Schroeder, L. A. Barrie, A. Steffen, H. E. Welch, K. Martin, L. Lockhart, R. V. Hunt, G. Boila, and A. Richter, "Magnification of atmospheric mercury deposition to polar regions in springtime: the link to tropospheric ozone chemistry," *Geophys. Res. Lett.*, vol. 28, no. 17, pp. 3219-3222, 2001.
- [26] A. Steffen, T. Douglas, M. Amyot, P. Ariya, K. Aspmo, T. Berg, J. Bottenheim, S. Brooks, F. Cobbett, A. Dastoor, A. Dommergue, R. Ebinghaus, C. Ferrari, K. Gardfeldt, M. E. Goodsite, D. Lean, A. J. Poulain, C. Scherz, H. Skov, J. Sommar, and C. Temme, "A synthesis of atmospheric mercury depletion event chemistry in the atmosphere and snow," *Atmos. Chem. Phys.*, vol. 8, pp. 1445-1482, 2008.
- [27] P. Wennberg, "Atmospheric chemistry – Bromine explosion," *Nature*, vol. 397, pp. 299-301, 1999.
- [28] J.-C. Gascard, Jean Festy, H. le Goff, M. Weber, B. Bruemmer, M. Offermann, M. Doble, P. Wadhams, R. Forsberg, S. Hanson, H. Skourup, S. Gerland, M. Nicolaus, J.-P. Metaxian, J. Grangeon, J. Haapala, E. Rinne, C. Haas, G. Heygster, E. Jakobson, T. Palo, J. Wilkinson, L. Kaleschke, K. Claffey, B. Elder, and J. Bottenheim, "Exploring Arctic transpolar drift during dramatic sea ice retreat," *EOS Trans. AGU*, vol. 89, no. 3, pp. 21-22, doi:10.1029/2008EO160002, 2008.
- [29] J. W. Bottenheim, S. Netcheva, S. Morin, and S. V. Nghiem, "Ozone in the Boundary Layer Air over the Arctic Ocean: Measurements during the TARA Transpolar Drift 2006-2008," *Atmos. Chem. Phys.*, vol. 9, pp. 4545-4557, 2009.
- [30] S. V. Nghiem, "Implications of Arctic Sea Ice Reduction on Arctic Tropospheric Chemical Change," *Eos Trans. AGU*, vol. 90, no. 52, Fall Meet. Suppl., Abst. A24B-01, 29 December, 2009
- [31] S. V. Nghiem, I. G. Rigor, P. Clemente-Colón, A. Freeman, A. Richter, J. P. Burrows, P. B. Shepson, J. Bottenheim, D. G. Barber, W. Simpson, D. K. Perovich, M. Sturm, A. Steffen, L. Kaleschke, D. K. Hall, T. Markus, H. Eicken, and G. Neumann, "Rejuvenation of Arctic sea ice and tropospheric chemical change," *Abs. C43D-0580*, AGU Fall Meeting, San Francisco, Calif., Dec. 13-17, 2010.
- [32] Zhang, J., R. Lindsay, M. Steele, and A. Schweiger, "What drove the dramatic retreat of arctic sea ice during summer 2007?" *Geophys. Res. Lett.*, vol. 35, L11505, doi:10.1029/2008GL034005, 2008.
- [33] Wang, J., J. Zhang, E. Watanabe, M. Ikeda, K. Mizobata, J. E. Walsh, X. Bai, and B. Wu, "Is the Dipole Anomaly a major driver to record lows in Arctic summer sea ice extent?" *Geophys. Res. Lett.*, vol. 36, L05706, doi:10.1029/2008GL036706, 2009.
- [34] U.S. Commission on Ocean Policy, *An Ocean Blueprint for the 21st Century*, Final Rep., Washington, DC, 2004.
- [35] V. Jayaraman, V. S. Hedge, M. Rao, and H. H. Gowda, "Future Earth observation missions for oceanographic applications: Indian perspectives," *Acta Astronautica*, vol. 44, no. 7-12, pp. 667-674, 1999.
- [36] X. Dong, K. Xu, H. Liu, and J. Jiang, "The radar altimeter and scatterometer of China's HY-2 satellite," *Proc. Geosci. Remote Sens. Symp., IGARSS*, vol. 3, pp. 1703-1706, doi:10.1109/IGARSS.2004.1370659, 2004.
- [37] National Research Council, *Earth Science and Applications from Space: National Imperatives for the Next Decade and Beyond*, the National Academies Press, Washington, D.C., 2007.
- [38] UNEP, *Report of the intergovernmental negotiation committee to prepare a global legally binding instrument on mercury on the work of its second session*, UNEP(DTIE)/Hg/INC.2/20, Chiba, Japan, 2011.

Complex Approach to Oil Spill Utilization

E.M. Sulman, M.G. Sulman, E.A. Prutenskaya, E.V. Selivanova, M.Yu. Rakitin

Tver Technical University

Tver, Russia

e-mail: sulman@online.tver.ru

Abstract— In the course of oil extracting on oilfield, and also at oil transportation inevitably there are oil spills leading to ecological balance disruption and bringing a doubtless loss to natural ecosystems. Bioremediation is the safest way of neutralization of the soils polluted with oil spill products. The highest degree of polluted soil clearing is observed while using of oil-slime pretreatment and its further additional cleaning by a consortium of not pathogenic petrooxidizing microorganisms. Complex method of neutralization of spills and wastes polluted by oil hydrocarbons allows converting more than 85 % of oil hydrocarbons from the initial concentration in samples within two weeks. Developed scientific and technical production has advantage in comparison with analogs and includes the use of ultrasonic pretreatment. The basic advantage of ultrasonic processing is its sufficient quickness, profitability and ecological harmlessness, and possibility to destroy C-C bonds in paraffin molecules.

Keywords— oil spill, ultrasound, pretreatment, biological degradation

I. INTRODUCTION

As a result of development of new and operation of already functioning oil deposits the environment undergoes considerable changes. Owing to emergency oil products spill on oilfields a considerable amount of oil hydrocarbons and also the chemical reagents used at extraction pollutes the environment.

Oil and oil-slime polluting the environment as a result of emergencies at spilling, extraction, transportation, storage and treatment, are the reason of numerous environmental problems [1, 2]. Unfavorable impact of oil on environment and nonrenewing of hydrocarbonic raw materials make a problem of waste treatment a rather actual.

Applied technologies of soil bioremediation are possible to be divided in two groups: methods *in situ* and methods *ex situ*. Bioremediation *in situ* is based on clearing of spill from pollutants without removal of the polluted soil from pollution area. The most perspective is bioremediation *ex situ*, which is based on removal of a layer of the polluted soil and its clearing from pollutant outside of a pollution place. Technologies of this type have a number of advantages: they demand less time and provide complete control of clearing process.

Use of bioreactors is one of the types applied at bioremediation *ex situ* technologies. The polluted soil is placed in the bioreactor, necessary nutritious elements and microorganisms are loaded. Optimum conditions of microorganisms cultivation are provided. After completion of the clearing process the soil is dried and returned in environment.

Other approach of bioremediation *ex situ* consists in placement of the removed from a place of pollution soil in certain territory, it is provided with aeration, nutrients and water for stimulation of microorganism growth and a metabolism. In comparison with clearing by means of the bioreactors, this technology demands a lot of place and longer time.

The most effective way of oil hydrocarbonic fraction biodegradation by microorganisms is the method of the continuous cultivation, allowing maintaining a number of process parameters at the set level, and simultaneously carrying out selection of the most active microorganisms-destroyers.

The maximal degree of clearing, more than 60-90 %, is observed at use of oil-slime pretreatment and the further additional cleaning by a consortium of not pathogenic petrooxidizing microorganisms [4]. The most perspective method is preprocessing by ultrasound which plays a role of demulsifying agent and a dispergator. As a result of ultrasonic influence in a water solution there is a formation at first the emulsion of direct type which is in a condition of inversion of phases.

Then, starting from critical value of acoustic wave sound pressure, there is a cavitation in a liquid. C-C bonds in paraffin molecules get broken and owing to what there are changes of physical and chemical structure (reduction of molecular weight, temperatures of crystallization, etc.). After ultrasonic pretreatment the steady microemulsion is formed and concentration of an accessible source of carbon and mineral components increases.

Preprocessed oil-slime destruction is 10-30 %.

Thus the aim of this study is development of neutralization method of spills and a waste polluted by oil hydrocarbons.

II. EXPERIMENTAL

Oil of the Caspian deposit has been used as a model in this study. Some of the major characteristics of oil are the density and viscosity. The density of oil is 860 kg/m³. Oil

with relative density 0.86 is called average. Dynamic viscosity of oil ranges from 1.4 to 4.5 mP's and depends on chemical and fractional structure, in our case viscosity of oil makes 3.39 mP's.

Observable oil contains about 10 % of paraffin. Hence, it concerns to highwaxy substances. From ecological positions components sulfur presented in oil (elementary, hydrosulphuric, sulphidic, sour sulfur) are important compounds of it. Used oil contains 0.2 % of sulfur, therefore is low-sulphur. Mechanical impurity was also defined in the oil. Its general maintenance in the investigated sample doesn't exceed 0.01 %.

In experiments the modeling samples of the polluted soils consisting of soil and oil were used. The sample contained 15 % of oil. Combination of oil with soil spent within three days. Ultrasonic pretreatment of the modeling sample were carried out after that.

As each solvent possesses the characteristic properties, the correct choice of environment is very important for definition of optimum conditions of carrying out sonochemical processes. Selection of a leach, as a rule, is carried out purely empirically; scientific bases of the directed selection are developed in small degree because of a lack of the information about oil-slime structure and character of its interactions with solvents of the various nature.

After analysis of different methods of solvents activity effectiveness research dissolving ability of hydrocarbons for maintenance of the maximum accuracy of received results and an exception of a making error of the experiment caused by possible discrepancy of conditions of carrying out of experiences were defined

Thus for laboratory researches hexane, toluene, chloroform, benzene were used.

Ultrasonic generator IKASONIC U 50 was applied to raw materials treatment, working at frequency of 30 kHz. The device was completed with a nozzle of updating US 50-3 Sonotool with a diameter of 3 mm and maintenance of intensity to 460 Wt/cm².

The quantity of oil products in the modeling sample were defined by the gravimetric method. During experiments intensity of ultrasonic processing (from 230 Wt/cm² to 414 Wt/cm²) and extraction time from 1 till 25 minutes were varied. As a control, continuous extraction of hydrocarbons of oil from samples under normal conditions in conical flasks on a rocking chair of type AVU-1.

Extraction degree (W, %) of oil hydrocarbons from oil-slime were defined under the equation:

$$W = \frac{A * 100}{B},$$

where

A – amount of the producing hydrocarbons from oil-slime solvent quantity (g);

B – content (wt.) of oil in oil-slime (g).

Oil qualitative analysis was carried out via GC using chromatograph Kristallux-4000 equipped with FID, and capillary column Zebron ZB-FFAP 50, and GCMS-QP2010.

III. RESULTS AND DISCUSSION

Determination of leach:oil-slime optimum ratio the first investigation stage. During the experiments it has been established that the fullest extraction of hydrocarbons of oil from samples occurred at leach:oil-slime ratio – 4:1 (Figure 1). Experiments were carried out at all rates (from 230 Wt/cm² to 414 Wt/cm²) and in all investigated solvents.

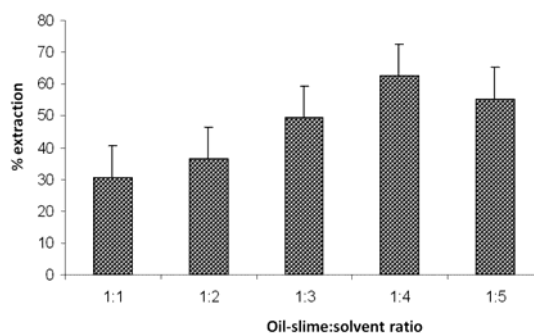


Figure 1. – Oil-slime hydrocarbons extraction degree at various oil-slime:solvent ratios (Solvent is chloroform, intensity of 414 Wt/cm²)

Optimum time of ultrasonic treatment has been also chosen, the range varied from 5 till 10 minutes depending on solvent (Figure 2).

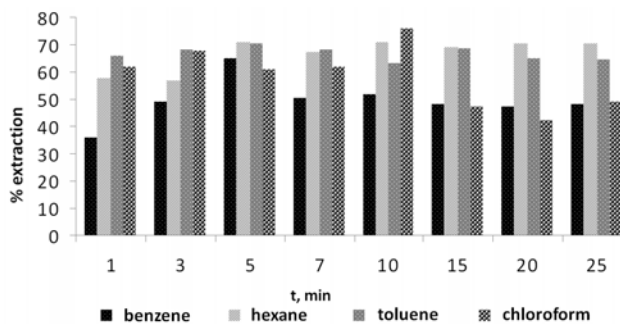


Figure 2. – Time of oil-slime ultrasonic treatment influence on degree of oil hydrocarbons extraction in solvent

On the basis of the obtained results it is possible to find an optimum range of ultrasonic extraction intensity (414 Wt/cm² – 460 Wt/cm²) at which there is the most effective extraction of oil hydrocarbons (Figure 3).

At fractional oil-slime extraction without ultrasonic treatment the maximum degree of oil hydrocarbons extraction has been reached in 1,5-2 hours and was 46, 48, 56, 66 % for chloroform, hexane, benzene and toluene, correspondingly. Thus it is possible to conclude that ultrasonic treatment intensifies process of oil hydrocarbons extraction from model samples.

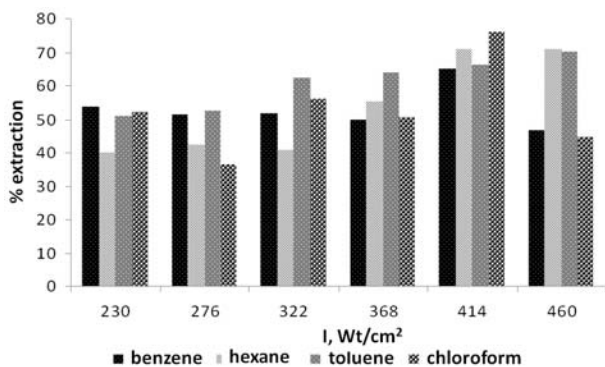


Figure 3. – Time of oil-slime ultrasonic treatment influence on degree of oil hydrocarbons extraction in solvent

It was shown that at ultrasonic influence the mineral oil temperature in the reactor increases on 7-10°C, in comparison with control. It likely occurs because of the acoustic energy dissipation (Figure 4).

During the sonochemical process particles in oil-slime make oscillative motions. Oscillative motion energy increases, in particular, at heating. As a result, the bonding between sand particles and hydrocarbon molecules is destructed, which leads to oil-slime structure weakening, but it is not enough for full extraction.

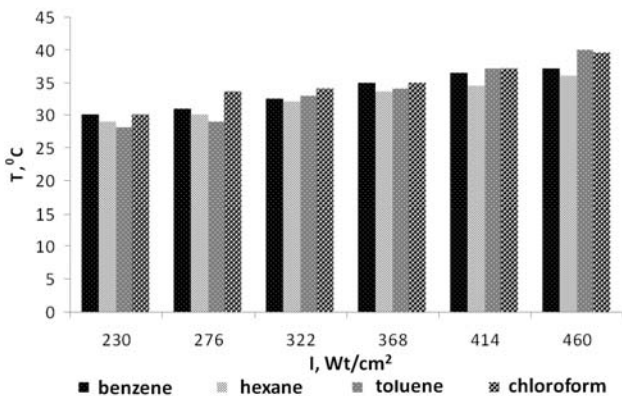


Figure 4. – Influence of ultrasonic treatment intensity on extraction temperature

However, even at higher temperature changes, limiting gradients of pressure can be reduced maximum in two-three times [5] (not in degrees, as it is necessary in many cases) since during the increase of the amount of free particles the probability of its collision and dynamic balance between process of hydrocarbons structure destruction and its restoration also increases. Thus, temperature rise owing to acoustic energy dissipation isn't the basic mechanism of oil-slime treatment from hydrocarbons though it plays a subsidiary role.

Following stage of the investigation was biodestruction of samples, polluted by oil hydrocarbons during sonochemical process. Collection cultures and the microorganisms secured in «Biotechnologies and chemistry» department of Tver Technical University were used in the

study. The phenotypic characteristic of new isolate was studied. It is shown that it concern barmy cultures of *Candida* genus (DK1, DK2, DK3, B3) and bacterial microorganisms of *Bacillus* genus. Oxidizehydrocarbon ability of studied microorganisms has been found (Figure 5).

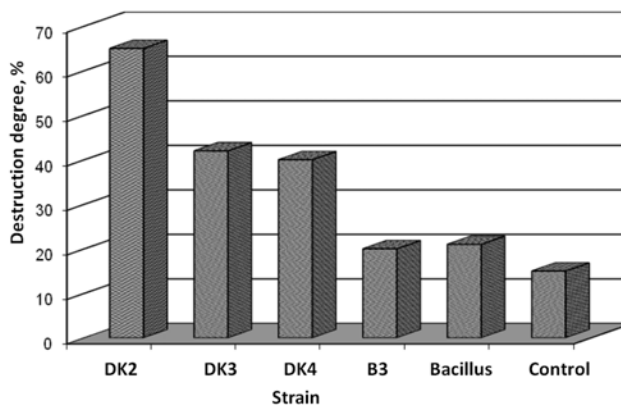
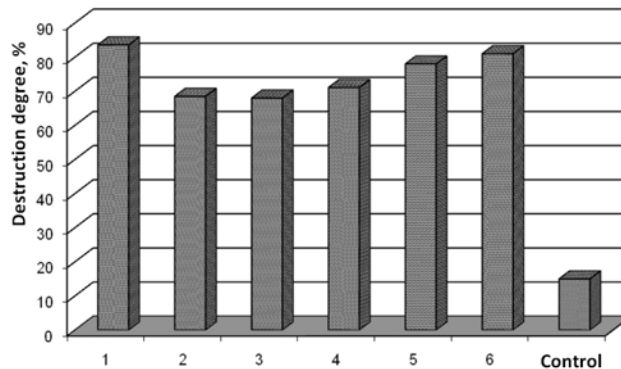


Figure 5. – Degree of oil hydrocarbons destruction by pure cultures

Optimum conditions of oil-slime biodestruction (temperature; pH; organic solvent, mineral salts and oil hydrocarbons concentrations) were chosen. It was shown that yeasts are the most effective destructor.

Further the consortium from allocated isolate was developed (Figure 6).



- 1 – strains DK2, DK 3, *Bacillus subtilis* in the ratio 1:1:1,
- 2- strains DK2 и DK3 in the ratio 2:1,
- 3- strains DK2 и DK3 in the ratio 3:1,
- 4- strains DK2 и DK3 in the ratio 1:3,
- 5- strains DK2, DK3, B3 in the ratio 1:1:1,
- 6- strains DK2 и DK3 in the ratio 1:1

Figure 6. – Oil hydrocarbons destruction in associations of microorganisms

Chosen consortium (1) is capable to decompose not only volatile fractions of oil, such as hexadecane, but also diesel fuel and heavier fractions of oil, for example black oil, i.e. destruct a wide spectrum of hydrocarbons. And the consortium doesn't lose the oxidizing activity at the

hexadecane, diesel fuel, oil and black oil maintenance at 5% (wt.).

CONCLUSIONS

Oil spill is a difficult engineering and microbiological problem which demands the complex approach for its solution. The developed method of oil spill recycling combines mechanical, physicochemical and biological methods.

Mechanical method means removal of oil spill from the polluted area and transferring it to the reactor for ultrasound extraction. Physicochemical method (ultrasound extraction) of oil spill pretreatment allows decreasing concentration of oil hydrocarbons up to atoxic level for microorganisms. Biological method allows destruction the remaining oil hydrocarbons up to maximum permissible concentration.

On the basis of experimental data optimum conditions of oil-slime ultrasonic pretreatment have been established: duration of process of 5-10 min, ultrasonic influence intensity of 368 Wt/cm² – 460 Wt/cm². From all studied solvents chloroform possessed the greatest extract ability for used samples. Thus the maximum degree of oil extraction from oil-slime was 75,9 %, at influence with intensity of 414 Wt/cm² and time of 10 minutes.

In process of biodestruction of the samples polluted by oil hydrocarbons after ultrasonic extraction, destruction degree has made more than 80 %.

Thus, the complex method of spills and a waste polluted by oil hydrocarbons neutralization, has allowed removing from it more than 85 % of oil hydrocarbons from the initial maintenance in samples within two weeks.

Developed scientific and technical production has advantage in comparison with analogs and includes use of ultrasonic treatment. The basic advantage of ultrasonic treatment consists of its sufficient quickness, profitability and ecological harmlessness. Besides, it allows destroying C-C bonds in paraffin molecules.

REFERENCES

- [1] M. Kumar, V. Leon, A. Materano, O.A. Ilzins, Enhancement of oil Degradation by Cop-Culture of Hydrocarbon degrading and Biosurfactant Producing Bacteria, Polish Journal of Microbiology.-2006.-A(2).-P.139-146.
- [2] G.G. Yagafarova, S.V. Leontjeva, A.H. Safarov, I.R. Yagafarov, M.V. Golovtsov, Complex technology of oil-slime purification, Oil-treatment-2008: international scientific-practical conference. – Ufa, 2008. – P. 330-331 (in Russian).
- [3] T.V. Mikhailova, S.V. Leonova, Problems of oil-slime treatment, Industrial ecology.-2009.-1. –P.10 (in Russian).
- [4] Isolation of autichthonous non-white rot fungi with potential for enzymatic upgrading of Venezuelan extra-heavy crude oil./ Naranjo, Urbina H., Leon V// Biocatal Biotransformation.-2007.-F(25).-P.341-349
- [5] R. Baldev, V. Randjendran, P. Palanichami, Ultrasound application, Moscow: Technosphere.-2006.-576 pp. (in Russian).

Glycoside hydrolases of marine bacteria are promising tools in haemotherapy

L.A. Balabanova, I.Y. Bakunina, G.N. Likhatskaya, T.N. Zvyagintseva, V.A. Rasskazov

Marine Biochemistry, Enzymatic Chemistry, Bioassay
Pacific Institute of Bioorganic Chemistry
Vladivostok, Russian Federation
balaban@piboc.dvo.ru

Abstract— Universal donor blood of group O is widely used on an emergency basis when it is impossible to define for some reasons a blood type of the recipient, for pediatric transfusions, and, especially, in cases when the blood of unusual or rare phenotypes. For today in transfusion medicine, still there is a problem of production of a qualitative donor blood in necessary quantity. Despite occurrence of techniques of enzymatic production of a donor blood, it cannot widely be applied in clinical practice because the enzymes being used for blood groups conversion are isolated from pathogenic microbial strains or/and produce up to 70 % injuring erythrocytes. Herein, alpha-N-acetylgalactosaminidase and α -galactosidase of marine bacteria, operating at neutral values of pH, have been suggested for conversion of erythrocytes of blood group A, B and AB to O in biotechnological production of universal donor blood. Alpha-N-acetylgalactosaminidase isolated from marine bacterium *Arenibacter latericius* has found to be uncommon enzyme. It shows the maximum activity at pH 7.0-8.0 and remains stable up to 50°C. The enzyme does not cause nonspecific agglutination of erythrocytes and their hemolysis and unlike known analogs modifies erythrocytes of blood subgroup A2 and A1 into erythrocytes of blood group O. Characterization of the sequences encoding glycoside hydrolases of marine bacteria revealed that they shared about 20-40% overall amino acid identity with their terrestrial counterparts. For further comparison of *A. latericius* alpha-N-acetylgalactosaminidase gene family, the gene sequence was isolated and characterized. It has a single open-reading frame consisting of 1287 base pairs, and the deduced amino acid sequence revealed that the mature enzyme consisted of 428 amino acid residues. The enzyme was estimated to be a homodimer with a molecular mass of subunit 48.2 kDa. The *Arenibacter* enzyme has a conserved common gene structure with a new glycoside hydrolases family 109. The structure of the putative binding sites of *A. latericius* alpha-N-acetylgalactosaminidase with NAD⁺ and blood group A antigen was predicted by molecular docking.

Keywords- marine bacteria, glycosidase, alpha-N-acetylgalactosaminidase, homology model, blood group conversion, erythrocytes

I. INTRODUCTION

Unlike known analogs, the enzymes from marine bacteria seem to be more suitable for use in biotechnology of production of a universal blood: a comfortable interval of pH for keeping the vital activity of erythrocytes, high

specific activity and demanded specificity that does a transfusion as much as possible effective, safe and economic. Recent characterization of alpha-galactosidase isolated from marine bacterium *Pseudoalteromonas* sp. KMM701 showed that the enzyme has a maximum activity at pH 6.7-7.7 at 22°C [1]. Alpha-galactosidase splits off galactose from melibiose, disaccharide Gala-1,3Gal and trisaccharide Gal₁, 3(Fucal,2)Gal that is a terminal structural element of the B antigen on erythrocytes of a blood type B. The results of immunological investigation of erythrocytes have shown that B antigens are completely transformed to H antigens in absence of aggregation of erythrocytes and their hemolysis. Enzyme does not show activity towards antigens A and H that is very important. Alpha-N-acetylgalactosaminidases (EC 3.2.49), that is capable of removing alpha-1,3-bound residues of N-acetylgalactosamine from glycoproteins of blood group substances and A-erythrocytes at neutral pH, converting them into O group substances are of more greater practical interest. For example, alpha-N-acetylgalactosaminidase from chicken liver carries out conversion only blood subgroup A2 that is not a sufficient condition for complete conversion of erythrocytes of type A, and the enzyme works at value of acidic pH, that in its turn produces 70 % injuring erythrocytes [2]. The enzymes from *Clostridium perfringens* and *Elisabethkingia meningosepticum* recently characterized are unsafe for recipients because of their pathogenic microbial sources [3, 4].

We studied the distribution of microbial producers of alpha-N-acetylgalactosaminidases among 860 bacterial isolates from water, bottom sediment, algae, and animals collected in different regions of the Pacific, Indian, and Atlantic oceans (Collection of Marine Microorganisms of PIBOC FEB RAS). Only nineteen percent of the microorganisms tested synthesized the enzyme with the different level of activity and specificity towards A-erythrocytes [5]. In view of this application, we have selected N-acetylgalactosaminidase of marine bacterium *Arenibacter latericius* for future characterization [6]. In this paper, the molecular structure of *A. latericius* alpha-N-acetylgalactosaminidase and catalytic mechanism of blood group A antigen hydrolyzing are suggested.

II. MATERIAL AND METHODS

A. Bacterium characterization and culture conditions

Arenibacter latericius KMM 426^T was isolated from sandy sediment sample collected from a depth of 20m (salinity, 32; temperature, 18 °C) in the South China Sea, near the island of Ku-Lao-Re (lat152108N, long1090702E). The bacterial strain KMM 426^T was cultivated on medium containing 5.0 g/liter bactopectone from Difco (USA), 1.0 g/liter glucose, 0.2 g/liter K₂HPO₄, 500 ml of distilled water, 500 ml of sea water, pH 7.8. Seeding material was grown on a shaker (150 rpm) in 250-ml shaker flasks (with medium of 50 ml) for 24-30 h at 25°C to the density 10⁹ cells/ml. The resulting material was inoculated into 1000-ml flasks with 500 ml of the same fermentative medium.

B. Alpha-N-acetylgalactosaminidase purification

The bacterial cells were suspended in 0.01 M Na⁺-phosphate buffer, pH 7.2, and sonicated. Proteins were precipitated from the supernatant with 50-70% ammonium sulfate, and the resulting pellet was resolved and dialyzed in 0.01 M Na⁺-phosphate buffer, pH 7.2. The solution was loaded onto DEAE-Sephacel CL-6B (15.0×2.8 cm), and then on DEAE-Toyopearl 650 M (Toyo Soda) (15.5×2.0 cm) in the same buffer, pH 7.2. Alpha-N-acetylgalactosaminidase activity was eluted with gradient of 0–1 M and 0–0.5 M NaCl, respectively. Active fractions were concentrated.

C. Effect of enzyme on erythrocytes blood group-specific glycoproteins

Erythrocytes washed with physiological solution were mixed with the enzyme solution (2 U/ml) in isotonic phosphate buffer, pH 7.3. After 24 h incubation with stirring at 36°C, the erythrocytes were washed thrice with physiological solution (pH 7.3) and mixed with corresponding sera in a series of double dilutions on the plates. Agglutination titer was read after 1 h incubation at room temperature. Excision of N-acetylgalactosamine from BGG A +H was registered by an amino acid analyzer after acidic hydrolysis of low-molecular-weight fraction of the products of fermentolysis obtained by gel chromatography on Sephadex G-15.

D. Molecular cloning and sequence analysis

Recombinant DNA technique was performed using Ins T/Aclone[™] PCR Product Cloning Kit, restriction endonucleases, T4 DNA ligase, Long PCR mix (Fermentas), Smart Taq Polymerase (Topotili), automatic amplifier (Eppendorf). Two pair of primers (For1 - 5'-GG(G/A/T)GC(A/T)AA(A/G)TA(T/C)ATG GGN GGN TT (T/C)TC-3' and Rev1 - 5'-GG (A/G)TG (G/A)TC (G/A)TA (C/T)TT N TC-3; For2 - 5'-ATG ATG ATG GA(A/G)

AA(T/C)GTN AA(T/C)TA-3' and Rev2 - 5'-GG (A/G)TG (G/A)TC (G/A)TA (C/T)TT N TC-3') were synthesized on the base of known alpha-N-acetylgalactosaminidase homologue sequences to amplify the active site region of alpha-N-acetylgalactosaminidase using *A. latericius* chromosomal DNA as a template. The C-termini region coding sequence was determined using only forward primers (F1 and F2). PCR products were cloned and sequenced using the automated PE/ABI 310 DNA sequencer and PE/ABI-ABI PRISM BigDye Terminator cycle sequencing Ready Reaction Kit (PE Applied Biosystems). *Escherichia coli* strains TOP10 or XL1 (Evrogen) were used for standard cloning procedures. Nucleotide and amino acid sequences analysis were performed with Chromas, GenRunner. Nucleotide and amino acid sequences homology and similarity searches and alignments were carried out by using the BLAST and ClustalW, MUSCLE facilities. The Molecular Operating Environment version 2010.10 software [7] was used for 3D-structure modeling and visualization. The theoretical model of *A. latericius* alpha-N-acetylgalactosaminidase 3D-structure was constructed with the use of Homology module of MOE package on the based of X-ray structure of *E. meningosepticum* alpha-N-acetylgalactosaminidase (PDB ID: 2IXB) as template. Molecular docking alpha-N-acetylgalactosaminidase with blood group A antigen was performed with the use of Docking module of MOE.

III. RESULTS AND DISCUSSION

The distribution of alpha-N-acetylgalactosaminidase activity in marine bacteria showed that the enzyme is rare and a highest number of its producers occurred as a free-living or marine animal-associated bacteria in tropical water of Pacific Ocean [5]. The extracellular glycosidase activity suggests that the bacterium is able to hydrolyze organic materials in the marine environment [8]. The enzyme exhibiting a high alpha-N-acetylgalactosaminidase activity isolated from marine bacterium *A. latericius* KMM 426^T, new genus of the family *Flavobacteriaceae*, was found to be unusual alpha-N-acetylgalactosaminidase. After three purification stages, the enzyme was homogenous and not contaminated with other glycosidase activities. It shows the maximum activity at pH 7.0-8.0 and stability up to 50°C during 30 min. The enzyme has exogenous mode of action. The enzyme does not cause nonspecific agglutination of erythrocytes and their hemolysis and unlike known analogs completely modifies erythrocytes of both blood subgroup A2 and A1 into erythrocytes of blood group O (Fig. 1, Table 1).

The enzyme properties provide a significant advantage of the enzyme over the alpha-N-acetylgalactosaminidase from liver that have optimum activity at pH less than 5.5 [2]. Characterization of the *A. latericius* alpha-N-acetylgalactosaminidase gene sequence (accession n.HQ108058) revealed that the enzymes shared about 84%

and 70% overall amino acid homology with uncharacterized proteins of *Flavobacteria bacterium* и *Akkermansia muciniphila*, respectively, and 37% identity and 50% homology with its terrestrial prototype from *E. meningosepticum*. It has a single open-reading frame consisting of 1287 base pairs, and the deduced amino acid sequence revealed that the mature enzyme consisted of 428 amino acid residues. The enzyme was estimated to be a homodimer with a molecular mass of subunits 48.2 kDa and pI 7.99. *A. latericius* alpha-N-acetylgalactosaminidase is characterized by a high content of Gly (10.51%) Glu (7.24%) Leu (7.01%) Ala (6.78%) Lys (6.54%). Polar amino acid residues are predominant. A high content of glycine residues in the structure can be explained by psychrophility of most marine bacteria [8]. Despite the low level of identity and homology with the known alpha-N-acetylgalactosaminidases the tertiary structure analysis of the *Arenibacter* enzyme showed that it has a common molecular fold with a new glycosyl hydrolases family 109 (Fig. 2). It has been found that exogenous NAD⁺ does not influence on the *A. latericius* alpha-N-acetylgalactosaminidase activity. The structure superposition showed cofactor binding specificity and strength similarity to *E. meningosepticum* alpha-N-acetylgalactosaminidase, belonging to family 109 (Fig. 2). The structure of the putative binding site of blood group A antigen trisaccharide with *A. latericius* alpha-N-acetylgalactosaminidase was predicted by molecular docking (Fig. 3). The trisaccharide moiety was found to be close to NAD⁺ and residues Tyr 178, His 180, Tyr 209 and Tyr 292, which were invariant within the GH109 family.

Structurally functional researches of glycosidases of marine bacteria will create a basis for optimal genetic construction of recombinant protein for working out of a new highly effective and hi-tech method of universal donor blood production for a safe and easy accessible transfusion.

TABLE I.

Polyclone-A	Agglutination titer of donor A erythrocytes before and after <i>A. latericius</i> enzyme treatment								
	2	4	8	16	32	64	128	256	512
Anty-A+ transformed erythrocytes	-	-	-	-	-	-	-	-	-
Anty-A+ non transform eruthrocytes	+	+	+	+	+	+	+	+	-

Galβ1-R 2 1 Fuca	GalNAcα1-3Galβ1-R 2 1 Fuca
H antigen	A antigen

Figure 1. H and A antigen structures.

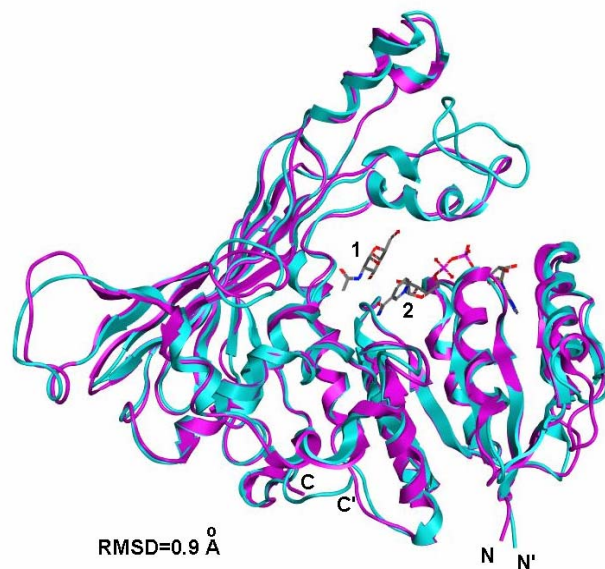


Figure 2. The ribbon diagram of superposition of the homology model of alpha-N-acetylgalactosaminidase from *Arenibacter latericius* KMM 426^T (magenta) and crystal structure of the complex of alpha-N-acetylgalactosaminidase from *Flavobacterium meningosepticum* (cyan) with N-acetyl-2-deoxy-2-amino-galactose (1) and NAD⁺ (2).

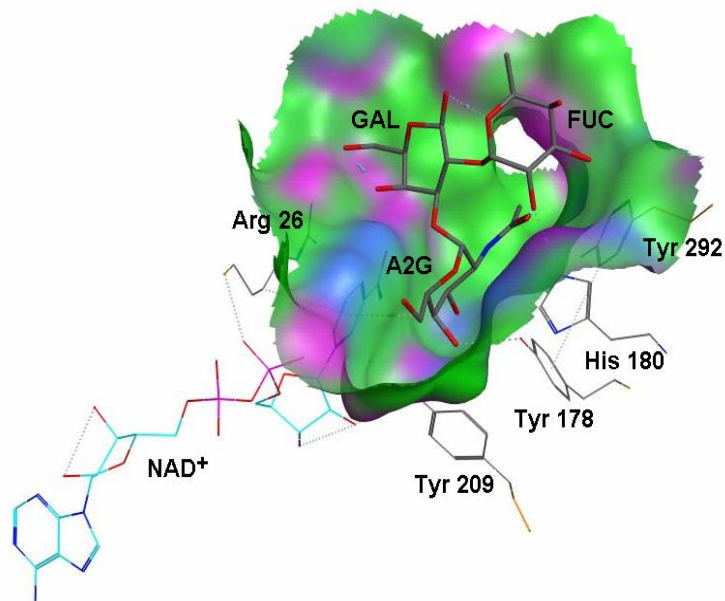


Figure 3. The putative binding site of alpha-N-acetylgalactosaminidase *Arenibacter latericius* KMM 426^T with blood group A trisaccharide. Molecular surface near trisaccharide is shown in magenta for H-binding, blue for mild polar and green for hydrophobic.

ACKNOWLEDGMENT

This work was supported with funding by grants of FEB RAS n. 09-III-A-05-143 and 09-III-A-05-150, RFBR n. 11-08-01200-a and the grant of the Russian Academy of Sciences on Program of Fundamental Research “Physicochemical biology FEB RAS” n. 09-I-II22-05.

REFERENCES

- [1] L.A. Balabanova, I.Y. Bakunina, O.I. Nedashkovskaya, I.D. Makarenkova, T.S. Zaporozhets, N.N. Besednova, T.N. Zvyagintseva, V.A. Rasskazov. “Molecular characterization and therapeutic potential of a marine bacterium *Pseudoalteromonas* sp. KMM 701 α -galactosidase”, *Mar. Biotechnol.*, vol. 12, 2010, pp. 111-120.
- [2] J. Hata, M. Dhar, M. Mitra, M. Harmata, P. Haibach, P. Sun, D. Smith. “Purification and characterization of N-acetyl- α -D-galactosaminidase from *Gallus domesticus*”. *Biochem. Int.*, vol. 28, 1992, pp. 77-86.
- [3] M.J. Calcutt, H.Y. Hsieh, L.F. Chapman, D.S. Smith. “Identification, molecular cloning and expression of an α -N-acetylgalactosaminidase gene from *Clostridium perfringens*”. *FEMS Microbiol. Lett.*, vol. 214, 2002, pp. 77-80.
- [4] Q.P. Liu, G. Sulzenbacher, H. Yuan, E.P. Bennett, G. Pietz, K. Saunders, J. Spence, E. Nudelman, S.B. Levery, T. White, J.M. Neveu, W.S. Lane, Y. Bourne, M.L. Olsson, B. Henrissat & H. Clausen. “Bacterial glycosidases for the production of universal red blood cells”. *Nat. Biotechnol.*, vol. 25, 2007, pp. 454 - 464.
- [5] E. P. Ivanova, I. Yu. Bakunina, O. I. Nedashkovskaya, N. M. Gorshkova, V. V. Mikhailov, and L. A. Elyakova. “Incidence of Marine Microorganisms Producing α -N-Acetylglucosaminidases, α -Galactosidases and α -N-Acetylgalactosaminidases”. *Russian Journal of Marine Biology*, vol. 24, 1998, pp. 365–372.
- [6] I. Yu. Bakunina, R. A. Kuhlmann , L. M. Likhoshesterov, M. D. Martynova, O. I. Nedashkovskaya, V. V. Mikhailov, and L. A. Elyakova. “ α -N-Acetylgalactosaminidase from Marine Bacterium *Arenibacter latericius* KMM 426T Removing Blood Type Specificity of A Erythrocytes”. *Biochemistry (Moscow)*, Vol. 67, No. 6, 2002, pp. 689-695.
- [7] *Molecular Operating Environment (MOE)*, 2010.10; Chemical Computing Group Inc., 1010 Sherbooke St. West, Suite #910, Montreal, QC, Canada, H3A 2R7, 2010.
- [8] Q.L. Qin , X.Y. Zhang , X.M. Wang, G.M. Liu , X.L. Chen , B.B. Xie, H.Y. Dang, B.C. Zhou, J. Yu, Y.Z. Zhang. “The complete genome of *Zunongwangia profunda* SM-A87 reveals its adaptation to the deep-sea environment and ecological role in sedimentary organic nitrogen degradation”. *BMC Genomics*, vol. 11, 2010, pp. 247-247.

Biocalcification of Corals and their Response to Global Climate Change

M. Azizur Rahman^{1,2} and Ryuichi Shinjo²

¹Department of Earth and Environmental Sciences
Palaeontology & Geobiology

Ludwig-Maximilians-University of Munich, Germany

²Department of Physics and Earth Sciences
University of the Ryukyus, Okinawa, Japan

Email: a.rahman@lrz.uni-muenchen.de, azizur31@yahoo.com

Abstract—The response of calcifying marine organisms, especially from corals – arguably among the most biologically diverse and ecologically important ecosystems on the planet – could have a potential mitigating role in buffering atmospheric CO₂. Here we report that the organic substances that participate in biocalcification in coral skeletons contain a carbonic anhydrase (CA) enzyme which is a biological catalyst responsible for the interconversion of CO₂ and bicarbonate. Also, it appears that the internal physiological condition of the body of corals has precisely evolved to respond to external environmental conditions. We find that the CA in the organic matrix acts as “keys” to control those internal conditions to enable a response to external environmental change. This study of biocalcification process can be used as a tool for understanding coral mineralization in nature and global climate change, and also has implications for CO₂ capture from the atmosphere.

Keywords- biocalcification; coral mineralization; carbonic anhydrase ; climate change; organic matrix

I. INTRODUCTION

Calcifying marine organisms make extensive use of calcium carbonate (CaCO₃), one of the most abundant minerals in nature, as a structural or protective material. Biologically formed calcium carbonates are mainly calcite, aragonite and vaterite as well as high Mg-calcites. During the work on biocalcification, it is seen that morphology, mineralogy and chemistry of biologically formed calcium carbonate are largely dependent on both biological species and physical-chemical environmental conditions. Proteins and enzymes may act as “keys” to control internal conditions and respond to external environmental change.

Identification and elucidation of proteins and their enzyme activity involved in calcium carbonate skeleton or spicules formation in corals are very important to understand the calcification process, biodiversity of their ecosystems and carbon cycling, along with global environmental change. Atmospheric CO₂ is expected to reach double the preindustrial levels by the year 2065. It is believed that the

increase in CO₂ concentration is responsible for global warming. Biological sequestration of carbon dioxide (CO₂) in geological formations is one of the proposed methods to reduce the carbon dioxide released into the atmosphere. Mineralization of CO₂ can be achieved by direct contact of gaseous CO₂ with mineral sources of calcium or magnesium or by dissolving CO₂ in water and then bringing the solution into contact with the minerals. Either way will produce calcium or magnesium carbonate, which are solids and will precipitate [1, 2]. In the present work, the feasibility of using CA enzyme as a catalyst for hydration of CO₂, as well as its precipitation in the form of calcium carbonate, was studied. The effects of enzyme concentration and temperature on the hydration of CO₂ and formation of calcium carbonate were investigated. Here we applied CA enzyme extracted from the soft coral sclerites, *Sinularia polydactyla* as a model. The information gained from this study would be applicable in understanding the biomineralization process of corals and their response to global climate change.

II. MATERIALS AND METHODS

A. Sample preparation

Sclerites were separated from the coral colony (*Sinularia polydactyla*) according to the mechanical and chemical treatments followed by Rahman et al., 2006 [3]. Briefly, the collected sclerites were stirred vigorously in 1M NaOH for 2 hours and subsequently in 1% NaClO solution for 2 hours to remove the fleshy tissues and debris. Treated samples were washed under tap water until the sclerites were completely cleaned. Finally, samples were washed with distilled water (five times) to remove unwanted substances.

B. CA assay

To examine the CA activity, the chemically treated sclerites were decalcified in 0.5 M EDTA (pH 7.8) overnight, followed by dialysis against H₂O for 48 hours. Proteins were separated from the soluble organic matrix of sclerites using SDS-polyacrylamide gel electrophoresis according to the method of Laemmli [4]. After electrophoresis, the bands of interest were excised from the SDS-PAGE and the pure proteins were extracted by electro-elution treatment, using

the Electro-eluter (Model 422, Bio-Rad) according to the procedure of Rahman et al., [5]. The Micron centrifugal Filter Devices (Millipore) were used for further purification of the sample.

The amount of protein concentration in each fraction was measured by the method of Lowry et al. [6] using chicken ovalbumin (Kanto chemical) as a standard protein followed by a spectrophotometric assay of protein. We measured CA activity using the CO₂-Veronal indicator method [7] as follows. Six drops of phenol red, 3 ml of 20mM Veronal buffer (Sodium 5, 5-Diethylbarbiturate, pH 8.3), and 0.5 ml of a sample were mixed and placed in ice water; then the reaction was started by adding 2 ml of ice-cold water saturated with CO₂ followed by observation of the time until the color changed from red to yellow for a pH drop to 7.3. The EU was calculated according to the following equation.

$$\text{Activity unit (EU)} = (\text{To} - \text{T}) / \text{T}$$

[where T and To are the reaction times required for the pH change from 8.3 to 7.3 at 0°C with and without a catalyst, respectively].

C. Enzymatic Hydration of CO₂. Carbonic anhydrase catalyzes the hydration reaction of CO₂, and consequently, hydrogen ions are transferred between the active site of the enzyme. This results in a change in pH. Therefore, measuring pH via the delta pH method is a viable method to monitor the progress of this enzymatic reaction [8]

D. Enzymatic Precipitation of Calcium Carbonate.

The influence of CA enzyme on the precipitation of CO₂ in the form of calcium carbonate (CaCO₃) was studied according to Mirjafari et al [9] and Rahman et al. [10]

III. RESULTS AND DISCUSSION

A. Biocalcification

For understanding biocalcification process in corals and their response to climate change, we purified proteins and enzyme from a soft coral sclerites, *S. polydactyla*. The SDS-PAGE analysis of the preparation showed seven proteins with the apparent molecular masses of 109, 83, 70, 63, 41, 30 and 22 kDa (Fig. 1, lane 2) that we named SP-1 (*Sinularia polydactyla-1*), SP-2, SP-3, SP-4, SP-5, SP-6 and SP-7 respectively. In the present work, we purified a protein with a molecular mass of about 83-kDa (SP-2) (Fig. 1, lane 2), which has high CA activity (Fig. 2). We excised the protein bands from the SDS-PAGE and extracted the purified proteins by electro-elution treatment. We confirmed the CA protein (SP-2) followed by the technique as indicated above (Fig. 2).

In order to identify CA activity associated with the purified proteins, the samples were assayed independently. Fig. 3 shows that the SP-2 possessed specific CA activity; where other has lower activity. The CA activity of both the matrix protein (SP-2) and bovine erythrocyte enzyme (BECA) was inactivated by heat treatment at 100°C for 10 min, which showed no activity. Since SP-2 showed the highest and most significant activity among the seven proteins, we can

consider only SP-2 to be a CA domain protein in *S. Polydactyla*.

Internal and external reactions of coral body including hard endoskeleton of sclerites are occurred with biocalcification process. In the mineralization of CO₂, calcium carbonate is produced through a reaction between calcium ions and aqueous CO₂. The following reactions take place in this process:

(1) First, gaseous CO₂ dissolves in water to form aqueous CO₂.



(2) Then, aqueous CO₂ reacts with water to form carbonic acid:

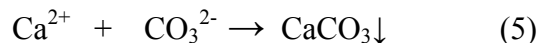


(3) In the next step, carbonic acid dissociates to bicarbonate and carbonate ions in the presence of CA enzyme:



Reaction 3 is very rapid and is virtually diffusion controlled.

(4) At the end, in the presence of calcium cations, calcium carbonate forms and precipitates:



Among reactions 1–5, reaction 2 is the slowest, and it is the rate-limiting step. It is proposed that a biological catalyst be used to increase the rate of this reaction.[11-13]. The biological catalyst for this reaction is enzyme carbonic anhydrase.

B. Enzymatic Precipitation of Calcium Carbonate

The amount of CaCO₃ decreased as the temperature increased. The weight of CaCO₃ at 0, 30, and 50 °C was 0.2097, 0.1282, and 0.095 g, respectively. This is because the solubility of CO₂ in water decreases with increasing temperature [14]. This result did not depend on the temperature or concentration of the enzyme. When the buffer is absent from the reaction mixture, addition of CO₂ to the mixture drives the pH down to low values (near 4). The chemistry of CO₂ hydration and bicarbonate dissociation shows that, in low pH, there is not enough carbonate ion present [15]. As a result, the solution does not become saturated with CaCO₃. This is the reason precipitation was not observed in this condition.

In the absence of the enzyme, precipitation was observed after 2 h. The amount of CaCO₃ was almost the same as its amount in the presence of the enzyme (Table 1). However, Figure 3 indicates that precipitation of calcium carbonate was much faster in the presence of CA enzyme. This figure

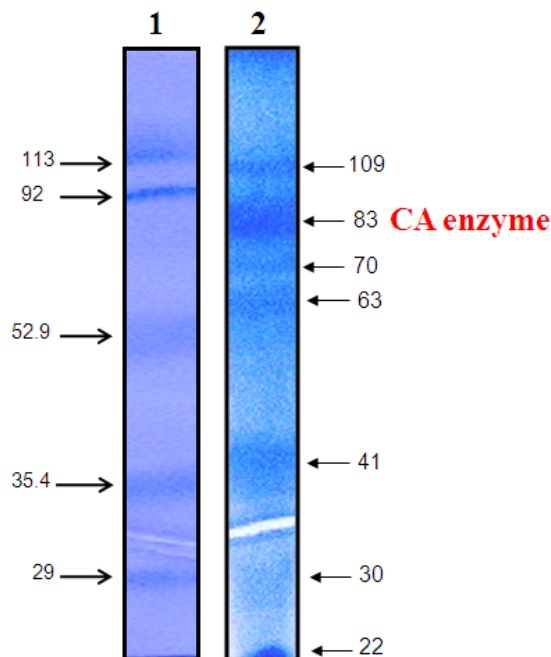


Figure 1: Identification of proteins. Lane 1, Protein marker, Lane 2, SDS-PAGE separation of the total assemblage of soluble matrix proteins with CBB staining. Arrows indicate significant protein bands.

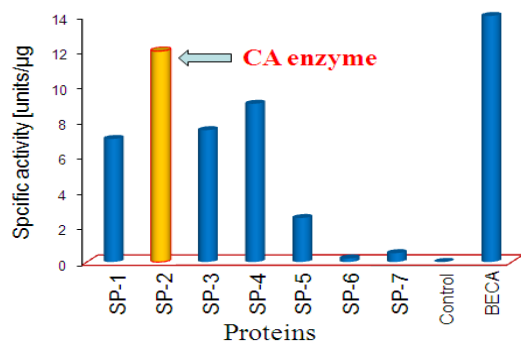


Figure 2: Determination of CA activity with purified matrix proteins. Specific activity was measured in the presence of matrix proteins at concentration of 1.5 ml (contain 30μg protein) for each protein; SP-2 showed the highest activity. H₂O (control) and bovine erythrocyte CA (BECA) was used as a standard in comparing the efficacy of CA proteins. Ten experiments were conducted for each protein. The novel matrix protein of SP-2 showed significant CA activity.

presents a comparison of the precipitation in the presence and absence of the enzyme. It is clearly seen that, in the presence of the enzyme, CaCO₃ reached its maximum value in less than 10 min; however, when no enzyme was added to the reaction mixture, the formation of calcium carbonate took place very slowly.

Carbonic anhydrases are very well-known enzymes that are ubiquitous in nature. They can be found in animals and plants and even in the human erythrocyte. They exist in different forms, with different structures and molecular

weights, and their activities vary from one to another. They are among the fastest enzymes known. For instance, each molecule of isozyme C from the human body can catalyze 1.4×10^6 molecules of CO₂ in 1 s [16].

In the presence of an anhydrase enzyme, the mechanism of hydration of CO₂ changes completely. The evidence suggests that the catalysis of CO₂ hydration is initiated by the nucleophilic attack on the carbon atom of CO₂, by zinc-bound OH⁻, to produce bicarbonate, which is then displaced from zinc by a water molecule [17]. In this study, the Mineralization of carbon dioxide is investigated as a method of converting CO₂ to mineral carbonates. The slow rate of hydration of CO₂ has been a limiting factor to make this

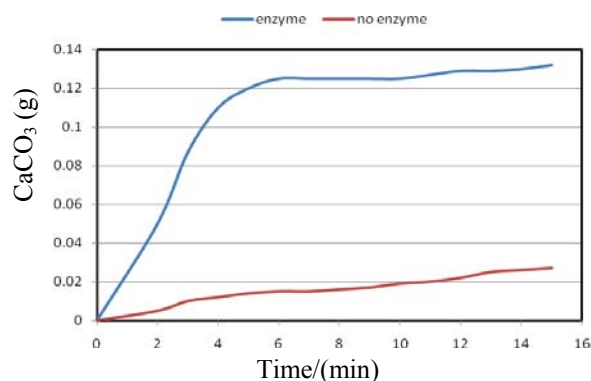


Figure 3: Comparison of precipitation with and without enzyme.

Table 1: Summary of CaCO₃ Precipitations

Set	Temp (°C)	Enzyme con. (μM)	Wt. of precipitate (g)	No. of units	Error (%)
1	0	3	0.2097	2	0.1
2	0	6	0.2105	4	4.2
3	0	6	0	3	N/A
4	0	No enzyme	0.18	2	1
5	30	3	0.1279	2	0.16
6	30	6	0.1282	4	1.8
7	50	6	0.095	3	1.7
8	50	No enzyme	0.0940	2	1.5

method widely accepted. Carbonic anhydrase enzyme isolated from soft corals sclerites has been shown to be credible as biological catalysts to overcome this shortcoming. The results showed that this enzyme was a very effective catalyst for coral mineralization. Overall, it promoted the hydration of CO₂ and, consequently, the precipitation of CaCO₃.

ACKNOWLEDGMENT

This work was supported by the Alexander Von Humboldt Foundation, Germany and Japan Society for the Promotion of Science (JSPS).

REFERENCES

- [1] K. S. Lackner, D. P. Butt, C. H. Wendt, and D. H. Sharp, "Carbon dioxide disposal in solid form," Proceedings of the 21st International Conference on Coal Utilization and Fuel Systems, Clearwater, FL, March 1996, pp. 18–21.
- [2] K. S. Lackner, C. H. D. P. Wendt, E. L. Joyce, and D. H. Sharp, "Carbon dioxide disposal in carbonate Minerals," *Energy* Vol. 20, 1995, pp. 1153–1170.
- [3] M.A. Rahman, Y. Isa, T. Uehara, "Studies on two Closely Related Species of Octocorallians: Biochemical and Molecular Characteristics of the Organic Matrices of Endoskeletal Sclerites," *Mar. Biotechnol.*, Vol. 8, 2006, pp. 415-424.
- [4] U.K. Laemmli, "Cleavage of structural proteins during assembly of the head of Bacteriophage," *Nature* Vol. 227, 1970, pp. 680-685.
- [5] M.A. Rahman, Y. Isa, T. Uehara, "Proteins of calcified endoskeleton: II. Partial amino acid sequences of endoskeletal proteins and the characterization of proteinaceous organic matrix of spicules from the alcyonarian, *Simularia polydactyla*," *Proteomics* Vol. 5, 2005, pp. 885-893.
- [6] O.H. Lowry, N.J. Rosebrough, A.L. Farr, R.J. Randall, "Protein measurement with the Folin phenol Reagent," *J. Biol. Chem.*, Vol. 193, 1951, pp. 265-275.
- [7] S-Y. Yang, M. Tsuzuki, S. Miyachi, "Carbonic anhydrase of chlamydomonas: Purification and studies on its induction using antiserum against chlamydomonas carbonic anhydrase," *Plant Cell. Physiol.* Vol. 26, 1985, pp. 25-34.
- [8] R. P. Henry, "The carbonic anhydrase: cellular physiology and molecular genetics" Plenum Press: 1991, New York,
- [9] P. Mirjafari, K. Asghari, and N. Mahinpey, "Investigating the Application of Enzyme Carbonic Anhydrase for CO₂ Sequestration Purposes" *Ind. Eng. Chem. Res.* Vol. 46, 2007, pp. 921–926.
- [10] M. A. Rahman, T. Oomori, T. Uehara, "Carbonic anhydrase in calcified endoskeleton: Novel activity in biocalcification in alcyonarian" *Mar. Biotechnol.*, Vol. 10, 2008, pp. 31-38.
- [11] G. M. Bond, G. Egeland, D. K. Brandvold, M. G. Medina, F. A. Simsek, J. Stringer, "Enzymatic catalysis and CO₂ sequestration," *World Resour. Rev.* Vol. 11, 1999, pp. 603–618.
- [12] G. M. Bond, G. Egeland, D. K. Brandvold, M. G. Medina, J. Stringer, "CO₂ sequestration via a biomimetic approach. *EPD Congress: Proceedings of sessions and symposia* 1999; pp. 763–781.
- [13] G. M Bond, J Stringer, D. K Brandvold, F. A Simsek, M. G Medina, G. Egeland, "Development of integrated system for biomimetic CO₂ sequestration using the enzyme carbonic anhydrase," *Energy Fuels*, Vol. 15, 2001, 309–316.
- [14] Green, P. *Perry's Chemical Engineering Handbook*, 7th ed.; McGraw-Hill: 1997, New York.
- [15] S. Morgan, *Aquatic chemistry, Chemical Equilibria and Rates in Natural Waters*; Wiley-Interscience: 1996, New York.
- [16] R. C. Khalifah, The carbon dioxide hydration activity of carbonic anhydrase. *J. Biol. Chem.* Vol. 246, 1971, pp. 2561–2573.
- [17] W. R. Chegwidden, N. D. Carter, Y. H. Edwards, "The carbonic anhydrase new horizons," Birkhäuser Verlag: 2000, Basel, Switzerland.